

Function of *MAP20* and *MYB103* in Cellulose and Lignin Formation of Xylem Secondary Cell Walls

David Öhman

Faculty of Forest Sciences

Department of Forest Genetics and Plant Physiology

Umeå

Doctoral Thesis

Swedish University of Agricultural Sciences

Umeå 2014

Acta Universitatis Agriculturae Sueciae

2014:4

Cover: Live cell imaging of cortical microtubule dynamics in tobacco leaves
(photo: S. Miroshnichenko)

ISSN 1652-6880

ISBN (print version) 978-91-576-7956-7

ISBN (electronic version) 978-91-576-7957-4

© 2014 David Öhman, Umeå

Print: Arkitektkopia, Umeå 2014

Function of *MAP20* and *MYB103* in Cellulose and Lignin Formation of Xylem Secondary Cell Walls

Abstract

Lignocellulose from trees and other crops will have tremendous impact on the next generation of sustainable biofuels and biomaterials. To take advantage of modern breeding tools, it is therefore important to understand the genetic and molecular regulation underlying secondary cell wall formation. Here, functional analysis was performed on two genes specifically involved in secondary cell wall formation, using *Arabidopsis* and *Populus* as model species.

PttMAP20 was earlier identified as a wood-specific microtubule-associated protein in hybrid aspen, but not functionally assessed [Rajangam *et al.* (2008). *Plant Physiology*, pp. 1283–1294]. In this thesis, AtMAP20 was found to be generally expressed in secondary wall forming cell types in *Arabidopsis*, including xylem cells, and its binding to microtubules was confirmed. A domain-mapping study showed that its central TPX2 domain, together with the N- and/or C-terminal domain, is required for complete microtubule binding. Overexpression of *AtMAP20* induced shorter roots and right-handed twisting, mimicking treatment with the microtubule-stabilizing drug taxol. Loss-of-function *map20* mutants had longer etiolated hypocotyls and altered cell wall chemistry. This phenotype was interpreted as resulting from mechanical weakening in the secondary walls of their spiral protoxylem vessels. In line with this, overexpression of *PttMAP20* in hybrid aspen affected cellulose microfibril angle. Taken together, MAP20 is a novel microtubule-stabilizing protein, specifically active during secondary cell wall formation and important for the patterning of cellulose microfibrils.

MYB103 is a xylem-specific transcription factor, previously demonstrated to be directly activated by the secondary wall NAC master switches SND1/NST1 and VND6/VND7 [Zhong *et al.* (2008). *Plant Cell*, pp. 2763–2782]. This thesis demonstrates that loss-of-function *Arabidopsis myb103* mutants have reduced levels of syringyl lignin in their basal stems. This was compensated for by an increase in guaiacyl lignin, resulting in a modified syringyl to guaiacyl ratio. The altered lignin composition, characterized by Py/GC-MS, FT-IR microspectroscopy and 2D NMR, was caused by a suppression of *F5H*, a key gene in syringyl lignin biosynthesis. Thus, it is concluded that MYB103 is required for *F5H* expression.

Taken together, this thesis presents novel knowledge on function of genes important for secondary cell wall formation and, hence, wood formation. These findings have the potential to improve wood characteristics to benefit forest growers and industries.

Keywords: *MAP20*, *MYB103*, microtubule-associated protein (MAP), transcription factor, secondary cell wall, xylem, lignin, cellulose, *Arabidopsis thaliana*, *Populus*

Author's address: David Öhman, SLU, Department of Forest Genetics and Plant Physiology, SE-901 83 Umeå, Sweden.

E-mail: David.Ohman@slu.se

Imagination is more important than knowledge.

Einstein

Contents

List of Publications	7
Abbreviations	9
1 Introduction	11
1.1 Formation and Characterization of Wood	12
1.1.1 Cambial Growth	12
1.1.2 Differentiation of a Wood Cell	13
1.1.3 Mechanics and Chemistry of Wood	13
1.2 Primary Cell Walls and Their Expansion in Developing Wood	15
1.3 Exploring Genes Involved in Secondary Cell Wall Formation	18
1.4 Cellulose Deposition and Its Dependency on the Cytoskeleton	19
1.4.1 Cellulose Biosynthesis	19
1.4.2 Cellulose Microfibrils Align with Cortical Microtubules	22
1.4.3 Microtubule Structure, Dynamic Instability and Reorientation	25
1.4.4 Microtubule Mutants Display Twisting and Modified Microfibril Angle in Their Cell Walls	26
1.5 Microtubule-Associated Proteins – MAPs	27
1.5.1 MAPs Affecting Primary Cell Wall Expansion	27
1.5.2 Bundling of Cortical Microtubules by MAPs – A Requirement for Secondary Cell Wall Formation	29
1.5.3 MAPs Regulating Local Initiation and Prevention of Secondary Cell Wall Deposition	30
1.5.4 MAPs Implicated in the Ordered Deposition of Cellulose Microfibrils	32
1.6 Lignin Biosynthesis and Structure	34
1.6.1 Biosynthesis of Lignin Monomers	34
1.6.2 Monolignol Transport	34
1.6.3 Lignin Nucleation and Polymerization in the Apoplast	35
1.6.4 Lignin Engineering – Modifying Syringyl to Guaiacyl Ratios	36
1.7 Transcriptional Networks Regulating Secondary Cell Wall Formation	37
1.7.1 First Level Master Switches – The NAC Family	37
1.7.2 Second Level Master Switches – The MYB and KNAT Families	40
2 Objectives	45
2.1 In General	45
2.2 In Particular	45

3	Methodological Considerations	47
3.1	<i>Arabidopsis</i> and <i>Populus</i> as Model Systems to Study Secondary Growth	47
3.2	Generation of Transgenic Lines in Hybrid Aspen	48
3.3	Plant Materials and Growth Conditions for Hybrid Aspen	48
	3.3.1 Explant Shoots Grown <i>in Vitro</i>	48
	3.3.2 Greenhouse-Grown Trees	49
3.4	Promoter–GUS Analysis in Hybrid Aspen	49
3.5	Gene Expression Analysis	49
	3.5.1 Quantitative PCR Analysis	49
	3.5.2 Microarray Analysis	50
3.6	Cellulose Microfibril Angle Measurements on Wood Fibres	51
3.7	Xylem Tracheary Element Cell Culture System in <i>Arabidopsis</i>	51
4	Results and Discussion	53
4.1	MAP20 – A Microtubule-Associated Protein Highly Expressed in <i>Populus</i> and <i>Arabidopsis</i> Xylem Tissues	53
	4.1.1 AtMAP20 Is a Novel Stabilizer of Microtubules in <i>Arabidopsis</i> (Paper I)	53
	4.1.2 AtMAP20 Is Functioning in Secondary-Walled Cell Types and Required for Proper Cell Wall Composition and Structure (Paper II)	56
	4.1.3 Exploring AtMAP20 Function by an <i>Arabidopsis</i> Cell Culture System, Induced to Differentiate into Xylem Tracheary Elements	58
	4.1.4 Mis-Regulation of <i>PttMAP20</i> Suggests a Function in Cellulose Microfibril Angle and Xylem Cell Dimension in <i>Populus</i>	61
	4.1.5 Summary of MAP20 Function in <i>Arabidopsis</i> and <i>Populus</i>	72
4.2	MYB103 Is Required for Syringyl Lignin Biosynthesis in <i>Arabidopsis</i> Inflorescence Stems (Paper III)	74
4.3	Analytical Pyrolysis, Coupled with Gas Chromatographic / Mass Spectrometric Separation, as a High-Throughput Method for Chemical Characterization of Lignocellulosic Plant Material (Paper IV)	78
5	Conclusions and Future Perspectives	81
5.1	Main Conclusions	81
5.2	Outlooks and Future Research Directions	82
	References	83
	Acknowledgements	104

List of Publications

This thesis is based on the work contained in the following papers, referred to by Roman numerals in the text:

- I Manoj Kumar, Sergey Miroshnichenko, **David Öhman**, Ines Ezcurra, Björn Sundberg and Edouard Pesquet. MAP20, a Novel Plant Specific Stabilizing Microtubule Associated Protein (Manuscript).
- II **David Öhman**, Sergey Miroshnichenko, Delphine Menard, Manoj Kumar, Lorenz Gerber, András Gorzsás, Edouard Pesquet and Björn Sundberg. *AtMAP20* is specifically expressed in cell types with secondary walls and involved in cell wall composition and structure (Manuscript).
- III **David Öhman***, Brecht Demedts*, Manoj Kumar, Lorenz Gerber, András Gorzsás, Geert Goeminne, Mattias Hedenström, Brian Ellis, Wout Boerjan and Björn Sundberg (2013). MYB103 is required for *FERULATE-5-HYDROXYLASE* expression and syringyl lignin biosynthesis in Arabidopsis stems. *The Plant Journal* 73, 63–76.
- IV Lorenz Gerber, **David Öhman**, Viet Mai Hoang, Thai Bui, Manoj Kumar, Philippe Ranocha, Deborah Goffner and Björn Sundberg. High-throughput microanalysis of large ligno-cellulosic sample sets by Pyrolysis-Gas Chromatography/Mass Spectrometry (Submitted to *New Phytologist*).

**These authors made equal contributions.*

Paper III is reproduced with the permission of the publisher.

The contribution of **David Öhman** to the papers included in this thesis was as follows:

- I David Öhman was involved in the planning and designing of experiments. He also performed experiments, including construction of transgenic plants and plant growth experiments. He participated in data analysis and writing, formatting and proofreading the manuscript. Concerning tables and figures, he contributed mainly to the bioinformatical part.
- II David Öhman planned and designed experiments. He isolated and performed molecular and phenotypic characterization of mutants, performed expression analysis and grew plants for supply of experimental material. He did wet chemical analysis and co-ordinated other chemical characterizations with collaborators. He analysed results and made a first draft of the manuscript, including formatting and proofreading. He made large contributions in producing tables and figures and had a main responsibility in assuring the accuracy and reliability of their contents.
- III David Öhman planned and designed the experiments. He isolated and performed molecular and phenotypic characterization of mutants, was responsible for plant growth and supply of experimental material and performed wet chemical analysis and co-ordinated other chemical characterizations with collaborators. He analysed results and made a first draft of the publication, where main contributions included formatting tables and figures and compile everything into a proof to submit.
- IV David Öhman was involved in planning, designing and performing experiments. Main responsibility was in growing, characterizing, preparing and supplying plant material for chemotyping of mutants. He also participated in data analysis and writing and formatting the manuscript.

Abbreviations

+TIP	Microtubule plus end tracking protein
2D NMR	Two-dimensional nuclear magnetic resonance spectroscopy
ABC	ATP-binding cassette-like
AF	Actin microfilament
<i>At</i>	<i>Arabidopsis thaliana</i>
BiFC	Bimolecular fluorescence complementation
ChIP	Chromatin immunoprecipitation
CHX	Cycloheximide
CMF	Cellulose microfibril
CMT	Cortical microtubule
Co-IP	Co-immunoprecipitation
CSC	Cellulose synthase complex
CWM	Cell wall material
DEX	Dexamethasone
DR	Dominant repression
EMSA	Electrophoretic mobility shift assay
ER	Endoplasmic reticulum
F5H	FERULATE-5-HYDROXYLASE
FPA	Focal plane array
FT-IR	Fourier transform infrared
G	Guaiacyl/coniferyl
GT	Glucosyltransferase
H	<i>p</i> -hydroxyphenyl/ <i>p</i> -coumaryl
HG	Homogalacturonan
IF	Interfascicular fibre
JW	Juvenile wood
KO	Knockout
LAC	Laccase
M46RE	MYB46-responsive <i>cis</i> -regulatory element

MAP	Microtubule-associated protein
MASC	Microtubule-associated cellulose synthase compartment
MBD	Microtubule-binding domain
MCR-AR	Multivariate curve resolution by alternate least square
MFA	Microfibril angle
ML	Middle lamella
MT	Microtubule
MW	Mature wood
OE	Overexpression
OPLS-DA	Orthogonal projections to latent structures discriminant analysis
PCA	Principal component analysis
PCD	Programmed cell death
PCW	Primary cell wall
PM	Plasma membrane
PME	Pectin methyl esterase
<i>Pt</i>	<i>Populus trichocarpa</i>
<i>Ptt</i>	<i>Populus tremula</i> L. × <i>Populus tremuloides</i> Michx
PXV	Protoxylem vessel
Py-GC/MS	Pyrolysis-gas chromatography/mass spectrometry
RE	Radial expansion
RGI	Rhamnogalacturonan I
RGII	Rhamnogalacturonan II
S	Syringyl/sinapyl
SCW	Secondary cell wall
SmaCC	Small CESA compartment
SMRE	Secondary wall MYB-responsive element
SNBE	Secondary wall NAC binding element
SWN	Secondary wall NAC
SX	Secondary xylem
TE	Tracheary element
TFA	Trifluoroacetic acid
VC	Vascular cambium
VE	Vessel element
WT	Wild type
XET	Xyloglucan endotransglucosylase
XF	Xylem fibre
XG	Xyloglucan
XGA	Xylogalacturonan
XRD	X-ray diffraction
Y2H	Yeast two-hybrid

1 Introduction

In a world where fossil carbon is becoming limited and its use considered an environmental threat, alternative energy and material sources are becoming more attractive. Recent figures state that peak oil is already reached; *i.e.*, the global supply of petroleum has reached a maximum and is declining, whereas recovery has become more costly (Neff *et al.*, 2011). Therefore, to replace petrol, large investments are now made in research and development of bioenergy and biofuels from sustainable resources (Yuan *et al.*, 2008). One key to green and clean energy is the source of the biomass itself.

As a renewable resource, wood is of outmost importance. Forests cover about 30% of the terrestrial surface (equivalent to about four billion hectares), and Earth is estimated to contain 0.4×10^{12} m³ of wood (Albersheim *et al.*, 2011). With an annual growth rate of 3×10^{10} tons from fixed carbon, wood is also a major sink for CO₂. Not surprisingly, wood is considered one of the most important world trade products, providing energy, building material, pulp and paper and other materials (Plomion *et al.*, 2001).

Cellulose is the major compound in wood; it is used to produce pulp and a diverse range of materials, such as paper, packaging and tissues (Wertz *et al.*, 2010). It is also the major raw material for ethanol production from lignocellulose; although, this is not yet taking place on a significant commercial scale (Sims *et al.*, 2010).

After cellulose, lignin is the second most abundant biopolymer in wood. Large volumes of lignin are extracted from wood, in order to produce pulp. Lignin has mainly been considered as a rest product, used for industrial heating, but with the emerging vision of wood biorefineries, the commercial value of lignin is now heavily researched. Lignin is used on a small scale for several products, *e.g.*, in cement additives, as an environmentally sustainable dust suppression agent in roads and as a raw material for making phenols and vanillin; more lignin-based products are likely to be seen in the near future

(Arato *et al.*, 2005; Fellows *et al.*, 2011; Zakzeski *et al.*, 2012). Highly lignified wood is also durable and an excellent fuel, because lignin has a higher energy value than cellulose (Novaes *et al.*, 2010).

The large impact of wood as a global renewable raw material emphasizes the importance to study wood formation and lignocellulose biosynthesis in wood fibres. It is of particular interest to unravel genetic and molecular mechanisms regulating biomass production and other traits of energy crops to improve yield and value by molecular breeding (Demura & Ye, 2010). A key strategy is to identify genes involved in developmental programs and metabolic pathways for biosynthesis of cell walls. This thesis aims to shed light on some aspects of cellulose and lignin biosynthesis. It highlights how applied scientific problems can be addressed with basic scientific questions, by functional analysis of genes postulated to have a role in the production of biomass in trees, such as *Populus*, as well as the herbaceous model plant *Arabidopsis*.

1.1 Formation and Characterization of Wood

Wood, or secondary xylem (SX), in angiosperms is mostly composed of lignocellulosic xylem fibres (XFs), providing strength and support to woody stems; vessel/tracheary elements (VEs/TEs), facilitating long-distance water and nutrient transport from source to sink tissue and xylem ray parenchyma cells, facilitating short-distance transverse conduction and storage (Plomion *et al.*, 2001). The remarkable feature of wood enables a tree, with a life-span of decades up to centuries, to grow extensively in diameter and height.

The complete maturation of a SX cell is mainly a result from four major developmental steps:

1. Cell division in the vascular cambium (VC) and the formation of middle lamella (ML), cementing adjoining cells together.
2. Radial expansion (RE) and/or intrusive elongation of cells; *i.e.*, stretching of a thin and flexible primary cell wall (PCW) inside the ML.
3. Ordered deposition of a multi-layered secondary cell wall (SCW) and lignification of cell wall.
4. Programmed cell death (PCD).

1.1.1 Cambial Growth

SX and secondary phloem tissues originate from the activity of a cylindrical lateral meristem, the VC. The VC develops from joining fascicular cambia in the vascular bundles, thereby forming interfascicular cambia (Raven *et al.*, 1999; Déjardin *et al.*, 2010). The VC is made up of two different types of initial cells; fusiform initials and ray initials. The elongated fusiform initials

divide periclinally and produce SX towards the xylem side that differentiate mainly into axially elongated water-conducting VEs and supporting XFs. The radial isodiametric ray initials develop into radially elongated xylem ray parenchyma cells. Anticlinal (radial) cell divisions give rise to new fusiform initials and take place in synchrony with the increase in trunk diameter. Typically, the final composition of cell types (v/v) in *Populus* SX is usually 33% VEs, 53–55% XFs and 11–14% ray parenchyma cells (Mellerowicz *et al.*, 2001).

1.1.2 Differentiation of a Wood Cell

The developing SX cells expand radially, and XFs also elongate longitudinally by intrusive tip growth (Plomion *et al.*, 2001; Déjardin *et al.*, 2010). Once this process is completed, the SX cell starts to deposit the SCW inside the PCW. The SCW consists of up to three different layers, denoted S_1 , S_2 and S_3 , where cellulose β -(1,4)-glucan chains coalesce into cellulose microfibrils (CMFs). These are arranged in ordered, parallel-aligned arrays. On a larger scale, CMFs bundle into macrofibrils. CMFs are further embedded in matrix hemicelluloses (mainly xylan in angiosperms), which cross-link with cellulose and lignin to strengthen the SCW (Scheller & Ulvskog, 2010). During the course of SX development, lignin (an aromatic heteropolymer) is synthesized through a temporally and spatially regulated pattern (Boerjan *et al.*, 2003; Vanholme *et al.*, 2010). It is first deposited in the cell corners and progresses through the ML, PCW and SCW. Lignin forms a large, three-dimensional polymer that to a large extent is synthesized from syringyl (S) and guaiacyl (G) monomers. The lignin polymer associates with the hemicellulose matrix to provide compressive strength and water impermeability to plant cell walls. VEs and XFs undergo PCD through autolysis, accompanied by vacuolar rupture, as a last step in their differentiation (Bollhöner *et al.*, 2012). The onset of PCD in VEs and XFs is temporally separated. VEs undergo rapid deposition of SCWs and cell death to ensure a rapid maturation of a functional, water-conducting cell, whereas PCD in XFs is initiated much later, and they also disintegrate their cellular contents at a slower pace.

1.1.3 Mechanics and Chemistry of Wood

Mechanical and chemical properties of wood are to a large extent determined by the S_2 layer in XFs, because this makes up most of the woody biomass. Mechanical strength and stiffness are largely determined by the angle of CMFs with respect to the XF longitudinal axis. The CMF angle (MFA) varies between the SCW layers. In S_2 , the MFA is always right-handed and usually between 5–30° (Barnett & Bonham, 2004; Clair *et al.*, 2011). With increasing

MFA, wood becomes less stiff and its XFs exhibit lower tensile strength (Burgert & Keplinger, 2013). Tensile strength, in this sense, refers to the force required to pull, *e.g.*, a longitudinal–radial wood section, from both ends in opposite direction until it eventually ruptures and breaks, whereas tensile stiffness refers to the force required to displace (stretch) a similar wood section over a unit length. The MFA in wood formed from a young VC (referred to as juvenile wood, JW) is usually high, as compared to the MFA formed from an older VC (referred to as mature wood, MW). JW is normally formed during the first 10–20 years of a tree’s life, and the high MFA provides flexibility during growth and environmental stresses. Because of its lower stiffness and altered mechanical properties, however, presence of JW in only a part of a board reduces its usefulness as building material due to distortions. But JW is still beneficial for use as biofuels, pulp and paper, pellets and briquettes and particle and fibre boards (Antizar–Ladislao & Turrion–Gomez, 2008; Hinchee *et al.*, 2009; Stelte *et al.*, 2012). There are several different methods to measure the MFA, such as polarized light microscopy, pit angle measurement and X-ray diffraction (XRD). XRD is a preferred method if the aim is to have an average estimate of MFA from a larger population of SX cells (Burgert, 2006).

Chemically, wood is composed of 40–50% cellulose, 25–35% lignin and approximately 25% hemicellulose, with small amounts of pectin and proteins (Albersheim *et al.*, 2011). Traditionally, the chemical composition of wood has been analysed by means of wet chemistry (Rowell *et al.*, 2012). This includes different types of extractions from milled wood and analysis of desired wood components. Since wood is made up of multiple complex biopolymers, the extraction procedure is never complete and the extracted fractions are not pure. It is clear that modification of the cell wall structure in a mutant plant may result in an altered extractability of cell wall polymers, which then complicates comparison with wild type (WT) plants. In addition to wet chemistry, several complementary methods for chemical characterization of all components of a wood sample in the same analysis were used throughout the work of this thesis. These include analytical pyrolysis with gas chromatographic separation (Py-GC/MS), Fourier transform infrared (FT-IR) microspectroscopy and two-dimensional nuclear magnetic resonance spectroscopy (2D NMR). All these methods can be used to give an overall picture of every cell wall component from the same sample.

Py-GC/MS is a rapid, robust and highly reproducible method for chemical characterization of lignocellulose (Meier *et al.*, 2005; Gerber *et al.*, 2012). It provides a chemical fingerprint of the sample that can then be subjected to multivariate analysis, such as principal component analysis (PCA) and/or orthogonal projections to latent structures discriminant analysis (OPLS-DA),

capable of discriminating different samples (*e.g.*, transgenic from WT origin). The procedure for Py-GC/MS analysis requires drying, ball-milling, loading of a small sample amount in an auto sampler and about 20 min analysis. A data processing pipeline, based on multivariate curve resolution by alternate least square (MCR-AR) and automated group-wise peak identification and assignment, was recently established (Gerber *et al.*, 2012). This protocol enables the user to process multiple chromatograms in parallel, instead of the time-consuming sequential manual curation employed previously. This method development solved the last bottleneck to use Py-GC/MS for high-throughput characterization of lignocellulosic materials. In addition, the protocol also employs an automated Py-GC/MS data analysis approach, where pyrolytic degradation products are grouped according to a broad class of precursors, *e.g.*, *p*-hydroxyphenyl (H), G and S units and carbohydrates.

Similar to Py-GC/MS, FT-IR spectroscopy provides a chemical fingerprint of the sample and is an alternative high-throughput method for chemical characterization of wood powder and discrimination of cell wall composition against samples, using OPLS-DA (Gorzsás *et al.*, 2011; Gorzsás & Sundberg, 2014). Though, since many of the characteristic bands for the major cell wall components are overlapping in the FT-IR spectra, it is often difficult to determine the type of polymer that differs between samples (Gorzsás *et al.*, 2011). FT-IR microspectroscopy can also be used to acquire spatially resolved analysis of tissue sections (Gorzsás *et al.*, 2011). Combined with a focal plane array (FPA) detector, a large number of highly resolved spectra across the tissue section can be collected simultaneously, and XFs, VEs and ray parenchyma cells can be analysed individually in a feasible way. Thus, it can be evaluated if a cell wall mutant is modified in all cell types or only in specific ones.

Chemical analysis of the complete wood sample can also be performed by solution-state 2D NMR of the dissolved sample. In combination with multivariate analysis, a chemical fingerprint can be obtained that is more informative, as compared to Py-GC/MS and FT-IR (Hedenström *et al.*, 2009). Comparison of samples with OPLS-DA allows for visualization of highly informative loadings plots, showing compounds discriminating the samples.

1.2 Primary Cell Walls and Their Expansion in Developing Wood

Typically, the PCW of a SX cell resembles a fibreglass-like composite material, consisting of randomly or longitudinally oriented CMFs, embedded in a matrix of complex polysaccharides, such as hemicelluloses and pectin

(Mellerowicz *et al.*, 2001; Plomion *et al.*, 2001; Cosgrove, 2005; Cosgrove & Jarvis, 2012). In *Populus*, it is estimated to contain 47% pectin, 22% cellulose, 18% hemicelluloses (*e.g.*, xyloglucan, XG), 10% protein and 3% of other material (Mellerowicz *et al.*, 2001). In developing SX, it is synthesized as the cell expands during the stages of cell division and RE and is designed to resist the turgor pressure (wall stress) within the cell. Maintaining control over this complex physical process is important for cell expansion and shaping (Szymanski & Cosgrove, 2009).

Cell expansion is driven by turgor pressure that exerts a uniform, outward-pushing force, whereas CMFs in the wall exert a counteracting, resistance force (Crowell *et al.*, 2010b). Therefore, expansion of PCWs involves wall stress relaxation (wall loosening) and expansion through a process known as polymer creep; *i.e.*, an irreversible extension where CMFs and matrix polysaccharides slowly slide within the wall, thereby increasing cell wall surface area (Cosgrove, 2005). The transversely oriented CMFs provide high tensile strength in the radial direction; thus, permitting anisotropic (directional) growth in the longitudinal direction (Geitmann, 2010). As expected, CMFs are transversely oriented to the cell longitudinal axis in elongating *Arabidopsis* root cells (Sugimoto *et al.*, (2000). In addition, Baskin *et al.* (1999) concluded that CMFs regulate the direction, but not the degree, of cell elongation. This led Baskin *et al.* (2004) and Baskin (2005) to further suggest that global, rather than local, alignment of CMFs in neighbouring cells determines the degree of growth anisotropy. This is a modification of “Green’s hypothesis” (Green, 1965), originally based on the older “multinet growth hypothesis”, which has stood the test of time (Preston, 1982). They are both still relevant today in revised and updated models to explain the rationale behind the rise of the PCW, which is often described as a polylamellated, helicoidal-like structure (Evert, 2006); *i.e.*, multiple layers of CMFs deposited at multiple angles.

Cell expansion can occur by symplastic growth (neighbouring cells growing together) or by intrusive growth (moving past one another) (Mellerowicz & Sundberg, 2008). Intrusive growth is rather uncommon, but important for elongation of fusiform initials and differentiating SX cells. During intrusive growth, the XF tip penetrates the pectin-rich ML of neighbouring cells. Anticlinal divisions in the VC are oblique and therefore shorten the length of the fusiform initial (Larson, 1994; Fromm, 2013). The initial cell then elongates by intrusive tip growth in between each anticlinal division. This is of importance, since the lengths of developing VEs and XFs are dependent on the length of the initial cell. Whereas the length of a VE reflects the length of the initial, the developing XF will continue to elongate by intrusive tip growth (Larson, 1994; Fromm, 2013). Thus, SX cells develop by a balance of intrusive

and symplastic growth. As such, XFs expand radially in diameter by symplastic growth, but they rely fully on intrusive growth when elongating longitudinally at their tips (Larson, 1994; Fromm, 2013). Conversely, VEs only expand radially.

Cell expansion is promoted by pH-dependent wall-loosening expansins that are bound to the wall and aid into the irreversible wall extension, without hydrolysing the wall polymers (Cosgrove, 2005). The mechanism is termed acid growth, but its mechanism remains largely unknown. The physical properties of the PCW are determined by cross-links and non-covalent bridges between the XG and pectin matrix and the CMFs (Cosgrove, 2005). Integration of newly secreted XG into the matrix is mediated by XG endotransglucosylase (XET), an enzyme that specifically cuts the XG backbone and re-joins a glycosidic bond with the free end of another XG chain. XET activity has been suggested to catalyse the rapid cell expansion observed during PCW restructuring, through reversible and irreversible loosening of wall material (Rose *et al.*, 2002). Interestingly, when XET activity was increased by overexpression (OE) of *PttXET16-34* across SX in transgenic *Populus* trees, it resulted in increased diameter in VEs, but not in XFs (Nishikubo *et al.*, 2011).

Pectin is a complex and heterogenous group of polysaccharides that are important determinants for PCW mechanical and porosity properties (Willats *et al.*, 2001), along with cell expansion and cell–cell adhesion (Mellerowicz *et al.*, 2001; Cosgrove, 2005; Harholt *et al.*, 2010). Pectin consists of distinctive domains known as homogalacturonan (HG), xylogalacturonan (XGA), rhamnogalacturonan I (RGI) and rhamnogalacturonan II (RGII). The carboxyl group of HG can be either methylesterified or freely available for Ca^{2+} -crosslinking, depending on the activity of pectin methyl esterase (PME). When pectin is Ca^{2+} -crosslinked, it forms stiff gels that push CMFs apart during wall expansion and cement cells together through the ML. Thus, the balance between methylated and demethylated pectin is important for wall flexibility and cell–cell adhesion of the growing SX cell (Mellerowicz & Sundberg, 2008). It was recently demonstrated that *PttPME1*, encoding a major PME in SX tissues of *Populus*, acts as a negative regulator of both symplastic and intrusive growth for XFs and VEs (Siedlecka *et al.*, 2008).

Once the SX cell has attained its final shape and size, the multi-layered SCW is deposited inside the PCW. This involves a reprogramming of the cell wall biosynthesis machinery.

1.3 Exploring Genes Involved in Secondary Cell Wall Formation

To identify genes important for wood formation, a pioneering global expression profiling across different developmental zones of SX tissues in *Populus* was performed by microarray analysis (Hertzberg *et al.*, 2001). A number of genes with homology to *Arabidopsis* genes, influencing cellulose, hemicellulose and lignin biosynthesis, were found to be expressed during PCW and SCW formation. Further, the differential expression patterns of these genes, putatively involved in biosynthesis of major wall components, co-regulated with TFs and genes coding for various signalling molecules.

In *Arabidopsis*, several similar microarray experiments were later made to address candidate genes involved in SX biosynthesis. In a study by Oh *et al.* (2003), *Arabidopsis* inflorescence stems were induced to undergo enhanced secondary growth by decapitation. The authors discovered that about 20% of the transcripts (corresponding to 1658 genes) were differentially expressed, compared with control, and therefore potentially involved in SX formation. Ko *et al.* (2004) applied an artificial weight on an immature *Arabidopsis* inflorescence stem to promote SX formation. They also placed agar blocks containing auxin on top of decapitated inflorescence stems, thereby inducing SX formation. About 700 genes were found to be differentially expressed in tissues stimulated to form secondary growth; more than 40% of the up-regulated (> 5-fold) genes were encoding TFs and proteins responsible for signalling by extracellular molecules. Ehling *et al.* (2005) used a microarray to explore differential expression patterns during the transition from primary to secondary growth in *Arabidopsis* inflorescence stems. They revealed many genes that they interpreted as involved in SX formation and cell wall biosynthesis. These represented, on the one hand, genes with known function, coding for, *e.g.*, TFs; in addition, genes involved in cellulose biosynthesis and the biosynthesis, transport and polymerization of monolignols were identified. On the other hand, the study also identified novel candidate genes, encoding enzymes in the shikimate and phenylpropanoid pathway, and TFs, potentially regulating interfascicular fibre (IF) and XF differentiation and maturation.

Brown *et al.* (2005) analysed genes highly co-expressed with two SCW cellulose biosynthesis genes; *CESA7* and *CESA8*. They initially produced a microarray data set across tissues of leaf, hypocotyl and four different stages of stem development in *Arabidopsis*. Through cluster analysis and profile filtering, 200 genes with expression profiles closely matching those of SCW *CESAs* were included for further study. In the next step, a publically available *Arabidopsis* root microarray data set with cellular resolution (Birnbaum *et al.*, 2003) was used to identify which genes out of the 200 selected candidates co-regulated with *CESA7* and *CESA8* in this data set. Finally, co-regulation of the

candidates with *CESA7* was mined in a large number of publically available microarray data sets through pairwise comparison with a two-gene scatterplot. From this data filtering, 16 candidate genes were selected and functionally analysed for collapsed VEs in the xylem, using T-DNA mutants. Seven of them gave a clear *irx* (short for *irregular xylem*) phenotype (*i.e.*, collapsed VEs) in their corresponding mutant plants and revealed several novel key players required for SCW formation. Among the identified genes were *COBL4*, putatively involved in cellulose biosynthesis, and *IRX7* (*FRA8*), *IRX8* and *IRX9*, which encode putative glucosyltransferases (GTs), involved in xylan biosynthesis.

In a parallel work, Persson *et al.* (2005) carried out a slightly different co-expression study, using regression analysis of public microarray data sets. They reported, in particular, on four candidate genes that strictly co-regulated with *CESA4*, *CESA7* and *CESA8*; thus, putatively influencing SCW biosynthesis. Analysis of their corresponding T-DNA mutants revealed that two of them exhibited *irx* phenotypes, accompanied by a reduction in cellulose. These were recognized as *irx8* and *irx13* (*IRX13* encodes FLA11). The remaining two, one encoding an unknown function protein (AT4G27435) and the other a CTL1-LIKE protein, did not show any aberrant stem anatomy. Interestingly, more than half of the top 25 candidate genes that co-regulated with *CESA7* in the study of Brown *et al.* (2005) were in common with the candidate genes that co-expressed with SCW *CESAs* in the study of Persson *et al.* (2005).

1.4 Cellulose Deposition and Its Dependency on the Cytoskeleton

1.4.1 Cellulose Biosynthesis

Cellulose is synthesized *in planta* by catalytic transmembrane-spanning cellulose synthases, encoded by *CESA* genes (Endler & Persson, 2011). These are organized as rosette-like hexamers of ≈ 25 nm in diameter, referred to as cellulose synthase complexes (CSCs), situated in the plasma membrane (PM) (**Figure 1**) (Kimura *et al.*, 1999). The cytoplasmic domain of the CSC has been demonstrated to contribute substantially to the overall size, in contrast to the smaller hexagonal structure, as observed by freeze-fracture techniques of the PM (Bowling & Brown, 2008). Given the size initially estimated of one CMF (≈ 3.5 nm), the CSC was calculated to contain 6×6 *CESAs*, each producing one β -(1,4)-glucan chain (Doblin *et al.*, 2002). Each subunit (containing six *CESA* isoforms) of the hexameric CSC was further hypothesized to be composed of at least three essential and unique *CESA* isoforms, as deduced

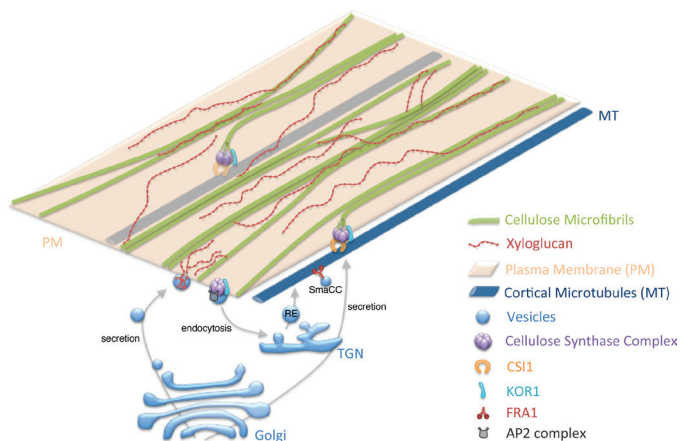


Figure 1. Simplified schematic representation of some important trafficking pathways and components for cell wall biosynthesis and organization. Reprinted from Bashline *et al.* (2014): Cell Wall, Cytoskeleton, and Cell Expansion in Higher Plants, *Molecular Plant*, 7(4), p. 592, by permission of Oxford University Press.

conflicting data on more precise estimates of the CMF size, obtained by NMR studies, challenges the classic 36-chain model and instead proposes a mechanism that is likely to produce only 18 chains in onion/quince (Ha *et al.*, 1998) or 15–25 glucose chains in celery (Kennedy *et al.*, 2007). A recent study by Fernandes *et al.* (2011) in spruce further suggested a 24-chain model, since a 36-chain model would produce a CMF that is larger than expected (≈ 3.8 nm). In their model, each subunit instead synthesizes four β -(1,4)-glucan chains, rather than six, and the CMF was also suggested to be rectangular-shaped and twisted. Therefore, the number of cellulose chains in one CMF might not be universally fixed across species.

To date, 10 *CESA* genes have been described in *Arabidopsis*, and a unified nomenclature system has been developed for cross-species comparison (Kumar *et al.*, 2009). In *Populus trichocarpa*, sequences from 18 putative *CESA* genes, encoding 17 proteins with non-redundancy in their amino acid sequence, have been identified (Djerbi *et al.*, 2005). *CESA* genes expressed during SX formation were first identified in a mutant screen where *Arabidopsis* inflorescence stems displayed collapsed walls of mature VEs. This genetic screen identified *CESA4*, *CESA7* and *CESA8* (*IRX5*, *IRX3* and *IRX1*) as being active during SCW cellulose synthesis (Turner & Somerville, 1997). Co-immunoprecipitation (Co-IP) assays (Taylor *et al.*, 2003), together with membrane-based yeast two-hybrid (Y2H) approaches (Timmers *et al.*, 2009), revealed interactions between the three SCW CESAs, and that they are non-redundant. Even though the exact number and stoichiometry of CESAs in each

from mutant analysis in *Arabidopsis* (e.g., Arioli *et al.*, 1998). Thus, a model where 36 independent β -(1,4)-glucan chains would be produced from the rosette to align into highly organized and crystalline CMFs was proposed by Delmer *et al.*, (1999). Though,

subunit of the rosette remain unknown, the secondary CESAs were suggested to contribute equally to a functioning CSC (Gardiner *et al.*, 2003).

The remaining *CESA* genes in *Arabidopsis* are believed to be associated with PCW biosynthesis (Burn *et al.*, 2002). Of these, *CESA6* was shown by mutations to be partially functionally redundant with *CESA2* and *CESA5* (*CESA6*-related genes), competing for its position in the CSC in *Arabidopsis* hypocotyl and root tissue (Desprez *et al.*, 2007; Persson *et al.*, 2007). Recent findings by Carroll *et al.* (2012), however, suggest that PCW and SCW CESAs are interchangeable and therefore not functionally different. Thus, the authors argued that it is possible that the CSC consists of mixed CSCs during the transition between PCW and SCW biosynthesis. Several attempts have been made to purify an intact and functional CSC. The closest achievement so far is based on an epitope-tagging approach against *CESA7*, yielding purified oligomers, but not an active complex, of SCW CESAs under non-denaturing conditions (Atanasov *et al.*, 2009). Interestingly, no other protein appeared to be attached to the purified CSC.

One of the first steps in cellulose biosynthesis is thought to occur when the catalytic subunits of the *CESA* proteins are utilizing the sugar donor UDP-glucose to polymerize it into β -(1,4)-glucan chains (Guerriero *et al.*, 2010). This substrate, *per se*, is formed by either the cytosoluble enzyme UDP-glucose pyrophosphorylase, from UTP and glucose-1-phosphate, or the enzyme SUCROSE SYNTHASE (SUSY), which forms UDP-glucose from sucrose and UDP. It has further been proposed that a cytosolic/membrane-bound isoform(s) of SUSY is directly involved in channelling UDP-glucose to the catalytic site, facing the cytoplasm (Amor *et al.*, 1995; Fujii *et al.*, 2010). Another membrane-localized β -1,4-glucanase, KORRIGAN (KOR) (**Figure 1**), has also been suggested to be directly associated with the CESAs to remove non-crystalline glucan chains and/or relieve tensional stress of the growing polymer (Williamson *et al.*, 2002; Somerville, 2006).

COBRA (COB) and COB-LIKEs (COBLs) have been linked to aspects of cellulose biosynthesis. Mutations in *COB* alter directional cell expansion in roots and reduce the amount of crystalline cellulose in cell walls in the root growth zone (Schindelman *et al.*, 2001). Both COB and COBLs are required for the oriented deposition of CMFs in cells undergoing rapid elongation in developing organs and are regarded as key regulators of diffuse anisotropic expansion (Roudier *et al.*, 2002). Moreover, mutations in *BRITTLE CULM1* in rice (Li *et al.*, 2003) and *BRITTLE STALK2* in maize (Sindhu *et al.*, 2007) (both encoding COBLs) resulted in cell wall defects, accompanied by reduced cellulose content. One obvious phenotype was organ brittleness, *e.g.*, weaker stems that snapped easily when bent. Phylogenetically, these genes are

orthologous to *Arabidopsis COBLA*, which is expressed in secondary tissues, and co-regulates with secondary *CESAs* (Brown *et al.*, 2005).

1.4.2 Cellulose Microfibrils Align with Cortical Microtubules

It has long been known that the direction of cortical microtubules (CMTs) is parallel with the deposition of CMFs (Green, 1962). From this observation, it was implied that microtubules (MTs) directly guide self-propelled CSCs (*i.e.*, the rosette complex is pushed forward by the biosynthesis of cellulose itself) to move along the PM (**Figure 1**), the so-called MT–CMF alignment hypothesis (Wasteneys, 2004; Lloyd & Chan, 2008; Nick, 2008). Originally, this idea was further represented by two models. The first one, known as the monorail model (Heath, 1974), proposed that CSCs are physically linked to CMTs, which directly influence their movements. The second model, known as the guardrail (or bumper rail) model (Giddings & Staehelin, 1991), stated that CMTs are merely delimiting the pathway for passive movements of CSCs in between individual CMTs; thus, not directly interacting with them. Nevertheless, CMTs are generally believed to define the direction of CMF deposition, which *per se* controls anisotropic cell wall expansion (Nick, 2008).

Evidence has been obtained for and against the MT–CMF alignment hypothesis. Direct proof for the hypothesis was obtained by spinning disk confocal microscopy, where Paradez *et al.* (2006) demonstrated movements of CSCs along CMTs in etiolated hypocotyl cells of *Arabidopsis*. For individual fluorescent tracks, they also discovered that the motilities of CSCs were bidirectional. This indicates active guidance of two linear arrays of CSCs that run alongside of one CMT, rather than directly on top of it. In further support of the alignment hypothesis, DeBolt *et al.* (2007a) found that drug treatments with morlin, which disrupts the CMT array, caused reduced CSC movement. Moreover, when Fisher & Cyr (1998) treated tobacco protoplasts with isoxaben, which inhibits cellulose biosynthesis, CMTs became disorganized. The effect was reversible, implying that ordered CMFs are providing spatial cues for CMT organization. This prompted the authors to propose bidirectional cross-talks between the CMF and CMT network; a refinement of the alignment hypothesis. Evidence against the alignment hypothesis was presented by Baskin *et al.* (1999) and Sugimoto *et al.* (2000), who found that the CMT–CMF parallelism is uncoupled in the late elongation zone of roots. As cell elongation rate started to decline, CMTs gradually shifted from a predominantly transverse to an oblique and finally longitudinal orientation, whereas CMFs remained transverse; thus, implicating that the mechanism controlling growth rate is independent of CMT and CMF orientation. In another study, DeBolt *et al.* (2007b) reported that application of 2,6-

Dichlorobenzonitrile (DCB), a cellulose biosynthesis inhibitor, rapidly disrupted CSC motility, without affecting MT organization. Furthermore, Paradez *et al.* (2006) also observed in their study that CSCs actively continued their movements in aligned trajectories even after CMTs had been disrupted by oryzalin (an MT-destabilizing drug). This led them to conclude that CMTs might indeed transmit cues for the direction of CSC movement, but are not required for their motilities *per se*. Similarly, earlier data from an *Arabidopsis* root epidermal cell that exhibited radial swelling, caused by drugs and/or a mutation, also demonstrated that newly deposited CMFs can resume a parallel, transverse alignment in their trajectories, despite the absence of a pre-existing template of either transversely, well-organized CMTs or well-ordered CMFs (Himmelspach *et al.*, 2003; Sugimoto *et al.*, 2003). This suggests that, at least in some cases, CMT organization and CMF alignment are independent arrays, and that anisotropic expansion of the PCW is regulated by some other mechanism. Clearly, the relationship between cytoskeletal organizations, cellulose biosynthesis and cell morphogenesis is not as straightforward as previously thought when the alignment hypothesis was first launched. Moreover, the idea of a scaffold complex, or physical linkage molecule, actively interconnecting the CMTs with CSCs, challenges the passive guardrail model and prompts for further investigations to identify candidates for a hypothetical CMT–CSC linker (Lloyd, 2006).

Baskin (2001) argued for a template-incorporation model, where a newly produced CMF attach to a CMT-oriented scaffold made of protein(s) or polysaccharide(s). This scaffold was postulated to be situated in the cell wall and interlinked with PM proteins, either directly or through mediators, in a complex. It was further suggested to be able to rotate, thereby providing orientation for the CMFs that are continuously formed and aligned, as CSCs are guided by CMTs via the scaffold complex. In this model, established CMFs can continue to be deposited in the same orientation as the scaffold, regardless of whether organized CMTs remain in place or not, as hypothesized by Baskin (2001). Nevertheless, CSCs would still be dependent on CMT organization to change direction of their trajectories.

An alternative model for CMF patterning has been proposed in a series of publications by Emons and co-workers (Emons & Mulder, 1998, 2000; Emons *et al.*, 2002). This model is mainly built from observations of helicoidal cell walls in root hairs, where the CMT–CMF parallelism was not apparent (Emons, 1982). Briefly, it was hypothesized that CMFs self-align by exploiting the geometrical constraints imposed by the shape of the cell. This is best illustrated as wrapping strings with constant width around a cylinder (Emons, 1994). Emons *et al.* (2007) later reasoned that the ability of CSCs to self-align,

without any obvious guidance, could be a default mechanism employed in certain plant cell types and/or under certain conditions. Though, in most cell types, the CMT-driven guidance mechanism dominates.

MTs, together with actin microfilaments (AFs), have also been suggested to have a role in the transport of newly assembled CSCs and their insertion into the PM (Wightman & Turner, 2010). Despite that the AF and MT cytoskeletons have traditionally been regarded as two distinct networks with different functions in the cell cortex, recent live cell imaging studies by Sampathkumar *et al.* (2011) suggest a dynamic interaction and dependence between the two networks. For instance, Sampathkumar *et al.* (2013) noticed that organization of AFs in etiolated *Arabidopsis* hypocotyls regulates CSC delivery rate to, and lifetime at, the PM, affecting cellulose biosynthesis. Though, organization of the AF cytoskeleton had no effect on the targeted insertion of CSCs into the PM at sites where CMTs were present; *i.e.*, the AF cytoskeleton does not impact specific positional insertions of CSCs in the PM. Instead, MTs are believed to carry out that task (Wightman & Turner, 2010). Altogether, Sampathkumar and co-workers concluded that the AF cytoskeleton in plant cells indirectly governs cellulose deposition and cell wall patterning.

AFs have also been suggested to be involved in the insertion of newly synthesized CSCs. From studies of PCW biosynthesis, it was shown that CSCs are targeted and delivered to the PM either directly from Golgi bodies or from small CESA compartments (SmaCCs) (**Figure 1**) (Gutierrez *et al.*, 2009), also denoted MT-associated cellulose synthase compartments (MASCs) (Crowell *et al.*, 2009). Crowell *et al.* (2009, 2010a) and Gutierrez *et al.* (2009) argued for a model where AFs are required for the motility and distribution of these Golgi bodies, as well as the proper global organization and distribution of CSCs in the PM. CMTs were proposed to govern the fine-scale targeting of CSC delivery to the PM, but not their insertion *per se*. The authors further reasoned that SmaCCs/MASCs play a pivotal role in the recycling of old CSCs from the PM. During SCW biosynthesis of VEs in *Arabidopsis* roots, Wightman & Turner (2008) also observed that AF cables (although, they were thicker) accounted for the rapid and unidirectional trafficking of CSC-containing organelles; *i.e.*, same as for PCWs. AFs, rather than CMTs, however, appeared to mark the targets for CSC insertion into the PM. The authors further concluded that CMTs are more likely essential for maintaining the replenishment of CSCs in the PM. Taken together, the mechanism for CSC delivery to the PM appears to differ between PCW and SCW formation.

1.4.3 Microtubule Structure, Dynamic Instability and Reorientation

The undisputable role of CMTs in guiding CSCs and in patterning of CMFs directs the interest to the regulation of the CMT network. MTs can be regarded as hollow cables with a diameter of 25 nm built by polymers of α - and β -tubulin (TUA and TUB) heterodimers (Waterman–Storer & Salmon, 1997). The tubulin gene family is rather heterogenous in plants; *Arabidopsis* contains six *TUA* and nine *TUB* genes, whereas a relatively large suite of eight *TUAs* and 20 *TUBs* is found in *Populus*, as surveyed by Oakley *et al.* (2007). In the same study, it was concluded that both *TUAs* and *TUBs* comprise distinct isoforms, some displaying high expression in SCW-forming tissues with the most abundant tubulin expression localized to developing XFs.

CMTs in plants can be regarded as a highly dynamic population of polymers (Dixit & Cyr, 2004a) that disassembles in the cold (Nick, 2012). In contrast to animal cells, these organize into specific arrays, without a centrally located centrosome as an MT-organizing centre; *i.e.*, they are self-organized. MTs are polarised through a γ -tubulin-containing nucleation (initiation) site, termed the lagging (minus) end, and a growing (plus) end (Ehrhardt & Shaw, 2006; Sedbrook & Kaloriti, 2008). The minus end comprises an α -subunit, whereas the plus end comprises a β -subunit. The tubulin heterodimers polymerize end to end in protofilaments, which form the basic structure of an MT (Wade & Hyman, 1997). These associate laterally in a ring of 13 protofilaments per MT, generating a spiral shape. MTs frequently experience cycles of polymerization of GTP tubulins, pausing and periods of rapid depolymerisation (catastrophe), caused by the loss of the GTP-cap. These cycles are collectively termed dynamic instability (Gardner *et al.*, 2013), and they couple with MT migration, known as hybrid treadmilling, along the PM. MT dynamicity should further be calculated as tubulin monomers gained or lost per unit time; *i.e.*, the sum of growth and shrinkage rates and the frequencies of catastrophe and rescue events (Abe & Hashimoto, 2005). The switch between catastrophe/shrinkage and growth (rescue) is mainly regulated by available amounts of free energy (in the form of GTP), the pool of tubulin monomers (Wade & Hyman, 1997) and, importantly, MT-associated proteins (MAPs) (Ivakov & Persson, 2013), as discussed in detail later in this thesis.

Growing MTs frequently encounter existing MTs, causing certain pre-determined events to occur (Ehrhardt, 2008). These are necessary for bundling and stabilizing MT polymers, in order for them to reorient into an organized and functional CMT array. A shallow-angled collision between a growing plus end and an existing MT results in bundling (zippering), whereas a steep-angled collision results in either a catastrophe or, less commonly, a crossing over of MTs (Dixit & Cyr, 2004b). Positioning of new nucleation sites beneath the

PM, in close association with the cell wall, secures that nascent MTs can orient and stabilize across the cell cortex. Severing events, by the protein katanin, is another MT-destabilizing process thought to be important for transition into an aligned array. For instance, Wightman & Turner (2007) showed that severing events occur almost exclusively at sites where one MT treadmills over another or a bundle. Thus, severing activity provides, on the one hand, a mechanism that efficiently removes unaligned MTs (*i.e.*, MTs not oriented with the majority) and, on the other hand, increased MT density. This favours array alignment and is likely to be an essential component distinguishing a net-like from an aligned MT array (Wightman & Turner, 2007, 2008).

Interestingly, CMT arrays are known to undergo oscillating rotations in *Arabidopsis* hypocotyl epidermal cells, putatively accounting for the multi-angled, polylamellated PCW observed (Chan *et al.*, 2007). These rotary movements translate into transverse, oblique and longitudinal CMTs, occurring simultaneously from the inner- to outer-facing epidermal PCW layer. It was concluded by Chan *et al.* (2010) that the clockwise, or counter clockwise, alignment of these MTs influences CESA trajectories, which affect wall lamellation pattern and overall texture (as deduced from GFP-CESA3). The authors also discovered that the trajectory rate of GFP-CESA3, *per se*, was uncoupled from MT rotation. In a follow-up study, Chan *et al.* (2011) further concluded that, in light-grown *Arabidopsis* hypocotyls, the alignment of CMTs and CMFs at the inner epidermal PCW is independent from the pattern of the outer PCW. Moreover, reorientation of the net alignment of CMF trajectories also occurs in elongating root cells, as demonstrated with live cell fluorescence confocal microscopy by Anderson *et al.* (2010). In contrast to hypocotyl cells, however, they concluded that CMFs are always deposited transversely and passively reorient towards the longitudinal axis (*i.e.*, no 360° rotation), and that this is rather caused by strain from turgor pressure driven cell expansion. A polylamellated PCW is also better adapted to resist straining forces from multiple directions during anisotropic cell expansion, accordingly.

Taken together, plant MT arrays are dispersed in nature and focus has been on identifying key proteins that interact with and regulate their spatial and dynamic properties (Wasteneys, 2002). Proper regulation of cellulose biosynthesis and wall patterning requires an aligned CMT array. This, in turn, is critical to determine the MFA.

1.4.4 Microtubule Mutants Display Twisting and Modified Microfibril Angle in Their Cell Walls

Twisting (*i.e.*, helical and skewed growth) of *Arabidopsis* seedlings growing on plates *in vitro* has been observed for mutants in *TUA* and *TUB* genes. These

have left- or right-handed (S- and Z-form, respectively) helical MT array organizations along the longitudinal axis of the plant, rather than transverse arrays, which is normally required for straight growth in rapidly expanding cells (Thitamadee *et al.*, 2002; Ishida *et al.*, 2007). The mechanism causing left- or right-handed CMT arrays in tubulin mutants remains to be identified. A common observation, however, is that tubulin mutants that twist either to the left or right have CMT arrays of opposite handedness; *i.e.*, left-handed helical twisting results from right-handed helical CMT arrays and *vice versa* (Hashimoto, 2013). Another notion is the causal relationship of more stable CMTs in left-handed arrays, whereas right-handed display more dynamic CMTs (Abe & Hashimoto, 2005). Though, it is still not clear how MT dynamics are related to handedness.

MT mutants have also been observed to be affected in MFA of the SCW. A study in *Eucalyptus* by Spokevicius *et al.* (2007) demonstrated that misregulation of *EgTUB1* caused an alteration in the MFA of nascent CMFs. Down-regulation of *EgTUB1* was associated with increased MFA, whereas up-regulation caused a decrease. In line with these observations, Qiu *et al.* (2008) studied global gene expression in TW in branches of *Eucalyptus* and discovered that expression of *EgTUB1*, along with some genes encoding FLAs, showed a strong negative correlation with MFA.

1.5 Microtubule-Associated Proteins – MAPs

1.5.1 MAPs Affecting Primary Cell Wall Expansion

MAPs have emerged as important and direct regulators of CMT bundling and cross-linking in plant cells; thus, playing significant roles in patterning of CMFs in SCWs of a SX cell (Oda *et al.*, 2005; Hamada, 2007; Kaloriti *et al.*, 2007; Oda & Fukuda, 2012b). A plant MAP is defined by its ability to physically bind to MTs and by its co-sedimentation with MTs *in vitro* (Chan *et al.*, 1999; Lloyd & Hussey, 2001; Sedbrook, 2004). In *Arabidopsis*, hundreds of candidate MAPs, established by bioinformatical analysis, in addition to novel ones, have already been enriched from cell suspension cultures and characterized biochemically by their ability to co-purify with MTs (Hamada *et al.*, 2013). The many aspects of MT dynamics, organization and function are reflected by the wide diversity of interacting MAPs in plants (Buschmann & Lloyd, 2008), most of them described from studies on cell division and PCW deposition during cell expansion and differentiation.

The *Arabidopsis* MICROTUBULE ORGANIZATION 1 (MOR1) was identified through its temperature-sensitive *mor1-1* mutant and found to be essential for CMT organization throughout plant development (Whittington *et*

al., 2001). In addition, MOR1 was observed to interact and modulate the activity of END BINDING1 (EB1), an MT plus end tracking protein (+TIP) (Kawamura & Wasteneys, 2008). Moreover, the +TIP MAP AUGMIN SUBUNIT8 (AUG8) is involved in a novel mechanism in promoting CMT reorientation, required for preventing cells from elongating in rapidly growing primary tissues, as presented by the work of Cao *et al.* (2013). Etiolated hypocotyls of *aug8* were longer and showed left-handed twisting of epidermal cell files, whereas shorter hypocotyls, without any twisting, were observed in AUG8-OE, as compared to WT. Likewise, light-grown roots were longer in *aug8*, showed left-handed helical twisting of epidermal cell files and skewed in one direction. On the contrary, AUG8-OE roots were shorter, displayed right-handed twisting and skewed in the other direction. In WT seedlings, expression of *AUG8* was higher in light-grown (where cell elongation is strongly inhibited by light) *vs* etiolated hypocotyls; thus, indicating that *AUG8* is repressed in rapidly elongating hypocotyls and induced when hypocotyl elongation declines or ceases.

Other important +TIP MAPs are SPIRAL1 (SPR1) and SPIRAL2 (SPR2) that have been suggested to control anisotropic cell expansion through MT-dependent processes (Nakajima *et al.*, 2004). Mutation in members of the *SPIRAL* (*SPR*) gene family results in right-handed helical twisting of epidermal cell files in roots and etiolated hypocotyls, according to a study by Furutani *et al.* (2000). Through genetic analysis, they also reasoned that SPR1 and SPR2 act on a similar process, but via different pathways, since the *spr1* and *spr2* phenotypes differ in affected tissues; *i.e.*, etiolated stem, hypocotyl and root for *spr1* phenotype *vs* petiole, petal and cauline leaf for *spr2* phenotype. The *spr1 spr2* double mutant further enhanced the anisotropic growth defects in these distinct tissues by a synergistic effect, according to the authors. Shoji *et al.* (2004) further noted that *spr2* exhibited a relatively milder MT defect phenotype than *spr1*, supporting a theory where other MAPs compensate for the function of SPR2. Interestingly, SPR1-OE led to enhanced resistance to MT-destabilizing drugs and increased hypocotyl elongation (Nakajima *et al.*, 2004), in contrast to AUG8-OE phenotype (Cao *et al.*, 2013). Therefore, the regulatory mechanisms of +TIP MAPs in the control of MT organization and orientation might function differently, but co-ordinately, in modulating anisotropic cell expansion.

Liu *et al.* (2013) found that WDL3 plays a negative role in light-regulated hypocotyl elongation by a mechanism that involves degradation of this MAP through the ubiquitin (UBQ) 26S proteasome dependent pathway in the dark. For light-grown hypocotyls, WDL3-RNAi lines were longer, whereas WDL3-OE lines were shorter and displayed a more stabilized CMT array, as compared

to WT. In contrast to AUG8 (Cao *et al.*, 2013), the length of etiolated hypocotyls in WDL3-OE and WDL3-RNAi lines were not obviously different from WT, reflecting the temporal separation in function of these two MAPs. In response to light treatment of etiolated hypocotyl cells, Liu *et al.* (2013) further showed that CMT reorganization was delayed in WDL3-RNAi lines and enhanced in WDL3-OE lines. Taken together, the work by Liu *et al.* (2013) demonstrates that the level of WDL3 in WT is present in light and absent in dark; thus, WDL3 is required for light-induced CMT reorganization from transverse to longitudinal orientation to prevent cells from elongating in the light.

Finally, MAP18 was demonstrated to be involved in regulating anisotropic cell expansion and CMT organization by destabilizing MTs, as assessed in a study by Wang *et al.* (2007). MAP18-OE seedlings grown *in vitro* on plates displayed pronounced helical handedness of epidermal cell layers and slanting/skewing of roots. The authors further noticed that CMTs in MAP18-OE hypocotyl cells were hypersensitive to oryzalin treatment, whereas CMTs in MAP18-RNAi were hyposensitive, in agreement with the proposed role of MAP18 as an MT destabilizer. Other MAPs, known to exert a destabilizing effect on the organization of CMTs, include MICROTUBULE-DESTABILIZING PROTEIN 25 (MDP25) (Li *et al.*, 2011b) and MDP40 (Wang *et al.*, 2012); the former was found to be a negative regulator of hypocotyl elongation, whereas the latter was found to be a positive regulator. Furthermore, as MDP25 responds to cytoplasmic levels of calcium to reorient the CMT array, MDP40 activity is regulated through a mechanism involving brassinosteroid phytohormone signalling to mediate hypocotyl growth.

Altogether, twisting features are characteristic of *Arabidopsis* MAP, as well as MT, mutants. In addition, application of low doses of MT-destabilizing drugs to WT seedlings reduces anisotropic growth, generating a phenotype similar to many MAP mutants (Nakamura *et al.*, 2004). In general, this causes left-handed twisting of elongating *Arabidopsis* epidermal cell files, reflecting right-handed helical net arrangement of CMT arrays. These defects are direct consequences of a disturbance in MT dynamics, affecting the proper organization/orientation of CMTs.

1.5.2 Bundling of Cortical Microtubules by MAPs – A Requirement for Secondary Cell Wall Formation

Local bundling of CMTs is normally required for determining the sites of SCW formation (Fujita *et al.*, 2011). The most potent candidates for MT bundling during SCW patterning are MAP65s, represented by a heterogeneous family of nine 65 kDa isomers in *Arabidopsis*. All MAP65s contain a domain capable of

binding to and bundle MTs *in vitro* (Sasabe & Machida, 2006). Though, they are believed to interact with MTs in slightly different manners and display slightly different intracellular localization patterns (Van Damme *et al.*, 2004; Mao *et al.*, 2005). A few observations support the idea that MAP65s are associated with SCW formation. Several *MAP65s* were up-regulated upon the induction of SCW formation in a *Zinnia elegans* TE differentiation system (Mao *et al.*, 2006). Moreover, *AtMAP65-8* co-regulated with SCW *CESAs* in an *Arabidopsis* TE differentiation system *in vitro* and was suggested to bundle CMTs in developing VEs (Kubo *et al.*, 2005). This is supported by *in silico* analysis of publically available microarray data sets in GeneCat (Mutwil *et al.*, 2008) and Genevestigator (<https://www.genevestigator.com/gv/plant.jsp>), which showed high expression of several *MAP65s* in basal *Arabidopsis* inflorescence stems. In contrast, Pesquet *et al.* (2010) concluded that no such co-regulation was observed in their *in vitro Arabidopsis* TE differentiation system upon induction by phytohormones. Functional analysis of *MAP65-8* to determine its role *in planta* is still missing.

1.5.3 MAPs Regulating Local Initiation and Prevention of Secondary Cell Wall Deposition

AtMAP70-5 belongs to a plant-specific multigene family encoding five isoforms of 70 kDa MAPs, where *AtMAP70-1* has been shown to stabilize MTs by means of its coil-coil domains (Korolev *et al.*, 2005). Interestingly, in a study by Korolev *et al.* (2007), *AtMAP70-5*, the most divergent member of the family, was able to form a complex, not only with itself, but also with *AtMAP70-1*. In the same study, OE of *AtMAP70-5* in *Arabidopsis* plants caused epidermal cell swelling, stunted growth and right-handed organ twisting, whereas RNAi caused reduced inflorescence stem length and diameter and abolished cell expansion. The authors concluded that *AtMAP70-5* is an MT stabilizer that acts synergistically with its binding partner, *AtMAP70-1*, to influence CMTs and cell wall patterning. Furthermore, among a screening of 200 putative MAPs investigated, Pesquet *et al.* (2010) could identify only one gene, *AtMAP70-5*, as being specifically up-regulated and associated with TE differentiation and SCW thickening in their *Arabidopsis* cell culture system. When modifying the expression of *AtMAP70-5* and *AtMAP70-1*, the authors observed that OE of *AtMAP70-5* and *AtMAP70-1* increased spiral patterns in TEs, whereas RNAi increased pitted patterns. OE of *AtMAP70-5* and *AtMAP70-1* in the same TE cell, however, resulted in more spiral patterns than single OE of either gene in separate cells, confirming the synergistic relationship between *MAP70-5* and *MAP70-1* and the idea that they are both required for normal SCW banding pattern and proper TE

development. Pesquet *et al.* (2010) further hypothesized that AtMAP70-5/AtMAP70-1 define the boundaries between spirals of SCW thickenings (where underlying CMTs bundle) and also define the free spaces in the characteristic TE cell. They thereby delimit the borders of each CMT bundle, forming arc-like divisions between adjacent CMT bundles.

MICROTUBULE DEPLETION DOMAIN 1 (MIDD1), a +TIP MAP, is also highly expressed during *Arabidopsis* TE SCW formation (Oda *et al.*, 2010). Similar to AtMAP70-5, it was implicated to regulate SCW patterning, preventing SCW deposition through local MT disassembly in PM domains of developing SCW pits. This MT depletion process is dependent upon the activity of KINESIN-13A, which depolymerises MTs both *in vitro* and *in vivo* (Oda & Fukuda, 2013b). MIDD1 binds and targets KINESIN-13A to CMTs. Furthermore, Oda & Fukuda (2012a) showed that locally activated ROP11 recruits and anchors MIDD1 at the PM beneath where future SCW pits are formed. Thus, it is plausible that a ROP11–MIDD1–KINESIN-13A complex serves as an important regulator of the dynamic interplay between PM domains and CMTs in SCW patterning (Oda & Fukuda, 2013a). Moreover, Oda & Fukuda (2012a) hypothesized that the function of AtMAP70-5 and MIDD1 is separated in time rather than space, because their actions are not antagonistic. These authors further suggested that MIDD1 promotes local depletion of CMTs, whereas members of the AtMAP70 family modify the shape of these MT-depleted domains and define the boundaries of SCWs. This suggests a tight relationship between the mode of action of AtMAP70-5/AtMAP70-1 and MIDD1 in regulating MT dynamics and SCW patterning in TEs. In agreement with Oda & Fukuda (2012a), Pesquet & Lloyd (2011) concluded that MAP70s, flanking MT thickening sites, and MIDD1, interconnecting future sites of MT growth, play a role in specifying the global SCW patterning. This is best manifested as a spatio–temporal balancing between assembly (MAP70s) and disassembly (MIDD1) of CMTs (Oda & Fukuda, 2013c). Regulation of this would promote formation of spiral patterns when the former prevails and pitted patterns when the latter prevails.

TRACHEARY ELEMENT DIFFERENTIATION-RELATED6 (TED6) and *TED7* were found to be co-regulated with SCW *CESAs* during *in vitro* *Zinnia* TE differentiation in a study by Endo *et al.* (2009). Using co-purification and Co-IP, they also showed that the *Arabidopsis* homolog to ZeTED6, AtTED6, associated with AtCESA7. Furthermore, ZeTED6-/ZeTED7-RNAi transformed suspension cultures displayed delayed TE differentiation, whereas ZeTED6-/ZeTED7-OE caused an increased rate of TE differentiation. In line with this, transient expression of AtTED6-/AtTED7-RNAi constructs in *Arabidopsis* seedlings resulted in reduction of SCW thickness, smoothness and symmetry in

root VEs. The authors argued for a functional association of TED6/TED7 with the SCW CSC, and that the cytoplasmic C-terminal domain of these proteins promotes SCW formation by some mechanism yet to be discovered. Taken together, Endo *et al.* (2009) proposed a model where TED6/TED7 predict future sites of SCW deposition. Therefore, Pesquet & Lloyd (2011) suggested that TED6/TED7 could be direct/indirect partners to MIDD1/MAP70s.

1.5.4 MAPs Implicated in the Ordered Deposition of Cellulose Microfibrils

Ever since the discovery of the CMT–CMF parallelism and the alignment (monorail) hypothesis was launched in 1974 by Heath, a linker between the CMTs and the CSC has been hypothesized. Such a protein was recently identified through a Y2H screen and found to interact with PCW CESA isoforms; hence, it was denoted CELLULOSE SYNTHASE INTERACTIVE PROTEIN 1 (CSII) (**Figure 1**) (Gu *et al.*, 2010). Loss-of-function *csi1* mutants displayed reduced hypocotyl length and increased diameter, compared with WT, and elongated less rapidly. The mutant also displayed organ and epidermal cell twisting in rosette leaves, roots and etiolated hypocotyls, reminiscent of phenotypes observed in MAP mutants. Intriguingly, the distribution and motility of CESA particles, as deduced from a YFP-CESA6 marker line, appeared affected in the mutant. Li *et al.*, (2012b) further observed that CSII not only directly interacted with CESA6, but also directly bound to MTs *in vitro*, thereby establishing this protein as a MAP and providing a putative direct mechanistic link between CMTs and CSCs. They also observed through live cell imaging that this MAP co-localized with CMTs and CSCs, further strengthening the hypothesis that the interaction between CMTs and CESAs is dependent on, and mediated by, the physical association with CSII. In another report, Bringmann *et al.* (2012b) showed that fluorescently labelled POM2, which is allelic to CSII, associated with both PM-localized CESAs and SmaCCs/MASCs. Loss of POM2/CSII function did not affect the rate of CSC insertions to the PM or to the localized insertions of CSCs adjacent to CMTs. Instead, the authors concluded that POM2/CSII activity is required for the guidance and maintenance of continuous CSC movements along CMTs; thus, mediating the co-alignment of these two networks, either directly or indirectly, in association with some other scaffold proteins. This prompts for yet another refinement of the conventional alignment hypothesis to also integrate this linkage protein as a new and critical accessory player that physically couples CMTs with CMFs through a molecular bridge during cellulose biosynthesis in PCWs (Bringmann *et al.*, (2012a). An analogous mechanism in SCWs still awaits discovery.

Two *Arabidopsis* SCW MAPs, characterized as *FRAGILE FIBER (FRA)* genes (though, not all identified *FRA* genes encode MAPs), exhibit aberrant MFA in their mutant plants. *FRA1* encodes a kinesin-like motor protein (**Figure 1**) and the *fra1* mutation results in less ordered CMFs in IFs and thus reduced mechanical strength of mature inflorescence stems (Zhong *et al.*, 2002). On the contrary, no change in CMT organization or cell wall thickness and composition was observed, suggesting that *FRA1* does not serve as a direct linker, but contributes to the ordered deposition of CMFs by another mechanism. *FRA1*-OE, on the other hand, led to reduced thickness and also increased number of layers in the SCW (Zhou *et al.*, 2007). Though, considering that *FRA1* is a mono-directional +TIP MAP that has the potential to transport cargo along CMTs at a speed 100 times faster than CSC movement (Zhu & Dixit, 2011), it is unlikely that this motor protein is directly associated with CMF deposition. *FRA2 (AtKTN1)* encodes a katanin MT-severing protein (Burk *et al.*, 2007) and the *fra2* mutant displays disorganized CMTs (Burk *et al.*, 2001), irregular deposition of CMFs and thinner and weaker cell walls of the IFs (Burk & Ye, 2002). Katanin is crucial for plant cells to form aligned CMT arrays (Stoppin-Mellet *et al.*, 2003). Though, increasing the severing activity by OE of *AtKTN1* does not increase CMT net alignment, according to a study by Stoppin-Mellet *et al.* (2006). They rather found that OE caused numerous thick CMT bundles to form, which eventually shortened and depolymerized. Interestingly, Wightman *et al.* (2013) discovered that, in *Arabidopsis*, *SPR2* is enriched at MT crossover sites where it interacts with *AtKTN1* and stabilizes these crossovers to prevent severing. Thus, katanin activity, and its outcome, depends upon the presence and modulating function of *SPR2*. The authors further suggested an additional role of *SPR2* in promoting complex crossovers at sites where more than two MTs intersect.

Another SCW-associated MAP suggested to be linked to cellulose deposition is *PttMAP20* in *Populus*, which together with its homolog in *Arabidopsis*, *AtMAP20*, constitute an important part of this thesis. *PttMAP20* was first identified in a study by Rajangam *et al.* (2008a) as highly up-regulated across SX in the stem of hybrid aspen and was found to co-regulate with SCW *CESAs*. *PttMAP20* encodes a small cytosolic protein with an estimated mass of 20.8 kDa and a pI of 9.65. Importantly, the authors also discovered that recombinant *PttMAP20* bound to taxol-stabilized MTs *in vitro*, and decorated CMTs of tobacco epidermal leaf cells when transiently expressed *in vivo*. It also presented a capacity to bind to DCB, suggesting an unknown molecular linkage to the CSC, since DCB disrupts cellulose biosynthesis by an unknown mechanism. Moreover, heterologous OE of *PttMAP20* in *Arabidopsis* resulted in skewed growth of roots on plates and

right-handed helical twisting of tissues and organs. MAP20s share the highly conserved TPX2 domain with *Xenopus* TPX2, a large multidomain MAP. TPX2, *per se*, is a MAP that has been shown to target a kinesin-like protein, XKLP2, in *Xenopus* to MT minus ends during mitosis and is important for spindle pole organization (Wittmann *et al.*, 2000).

1.6 Lignin Biosynthesis and Structure

1.6.1 Biosynthesis of Lignin Monomers

Lignin represents a class of complex natural polymers, displaying high structural diversity (Sederoff *et al.*, 1999). The currently accepted model states that the lignin polymer is formed by combinatorial-like phenolic oxidative coupling reactions (dehydrogenations) of radicals (primarily 4-hydroxyphenylpropanoids) generated by peroxidase–H₂O₂ / laccase (LAC)–O₂, in a random, yet chemically controlled, manner (Ralph *et al.*, 2004; Vanholme *et al.*, 2010). The most common lignin monomers are the three *p*-hydroxycinnamyl alcohols (monolignols): *p*-coumaryl (H), coniferyl (G) and sinapyl (S) alcohols. These monolignols react endwise, adding H, G and S units, respectively, to the growing racemic polymer. This coupling theory is supported by oligolignol profiling in lignified *Populus* SX tissue (Morreel *et al.*, 2004). Nevertheless, lignin biosynthesis shows remarkable plasticity, allowing for substitutions with other monomers; thus, influencing the final molecular structure (Ralph *et al.*, 2004; Vanholme *et al.*, 2008).

Composition of lignin monomers varies between taxa (Vanholme *et al.*, 2010). Angiosperm dicots contain both S and G units with trace amounts of H units, whereas gymnosperms contain mostly G units with low levels of H units. Angiosperm monocots (grasses), on the other hand, incorporate similar levels of S and G units and higher amounts of H units, as compared to dicots. Biosynthesis of the monolignols starts with the deamination of phenylalanine, derived from the shikimate biosynthetic pathway, and then flows through the general phenylpropanoid and monolignol-specific pathways (Vanholme *et al.*, 2010). These involve hydroxylation, transacylation, methylation and reduction into lignin monomeric precursors. These pathways have been under continuous revision, and studies of mutants for each step of the pathway have contributed to that (Boerjan *et al.*, 2003).

1.6.2 Monolignol Transport

The monolignols are synthesized in the symplast (cytoplasm) and therefore needs to be transported to the apoplast (cell wall) for incorporation into the lignin structure (Vanholme *et al.*, 2010). Different hypotheses how this could

be accomplished have been proposed, such as passive diffusion of the hydrophobic monolignols, vesicular trafficking and actively through specialized membrane transporters (Sibout & Höfte, 2012). The favoured Golgi-mediated vesicle transport model, where monolignols would have to accumulate within either the endoplasmic reticulum (ER) or the Golgi was challenged in a study using inhibitors against protein translation and phenylpropanoid metabolism in conifers by Kaneda *et al.*, (2008), who found no support for such a model. Rather, recent evidence is pointing towards a transporter-mediated export model, powered either directly via ATP-binding cassette-like (ABC) transporters, or indirectly via the proton gradient (Yazaki, 2006). The former idea has gained favour after a report from Miao & Liu (2010), who demonstrated with *in vitro* assays of isolated dicot membranes that ABC transporters are both involved in transporting lignin precursors across the PM and sequestration into vacuoles for storage.

Furthermore, in gymnosperms, and certain angiosperms, monolignols are often glycosylated by UDP-glucose coniferyl/sinapyl alcohol GT to form 4-*O*- β -D-glucosides; coniferin and syringin, respectively (Liu *et al.*, 2011). In their report, Miao & Liu (2010) concluded that glucosylation appears to be necessary to facilitate vacuolar storage, but is not required for transport to the apoplast in *Arabidopsis*. This implicates that both PM and vacuolar membrane vesicles selectively transport different chemical forms of monolignols; *i.e.*, different ABC transporters are able to discriminate against them.

1.6.3 Lignin Nucleation and Polymerization in the Apoplast

Lignification initiates at nucleation sites, where the lignin polymer can grow (Boerjan *et al.*, 2003). It has been observed that after S₁ layer formation of the SCW has started, lignin is first deposited in the ML and cell corners (Donaldson, 2001; Boerjan *et al.*, 2003). These structures have the highest concentration of lignin in the cell wall. Lignification is then believed to proceed throughout the SCW, both during and after formation of the polysaccharide matrix of the S₂ layer (Donaldson, 2001; Boerjan *et al.*, 2003). In fact, lignin deposition might be as most intense when matrix polysaccharides are incorporated into the S₃ layer, and it progresses towards the cell lumen until lignification of all SCW layers is finalized (Mellerowicz *et al.*, 2001). The SCW of VEs has higher lignin concentration and is enriched in G units, as compared to fibres (Donaldson, 2001; Boerjan *et al.*, 2003). Taken together, it can be concluded that there is a difference in the spatio-temporal regulation of deposited lignin content and monomeric composition (*i.e.*, S/G lignin ratio) across SX.

Moreover, there is also a variation in the spatio-temporal regulation of incorporation of different lignin monomers during wall formation, *per se*, resulting in a variation in lignin chemistry at specific regions within the wall (Chabannes *et al.*, 2001). In XFs of angiosperms, H units have been observed to be deposited first, succeeded by G units and finally S units (Donaldson, 2001; Boerjan *et al.*, 2003). In addition, Boerjan *et al.* (2003) further reasoned that the difference in the spatio-temporal regulation of monolignol incorporation into the growing lignin polymer is influenced by the chemical nature of matrix polysaccharides and MFA of the wall layers. For instance, in the ML and PCW, lignin forms spherical structures, whereas in the SCW, lignin deposition follows the orientation of CMFs (Roussel & Lim, 1995). Lignin composition further influences the interaction with matrix polysaccharides.

1.6.4 Lignin Engineering – Modifying Syringyl to Guaiacyl Ratios

Lignin removal from lignocellulosic biomass is an obstacle for efficient use of polymers for materials or energy (Weng *et al.*, 2008). It has long been proposed that genetic engineering of lignin content or structure could facilitate lignin separation during processing (Kraft pulping). This could be done either by modifying the expression of lignin biosynthesis genes or TFs that regulate lignin biosynthesis (Vanholme *et al.*, 2008, 2012).

Since G lignin is more cross-linked than S, wood with a high S/G ratio is easier to delignify and therefore a desirable trait (Boerjan *et al.*, 2003). The discovery of FERULATE-5-HYDROXYLASE (F5H) as a key enzyme in regulating the shunt of ferulic acid to sinapic acid opened up the perspective to genetically engineer the S/G ratio (Meyer *et al.*, 1996, 1998). OE of *F5H* in tobacco and *Populus*, under control of the *C4H* promoter, indeed resulted in higher S/G ratio and improved chemical pulping and bleaching efficiencies (Huntley *et al.*, 2003). Nevertheless, the efficiency of cellulose conversion to ethanol is to a large extent dependent on lignin content, as demonstrated in both *Populus* and *Arabidopsis* mutant plants (Mansfield *et al.*, 2012; Van Acker *et al.*, 2013). In a study of a natural population of *Populus* trees with a large variation in both lignin content and S/G ratio, however, Studer *et al.* (2011) found that, for high S/G ratios (> 2.0), there was no correlation between lignin content and enzymatic hydrolysis efficiency. Conversely, only for samples with low S/G ratios (< 2.0) could a strong negative correlation with lignin content be inferred. In addition, a sample set that exhibited average lignin content and S/G ratio still presented enzymatic hydrolysis rates higher than expected, which led the authors to suggest that factors other than lignin

content and S/G composition impact on cell wall recalcitrance to digestion with cellulolytic enzymes.

Unfortunately, decreasing lignin content is often achieved at the expense of plant fitness and viability, *e.g.*, weakening of cell walls in water-conducting VE, which may then collapse (Li *et al.*, 2008). This can be circumvented by using a conditional promoter that instead directs the modification to supporting fibres and sclerenchyma, leaving water-conducting VEs intact (Li *et al.*, 2008). As an alternative approach, the deficiency of the VE cell wall could be compensated for by expressing critical genes under the influence of a VE-specific promoter. In fact, this was demonstrated by Petersen *et al.* (2012), who restored the collapsed VEs and growth performance in some xylan deficient *irx* mutants by expressing xylan biosynthesis genes, driven by VE-specific promoters. Taken together, lignin engineering seems to be an attractive approach to enhance the bioconversion of lignocellulose into biofuels, and ways to avoid reduced plant fitness could be in reach.

1.7 Transcriptional Networks Regulating Secondary Cell Wall Formation

1.7.1 First Level Master Switches – The NAC Family

Almost every aspect of plant development, including SCW formation, is influenced by different plant hormones, such as auxin, ethylene and gibberellins (Groover & Robischon, 2006). Genetic evidence for a role of auxin in fibre wall formation was provided by the *Arabidopsis* knockout (KO) mutants of the tonoplast-located WAT1, which have strongly reduced SCWs in fibres of the inflorescence stem and in hypocotyls (Ranocha *et al.*, 2010). This protein was later demonstrated to be a transporter, facilitating auxin export from the vacuole to the cytosol (Ranocha *et al.*, 2013). The biosynthesis of SCWs is further transcriptionally regulated by a hierarchical network of TFs (**Figure 2**), where activation is governed by a few master switches (Zhong & Ye, 2007). The most important belong to the NAC (short for NAM, ATAF1/2 and CUC2) and MYB (short for MYELOBLASTOSIS) families, representing first and second hierarchical level of transcriptional control, respectively. Among the NACs, SECONDARY WALL-ASSOCIATED NAC DOMAIN PROTEIN1 (SND1), also known as NAC SECONDARY WALL THICKENING PROMOTING FACTOR3 (NST3), and NST1 were discovered as important first level transcriptional regulators of the SCW biosynthesis program of fibres in *Arabidopsis*, and they were found to be functionally redundant (Zhong *et al.*, 2006, 2007a; Mitsuda *et al.*, 2007). The double KO mutant exhibited suppressed SCW formation in IFs and XFs, but not in VEs.

Moreover, NST1 was also shown to act redundantly with NST2 in regulating SCW thickening of anther tissue, important for anther dehiscence (Mitsuda *et al.*, 2005).

In parallel with regulation of SCW deposition in fibres, VASCULAR-RELATED NAC-DOMAIN6 (VND6) and VND7 were identified as master regulators for SCW formation of VEs in *Arabidopsis* (Kubo *et al.*, 2005; Ohashi-Ito & Fukuda, 2010). Dominant repression (DR) of these genes in primary roots inhibited formation of metaxylem and protoxylem vessels (PXVs), respectively. VND6 was further demonstrated to directly regulate downstream target genes related to TE-specific PCD (Ohashi-Ito *et al.*, 2010). Finally, VND7 plays a central role in regulating the differentiation of all types of VEs in *Arabidopsis* shoots and roots and might also function together/redundantly with VND2–VND5, since their expression patterns overlap (Yamaguchi *et al.*, 2008).

In SND1-/NST1-RNAi plants, 11 TFs, belonging to the *NAC*, *MYB* and *KNOTTED ARABIDOPSIS THALIANA (KNAT) KNOTTED1-LIKE HOMEODOMAIN (KNOX)* gene families with vascular expression patterns, were found to be down-regulated (Zhong *et al.*, 2008), and these were recognized as SND2, SND3, MYB20, MYB42, MYB43, MYB52, MYB54, MYB69, MYB85, MYB103 and KNAT7 (encoded by a Class II *KNOX* gene). Down-regulation by RNAi or T-DNA mutation of these TFs did not induce any visible morphological phenotype in the study by Zhong *et al.* (2008), whereas their OE and DR affected SCW thickness of IFs and XFs. This suggested that they have a function in SCW formation as downstream targets of SND1/NST1. Through promoter transactivation studies and electrophoretic mobility shift assays (EMSAs), KNAT7, MYB46, MYB83, MYB103 and SND3 were all found to be direct targets of SND1/NST1 and NST2, as well as of VND6/VND7 (Zhong *et al.*, 2007b, 2008; McCarthy *et al.*, 2009; Ohashi-Ito *et al.*, 2010; Zhong *et al.*, 2010c; Yamaguchi *et al.*, 2011). The secondary wall NAC (SWN) master switches (SND1/NST1, NST2 and VND6/VND7) recognize and bind to a common *cis*-acting element, named SWN-binding element (SNBE). This is composed of an imperfect palindromic 19 bp consensus sequence, located in the promoters of their direct targets (McCarthy *et al.*, 2011). The target genes of VND6/VND7 also harbour a TE-specific 11 bp *cis*-element, TERE, in their promoters (Pyo *et al.*, 2007), important for SCW modification and onset of PCD in differentiating VEs. Complementation studies have demonstrated that SWN master switches can rescue the *snd1 nst1* double mutant and restore the SCWs in its IFs when driven by the *SND1* promoter (Zhong *et al.*, 2010c; Yamaguchi *et al.*, 2011). Thus, SND1/NST1, NST2 and VND6/VND7 have a set of common target genes and are

functionally interchangeable, but *in planta* they are active in fibres and VEs, respectively.

A more global approach to identify direct target genes of SND1 and VND7 was undertaken by Zhong *et al.* (2010c). They induced these genes in protoplasts using the estrogen (estradiol)-inducible system, combined with cycloheximide (CHX) treatment. They found that SND1 activated 138 genes, and VND7 activated 276 genes with an overlap of 89 genes between the two. In another study, Yamaguchi *et al.* (2011) studied direct target genes of VND7 in 10-day-old *Arabidopsis* seedlings. They took advantage of the glucocorticoid-mediated posttranslational induction system, described by Yamaguchi *et al.* (2010a), which effectively induces transdifferentiation of various cell types into VEs after treatment with dexamethasone (DEX). Treatment with DEX activates VND7, which binds to the promoters of its direct target genes, enabling transcription. After CHX treatment, 63 direct target genes of VND7 were identified. Taken together, these studies suggest that, within the SWN-mediated transcriptional network, SND1 and VND7 seem to directly regulate a large number of target genes in specific cell types (fibres and VEs, respectively) for the coordinated formation of SCWs.

NAC domain TFs appear to be controlled at the posttranscriptional level. Yamaguchi *et al.* (2010b) showed that VND-INTERACTING2 (VNI2) interacts with VND7 and was suggested to act as a transcriptional repressor upstream of VND7 to regulate its VE-specific expression. Further, the expression of AS2-LIKE19 (ASL19) / LBD30 and ASL20/LBD18 in immature VEs was demonstrated to be dependent on VND6/VND7 (Soyano *et al.*, 2008). OE of ASL19 and ASL20 induced ectopic formation of VEs in cells of non-vascular origin, similar to OE of VND6/VND7. DR of ASL19 and ASL20 generated abnormal VEs, verifying that ASL activity is required for proper VE differentiation. Thus, it was suggested that ASL19 and ASL20 are likely mediating a positive feedback loop downstream of VND6/VND7 (Soyano *et al.*, 2008).

Another gene involved in SCW formation is *XYLEM NAC DOMAIN1* (*XND1*), which is highly expressed in maturing xylem (Zhao *et al.*, 2005). *XND1* is believed to influence VE size and xylem maturation by negatively regulating SCW biosynthesis and PCD (Zhao *et al.*, 2008). *Arabidopsis xnd1* KO mutants exhibited shorter, but otherwise apparently normal, VEs in stems and hypocotyls, whereas OE of *XND1* completely suppressed formation of VE SCWs and PCD.

A group of *Populus trichocarpa* NAC domain TFs (PtrWNDs), preferentially expressed in SX, have been identified as functional orthologs to SND1 through complementation studies and promoter-binding assays (Zhong

et al., 2010b). These *Populus* NACs were able to directly activate four of the direct targets of SND1 in *Arabidopsis*, namely *KNAT7*, *MYB46*, *MYB103* and *SND3*. In a follow-up study by Zhong *et al.* (2011b), expression of 35S promoter driven PtrWND-OE and PtrWND-DR constructs in *Populus* led the authors to suggest a suite of downstream TFs and their putative target genes in wood-forming tissues. Interestingly, many of these targets had *Arabidopsis* orthologs with unknown or even different function during SCW biosynthesis. Hence, functional analyses of these *Populus* genes will be important and relevant. Nevertheless, PtrWNDs are generally believed to be functional orthologs to their *Arabidopsis* counterparts, since they also bind to the SNBE sequences in the promoters of their direct targets in *Arabidopsis* (Zhong *et al.*, 2013). Similarly, the rice and maize OsSWNs and ZmSWNs were also able to complement the *Arabidopsis* *snd1 nst1* double mutant, demonstrating that they are functional orthologs to *SND1* (Zhong *et al.*, 2011a). In addition, OE of *OsSWNs* and *ZmSWNs* in *Arabidopsis* activated the SCW transcriptional program through binding to SNBE sites in their downstream target promoters, inducing ectopic deposition of cellulose, lignin and xylan.

Phylogenetic data analysis, in combination with the heterologous complementation studies of functional orthologs, suggests that the SWN-mediated transcriptional network controlling SCW biosynthesis is an ancient mechanism that has been evolutionary conserved through all vascular plant lineages (Zhong *et al.*, 2010a). The emerging picture is that perennial species have a more complicated network than annual species. This is reflected in that some downstream TFs of PtrWNDs, mostly MYBs in perennials, seem to lack functional orthologs in some annual taxa.

1.7.2 Second Level Master Switches – The MYB and KNAT Families

To understand the mechanisms underlying the SCW biosynthesis program in xylem cells, it is important to link the function of SND1/NST1 and VND6/VND7 downstream TFs to the biosynthetic pathways of major SCW components (cellulose, lignin and xylan). MYB46 was shown to act as a master switch, similar to SND1/NST1 and VND6/VND7, regulating SCW formation in both fibres and VEs; thus, representing a secondary level of molecular switches downstream the primary ones (Zhong *et al.*, 2007b). DR of MYB46 resulted in drastic reduction of SCW thickness in VEs and fibres, whereas OE produced thicker cell walls and even gave ectopic sclerification of epidermal and cortical cells in the inflorescence stem. Ko *et al.* (2009) further identified a suite of SCW-related genes through OE of MYB46 under the control of a DEX-inducible promoter *in planta*. One of these, AtC3H14, was proposed as a second level master switch during SCW formation, next to

MYB46, since transactivation analyses of this TF, similar to MYB46, induced the expression of a selected subset of important cellulose, lignin and xylan biosynthesis genes.

Knowledge of the transcriptional network regulating the SCW biosynthesis program has been further enriched by McCarthy *et al.* (2009) who demonstrated that MYB83 is another direct target of SND1 and its close homologs; it acts redundantly with MYB46 in regulating SCW formation. In this study, a double KO mutant in *MYB83* and *MYB46* led to thinner walls of IFs and severely retarded growth, whereas single mutations in each gene did not result in any aberrant effect in SCW thickening or plant growth, similar to the *snd1*, *nst1*, *vnd6* and *vnd7* single mutants. Thus, MYB83, together with MYB46, represents second level master switches. These act in concert with primary level master switches, located upstream, in regulating common downstream targets through feed-forward loops (**Figure 2**).

MYB46/MYB83 directly activate TFs, such as AtC3H14, KNAT7, MYB52, MYB58 and MYB63, but also genes involved in lignin and polysaccharide biosynthesis, SCW modification, PCD, cytoskeletal organization and vesicle transport (Ko *et al.*, 2012; Zhong & Ye, 2012). Transactivation analysis, together with EMSA analysis, facilitated the identification and mapping of a 7 bp SCW MYB-responsive element (SMRE) consensus sequence as a target for MYB46/MYB83 (Zhong & Ye, 2012). In addition, it was found that this DNA-binding element is enriched in some targets, and can also harbour different binding affinities, determined by the different SMRE sequence variants. Interestingly, three of eight different variants of the conserved SMRE sequences are identical to the AC element, which is required for transcription of phenylpropanoid and monolignol biosynthesis genes (Raes *et al.*, 2003). In parallel, Kim *et al.*, (2012a) identified an 8 bp core motif as a MYB46-responsive *cis*-regulatory element (M46RE). This is highly enriched in the promoters of MYB46-regulated SCW genes. Importantly, all three SCW *CESAs* contain the M46RE motif, and it was recently demonstrated by means of EMSA and chromatin immunoprecipitation (ChIP) analysis that MYB46 binds to their promoters both *in vitro* and *in vivo* and directly activates and regulates their transcription (Kim *et al.*, 2012b). Later, genetic complementation of mutants in the SCW *CESA* genes by promoters with point mutations in the M46RE motif established that MYB46 is required for the transcriptional complex regulating functional expression of the SCW *CESA* genes (Kim *et al.*, 2013). Further research is required to deduce if/how SMRE and M46RE impact on SCW formation in different ways, and to explore any additional important promoter elements. Altogether, the notion that first level SND1/NST1 and VND6/VND7 and second level MYB46/MYB83

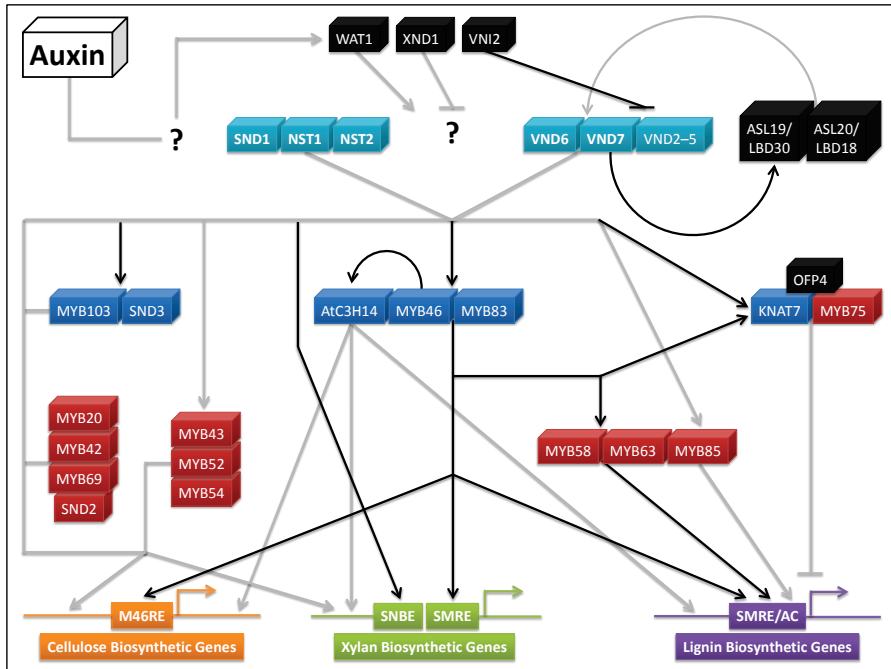


Figure 2. Simplified overview of the transcriptional network regulating the secondary cell wall biosynthesis program in *Arabidopsis*. Second level master switches are direct targets of first level master switches. Together, these activate a suite of, first, downstream transcription factors and, second, secondary cell wall biosynthetic genes through multi-levelled feed-forward/back loops. Black/grey arrows indicate direct/indirect activation, whereas black/grey horizontal strokes indicate direct/indirect repression, respectively. Based on the literature cited in this thesis.

master switches cooperatively and directly activate a suite of common downstream targets required for SCW biosynthesis suggests a complicated multi-levelled/-faceted feed-forward/back loop regulatory structure, instead of the previously thought simple linear top-down cascade (Wang & Dixon, 2011; Zhong & Ye, 2012).

The AC element has previously been recognized as a common *cis*-element located in the majority of monolignol biosynthesis genes and required for their expression in lignifying cells (Hatton *et al.*, 1995). Since then, major progress has been made in characterizing important regulators in the lignification process. For instance, MYB family TFs bind to the AC element (Sablowski *et al.*, 1994, 1995) and they are recognized to have a putative regulatory role in lignin biosynthesis in the SWN-regulated transcriptional network (Zhong & Ye, 2009; Nakano *et al.*, 2010). Indeed, functional analysis identified MYB58 and MYB63 as transcriptional activators of lignin biosynthesis, downstream of MYB46/MYB83 (Zhou *et al.*, 2009). OE of *MYB58* and *MYB63* specifically

activated lignin biosynthesis genes, but not SCW *CESA* or xylan genes. In these OE lines, ectopic deposition of lignin, but not cellulose or xylan, was observed in epidermal and cortical cells in the inflorescence stem. MYB58 was found to directly activate the expression of a SCW-associated *LAC* gene (*LAC4*), and all monolignol biosynthetic genes, except for *F5H*, which also lacks the AC element in its promoter. Zhao *et al.* (2010) further demonstrated, by promoter transactivation and EMSA assays, that *F5H* is directly activated by the SND1 master switch. They assessed, however, the *Arabidopsis* AtSND1 TF binding to the *Medicago truncatula* *MtF5H* promoter, which therefore not necessarily provide proof that this activation takes place in *Arabidopsis*. Taken together, MYB58 and MYB63 are the first true lignin-specific TFs identified in *Arabidopsis* (Zhou *et al.*, 2009; Zhao & Dixon, 2011).

MYB75, also known as *PRODUCTION OF ANTHOCYANIN PIGMENT 1* (*PAP1*), was first identified as a positive regulator of anthocyanin biosynthesis in *Arabidopsis* (Borevitz *et al.*, 2000). Interestingly, Bhargava *et al.* (2010) observed that basal stems of *myb75* had increased SCW thickness of IFs and XFs, higher lignin content and expression of several monolignol genes and a lower S/G ratio, compared with WT, whereas OE plants showed the opposite characteristics. When these contrasting phenotypes were taken into account, MYB75 was suggested to be a repressor of the lignin branch of the phenylpropanoid pathway, stimulating carbon flux towards flavonoid metabolism. In addition, the authors discovered protein interaction between MYB75 and KNAT7 in a Y2H assay and *in vivo* with a bimolecular fluorescence complementation (BiFC) study in *Arabidopsis* protoplasts. Bhargava *et al.* (2013) provided evidence that this interaction is dependent on the R3 domain of MYB75 and the KNOX2 domain of KNAT7. KNAT7 was further shown by Li *et al.* (2011a) to interact with OFP4, an OVATE FAMILY PROTEIN, in a Y2H assay and also *in vivo* with BiFC analysis. They both acted as transcriptional repressors in a protoplast transfection system and, when co-transfected, the repressor activity of KNAT7 was enhanced; thus, confirming interaction between the two proteins *in vivo*. A KO mutation in KNAT7 gives an *irx* phenotype, without any visible morphological defects, as described previously by Brown *et al.* (2005). Li *et al.* (2011a) further studied both *knat7* and *ofp4* single KO mutants and also the *knat7 ofp4* double mutant. Similar to *knat7*, *ofp4* also displayed collapsed VEs in the xylem vascular tissue system. Interestingly, the double mutant possesses the same *irx* phenotype as the corresponding single mutants, without any additive effect. Thus, this confirms that KNAT7 and OFP4 form a KNOX–OVATE regulatory complex, repressing certain aspects of SCW biosynthesis. Li *et al.* (2012a) further characterized *knat7* KO mutants more in-depth. Basal stems exhibited

thicker IFs with increased lignin amounts and enhanced expression of genes related to the three major components of the SCW. On the contrary, OE lines exhibited thicker SCW of the IFs. Taken into account the increase in lignin, coupled with the *irx* phenotype and thinner walls of VEs, Li *et al.* (2012a) postulated that KNAT7 regulates different aspects of SCW formation in a negative feedback loop by targeting different genes in different cell types. A model was suggested where a complex of KNAT7 and MYB75 are cooperating supplementary, rather than additively, in repressing SCW biosynthesis in general and lignin biosynthesis in particular. It was further suggested that this complex might consist of different interacting partners, depending on cell type. This model is strengthened by the overlapping expression pattern of KNAT7 with MYB75 (Bhargava *et al.*, 2010) and also implicates that MYB75, similar to KNAT7, is downstream the first and second level master switches.

MYB52 was initially identified by Zhong *et al.* (2008) as a downstream TF of SND1/NST1 master regulators. Cassan-Wang *et al.* (2013) found that a T-DNA KO mutant in *MYB52* had strongly lignified IFs and vascular bundle cells, suggesting that SX formation was enhanced and also appeared to take place earlier than in WT. Therefore, the authors proposed that MYB52 could be a potential repressor of SCW deposition and/or lignin biosynthesis. Nevertheless, Zhong *et al.* (2008) noticed thinner SCWs in plants harbouring a MYB52-DR construct; thus, reflecting additional functions from homologous TFs to MYB52, not detected in KO plants.

In the genus *Populus*, the MYB family is larger than any other angiosperm species with fully sequenced genome (Wilkins *et al.*, 2009), and the expansion was not only attributed to whole genome duplication, but also to diversification of specific clades (Wilkins *et al.*, 2009). Four *Populus* wood-associated MYB TFs, more specifically PtrMYB2, PtrMYB3, PtrMYB20 and PtrMYB21, were found by McCarthy *et al.* (2010) and Zhong *et al.* (2013) to activate expression of SCW biosynthetic genes and induce ectopic deposition of all three major SCW components during OE in *Arabidopsis*. They were also able to activate the promoters of *Populus* SCW biosynthetic genes. Interestingly, *PtrMYB3* and *PtrMYB20* are directly activated by PtrWND2 (McCarthy *et al.*, 2010), a close homolog to *SND1*. Moreover, *MYB46* and *MYB83* are, in fact, the closest functional *Arabidopsis* homologs to *PtrMYB3* and *PtrMYB20*, indicating a well-conserved transcriptional regulatory mechanism between *Populus* and *Arabidopsis*. Similar to their *Arabidopsis* counterparts, *Populus* MYB second level master switches also bind to SMRE sequences in the promoters of their direct target genes, activating their expression and the biosynthesis of cellulose, lignin and xylan (Zhong *et al.* 2013).

2 Objectives

2.1 In General

From a larger perspective, focus was set on studying genes and/or gene families with a potential role in influencing the lignocellulosic content and composition of xylem SCWs in stems of *Arabidopsis* and *Populus*.

2.2 In Particular

Functional genomics, bioinformatics and chemotyping tools were applied to investigate the following genes and their relation to cellulose/lignin biosynthesis:

- MAP20, a MAP displaying high expression across developing SX in *Populus* stems and implicated to have a direct/indirect regulatory role in biosynthesis of the cellulose polymer.
- MYB103, a TF, whose *Arabidopsis* loss-of-function mutants exhibited major wall chemistry alterations in the lignin polymer when their basal inflorescence stems were initially screened by Py-GC/MS.

3 Methodological Considerations

In this chapter, a brief overview and a more comprehensive description over the materials and methods used, not found in the attached papers, are given.

3.1 *Arabidopsis* and *Populus* as Model Systems to Study Secondary Growth

Arabidopsis thaliana (*At*) is recognized as a powerful plant model system to study genetics and genomics. It has a small genome (≈ 157 Mbps) that was the first plant genome to be sequenced (The Arabidopsis Genome Initiative, 2000). Because of its small physical size and short generation time, it is easy to grow in large numbers and ideal for genetic analysis. A number of molecular and computational tools have been developed for *Arabidopsis*, adapted to study molecular control of different traits. Of most importance are the publicly available T-DNA KO mutant libraries, annotation of genes (TAIR10 release, <http://www.arabidopsis.org/>) and bioinformatical tools.

The hypocotyl in *Arabidopsis* forms a VC that can undergo extensive secondary growth, particularly during short days (8 h light, 16 h dark) (Chaffey *et al.*, 2002; Nieminen *et al.*, 2004). Cambial growth and SX differentiation in *Arabidopsis* also occurs in roots and the inflorescence stem. Certain key regulators and regulatory networks controlling SX and vascular development are implied to be conserved between angiosperm herbaceous and tree species (Jansson & Douglas, 2007), facilitating comparative genomics and transfer of knowledge to angiosperm trees. Thus, *Arabidopsis* is a suitable model for cambial growth and SCW biosynthesis (Chaffey 2002; Liepman *et al.*, 2010; Zhang *et al.*, 2011). In addition, the inflorescence stem has also a measurable MFA in its xylem SCWs and mechanical testing, such as tensile strength and stiffness, as well as bending strength, can be performed (Strabala & MacMillan, 2013). Because of its short life cycle, however, *Arabidopsis* as a

model is somewhat limited when it comes to study certain aspects of wood formation, e.g., activity–dormancy transitions and maturation phenomena, such as the formation of early wood and late wood.

Because of its relatively small genome size (\approx 485 Mbps, 5-fold larger than *Arabidopsis thaliana*), rapid growth and ease to transform and propagate, *Populus* has emerged as a suitable tree model system (Taylor, 2002). The *Populus trichocarpa* (*Pt*) genome was the first tree genome to be sequenced (Tuskan *et al.*, 2006), facilitating the optimal use of fundamental bioinformatical and molecular tools, such as next generation sequencing, e.g., RNA (deep) sequencing (Wang *et al.*, 2009).

3.2 Generation of Transgenic Lines in Hybrid Aspen

Constructs were produced by Gateway cloning, according to manufacturer's instructions (Invitrogen, <http://www.lifetechnology.com/>), the insert of choice into Gateway-compatible binary destination vectors, provided by VIB–Ghent (Karimi *et al.*, 2002). In order to generate a promoter–GUS construct, a 2 kbp genomic DNA fragment upstream the start codon of *PtMAP20* was cloned into pENTR/D-TOPO vector (Invitrogen). This promoter fragment was subcloned into Gateway destination vector pKGWFS7 (Karimi *et al.*, 2002) to create the expression clone. Briefly, to create lines mis-regulated in *PttMAP20*, an EST clone with PU number PU02741 in PopulusDB (<http://www.populus.db.umu.se/>) (Sterky *et al.*, 2004) was cloned into vector pDONR221 (Invitrogen). This entry clone was subcloned into destination vector pK7GWIWG2(I), for RNAi, and pK2GW7, for OE, respectively (Karimi *et al.*, 2002).

All expression clones were further transformed into *Agrobacterium tumefaciens*, strain *GV3101::pMP90*, by electroporation. Then, in an in-house transformation facility, these binary plasmids were transformed into hybrid aspen (*Populus tremula* L. \times *Populus tremuloides* Michx, *Ptt*) WT (clone T89) trees by *Agrobacterium*-mediated transformation on appropriate antibiotic selection medium, using protocols developed at UPSC (<http://www.upsc.se/>).

3.3 Plant Materials and Growth Conditions for Hybrid Aspen

3.3.1 Explant Shoots Grown *in Vitro*

In vitro grown trees were propagated by transplanting new single axillary shoots to individual containers on fresh MS phytigel medium. These developed into stems that grew upright, without branching, under the following conditions: 18 h light / 6 h dark photoperiod, 22°C/18°C (day/night), 150 μ E ·

$\text{m}^{-2} \cdot \text{s}^{-1}$ and $\approx 60\%$ relative humidity. Shoots were harvested at a height of about 12 cm and their stems segmented, based on number of internodes counted from the apex.

3.3.2 Greenhouse-Grown Trees

Trees propagated *in vitro* were transplanted to soil and cultivated in the greenhouse under natural light conditions, supplemented with metal halogen lamps, with an 18 h light / 6 h dark photoperiod. Temperature was set to 22°C/15°C (day/night). After 10–11 weeks, trees had typically reached a height of about 160–180 cm and entire stems were harvested and analysed for growth characteristics on the same day. Stems were further divided into long and short segments, according to a predefined schedule, based on number of internodes counted from the apex and distance (cm) from the ground (soil).

3.4 Promoter–GUS Analysis in Hybrid Aspen

Basal 1 cm stem segments from trees grown *in vitro* were harvested, transferred to a microplate and prefixed with ice-cold 90% acetone for 10 min. Then, acetone was removed and samples were immersed in GUS staining solution (X-Gluc buffer), containing 1 mM X-Gluc (Thermo Fisher Scientific, <http://www.thermoscientificbio.com/>) dissolved in dimethylformamide; 50 mM sodium phosphate buffer, pH 7.2; 0.5 mM $\text{K}_3\text{Fe}(\text{CN})_6$ (potassium ferricyanide), M: 329.2 and 0.5 mM $\text{K}_4\text{Fe}(\text{CN})_6 \cdot 3 \text{H}_2\text{O}$ (potassium ferrocyanide), M: 422.4. Samples were subsequently vacuum-infiltrated for 20 min and incubated in the dark at 37°C for 16 h, for maximum visualization of GUS activity. For chlorophyll removal, samples were sequentially immersed in 25 and 50% ethanol. For fixation, 10 min incubation in FAA (formaldehyde – acetic acid – ethanol) solution was applied. Finally, stems were stored in 70% ethanol, prior to sectioning. Stems were then sectioned by freehand. Sections were subsequently washed in 50 mM sodium phosphate buffer (pH 7.2) and mounted in 50% glycerol on a microscope slide. Specimens were then studied under an Axioplan 2 Imaging light microscope (Carl Zeiss, <http://microscopy.zeiss.com/microscopy/>) and images captured with ZEN Lite software (Carl Zeiss).

3.5 Gene Expression Analysis

3.5.1 Quantitative PCR Analysis

Stems from greenhouse-grown trees were flash-frozen in N_2 . After debarking, the exposed developing SX was scraped with a scalpel and homogenized with

a mortar and pestle. Stem segments from *in vitro* grown trees were flash-frozen in N₂ and homogenized without debarking. Total RNA was isolated and DNase-treated with Aurum Total RNA Mini Kit #732-6820 (Bio-Rad, <http://www.bio-rad.com/>) and used to generate cDNA with iScript cDNA Synthesis Kit #170-8891 (Bio-Rad). Reaction mixture for qPCR contained 10 µL 2x iQ SYBR Green Supermix #170-8880 (Bio-Rad), 8 µL nuclease-free H₂O, 1 µL mixture of 10 µM forward/reverse primers and 1 µL cDNA template (diluted 1:10). Analysis was performed with Bio-Rad CFX96 Real-Time PCR detection system; 40 qPCR cycles were run under the following conditions: denaturation step, 95°C for 10 s; annealing step, 55°C for 10 s and elongation step, 72°C for 30 s.

Primers used were:

- ***PttMAP20* (Potri.T059900):**
FP, 5'-TTCCCCAAAGATCAAGCAGG-3';
RP, 5'-T TACTTAACAGGCTTCCAGGC-3'
- ***PttWDL3A* (Potri.010G076200):**
FP, 5'-AAGGACCAAGGAAGAGAAGGAGG-3';
RP, 5'-ATTTTGCACGTGTTGGTGGC-3'
- ***PttWDL4A* (Potri.006G200400):**
FP, 5'-AAAGAAGATACCGACTACTCGAGC-3';
RP, 5'-AGAAGTGGGCTGTGAGAAGC-3'
- ***PttUBQ10* (Potri.001G418500):**
FP, 5'-AGATGTGCTGTTCATGTTGTCC-3';
RP, 5'-ACAGCCACTCCAAACAGTACC-3'
- ***AtMAP20* (At5g37478):**
FP, 5'-AAGGAATGACCAAAGTGAACC-3';
RP, 5'-CACGTTTCACTGCTCTCTCG-3'
- ***AtCESA7* (At5g17420):**
FP, 5'-GGGTAGACAGAACAGAACAC-3';
RP, 5'-AACACTCTCGACAAAGTACAG-3'
- ***AtEF1-α* (At5g60390):**
FP, 5'-TCCAGCTAAGGGTGCC-3';
RP, 5'-GGTGGGTACTCGGAGA-3'

For data normalization, *PttUBQ10* was used as reference gene. Primers for *At* genes were used for the *Arabidopsis* cell culture system, described later.

3.5.2 Microarray Analysis

Total RNA from developing SX tissues (prepared as described earlier) was purified and concentrated with RNeasy MinElute Cleanup Kit #74204 (Qiagen, <http://www.qiagen.com/>). RNA quality and quantity were checked with the

Agilent 2100 Bioanalyzer (<http://www.agilent.com/>) and NanoDrop (<http://www.nanodrop.com/>), respectively. 4 µg per sample was submitted to Roche Nimblegen (<http://www.nimblegen.com/index.html>) and hybridized on whole-genome NimbleGen *Populus* 385K oligoarrays. Annotated gene models (**Table 4**) were based on *Pt* genome assembly v2.2 (Tuskan *et al.*, 2006; Phytozome, <http://www.phytozome.net/poplar>).

3.6 Cellulose Microfibril Angle Measurements on Wood Fibres

MFA measurements were essentially performed as described by Bjurhager *et al.* (2010). Briefly, \approx 4 cm wood blocks, harvested at the base of the stem (16–20 cm above soil), were prepared, containing a “clean” internode (*i.e.*, lacking leaf petioles) in the centre. Sections with a dimension of 40 µm thickness and 33 mm width were cut from wet samples in the longitudinal–radial direction with a microtome. Data was obtained by XRD (wide-angle X-ray scattering) (Nanostar, Bruker AXS, <http://www.bruker.com/>) with a sample-detector distance of 4.9 cm, using Cu K α radiation (wavelength 0.154 nm). The diffraction patterns were collected by a 2D position-sensitive (Hi-star) detector with a measuring time of 1 h. The intensity was plotted against the azimuthal angle. MFA was determined at three points for each sample.

3.7 Xylem Tracheary Element Cell Culture System in *Arabidopsis*

The *in vitro* system for inducible differentiation of *Arabidopsis* basal cells into TEs was previously described by Pesquet *et al.* (2010). Briefly, suspension cultures (Col-0 background) were cultivated in liquid MS medium (pH 6.0), supplemented with 3% sucrose, in the dark at 25°C with agitation (150 rpm). Every seventh day, periodic re-subcultivations were carried out into fresh liquid medium at a ratio of 1:10.

For hormonal induction of TE differentiation, 7-day-old cell cultures were diluted 1:10 with liquid MS medium (pH 6.0), supplemented with 3% sucrose, 100 mM 2-(N-morpholino)ethanesulfonic acid, 6 mg/L α -naphthalene acetic acid, 1 mg/L 6-benzylaminopurine, and 5 mM epibrassinolides. The induced cell cultures were then incubated in the dark at 25°C with agitation (150 rpm).

TE formation was monitored with an Axiovert 40 CFL bright-field microscope (Carl Zeiss), and cultures were sampled daily until day 9 after induction. Microscopy images of induced cells were acquired using AxioVision LE v.4.8.2.0 software (Carl Zeiss). To collect cells for downstream applications, aliquots of induced cell cultures were centrifuged for 5 min at 200

g. After estimation of fresh weight, the pelleted cells were flash-frozen in N₂ and stored at -80°C. RNA was then isolated, as described earlier.

In order to generate stable transgenic cell culture lines, basal cell cultures underwent *Agrobacterium*-mediated transformation. *Agrobacterium tumefaciens*, strain *GV3101::pMP90*, transformed with corresponding plant vector constructs, were grown in liquid LB medium, supplemented with selective antibiotics for 48 hours at 28°C with agitation (300 rpm). Then, 5 mL of 7-day-old cell cultures were diluted with 5 mL of fresh MS medium (pH 6.0), supplemented with 3% sucrose, and inoculated with 200 µL of *Agrobacterium* cultures.

After 48 hours of cultivation in the dark at 25°C with agitation (150 rpm), bacteria were washed away from the cell cultures 3 times by way of sequential centrifugation for 5 min at 200 g, and pelleted cells were resuspended in 10–15 mL of fresh MS medium, supplemented with 3% sucrose. After the final wash step, pelleted cells were plated on MS medium, supplemented with 3% sucrose, 0.8% agar, 250 µg/mL Cefotaxime and corresponding selective antibiotics. Plates were then incubated in the dark at 25°C, in order for transformed cells to develop into calli.

Transgenic calli were replaced to the same medium for additional incubation (2–3 weeks). Afterwards, individual calli were transferred to liquid MS medium (pH 6.0), supplemented with 3% glucose and selective antibiotics, and cultivated as separate transgenic lines for further characterization.

4 Results and Discussion

This thesis focuses on *MAP20* and *MYB103*, initially identified from transcriptome analysis as highly expressed in xylem tissue. *PttMAP20* first emerged from a transcript profiling by Hertzberg *et al.* (2001) as one of the genes with the highest relative expression across developing SX in hybrid aspen. It was characterized as an MT-binding protein by Rajangam *et al.* (2008a) and has been further characterized on a biochemical and physiological level in this thesis (**Paper I–II**). *MYB103* was identified by Zhong *et al.* (2008) as a TF downstream of SWN master switches, required for SCW formation in *Arabidopsis*, and was proposed to have a role in cellulose biosynthesis. *MYB103* later emerged from an *Arabidopsis* mutant screen of homologs to *Populus* genes down-regulated in relation to tension wood formation in *Populus tremula* (unpublished data). This screen was performed by high-throughput Py-GC/MS (**Paper IV**) that revealed a major chemotype in isolated *myb103* mutant plants, due to an altered S/G lignin ratio (**Paper III**). Here, loss-of-function mutants in *MYB103* were characterized to establish its role in the regulation of *F5H* expression; in conclusion, it was found to be required for S lignin biosynthesis.

4.1 MAP20 – A Microtubule-Associated Protein Highly Expressed in *Populus* and *Arabidopsis* Xylem Tissues

4.1.1 AtMAP20 Is a Novel Stabilizer of Microtubules in *Arabidopsis* (**Paper I**)

MAP20 contains a TPX2 domain, known to associate with MTs. Rajangam *et al.* (2008a) demonstrated, *de facto*, that hybrid aspen PttMAP20 binds to MTs, both *in vitro* and *in vivo*. TPX2 family proteins, *per se*, belong to a highly diverse family with variable molecular weights and low sequence similarity outside the TPX2 domain. A phylogenetic analysis by Rajangam *et al.* (2008b) of all TPX2 family proteins in *Populus* and *Arabidopsis* revealed 18 *Populus*

and 15 *Arabidopsis* gene models; *MAP20* was a single gene in each species. AtMAP20 in *Arabidopsis* consists of a conserved and centrally located TPX2 consensus domain (PF06886), a conserved C-terminal domain (PB004810) and a non-conserved, variable N-terminal region (**Figure 1, Paper I**).

As a part of AtMAP20 characterization, a domain-mapping study was performed. This was based on a complementary phylogenetic and domain architecture analysis on all TPX2 family proteins. A total of 166 UniProt TPX2 domain containing sequences from 28 different species were classified into 19 different domain architectures, built from 12 unique component domains (**Table 2, Paper I**). From this, it was concluded that TPX2 family proteins are constructed by adding distinct supplementary domains, with structural limitations, to the N- and C-terminal sides of the central TPX2 domain (**Figure 2b, Paper I**). This is in contrast to canonical domain architectures, typical for other MAP families described earlier in this thesis. The classification of *Populus* and *Arabidopsis* TPX2 domain containing proteins grouped them into a MAP20, a TPX2 and a WVD2/WDL clade, all with full and up-to-date gene nomenclatures (**Table 1 & Figure 2a, Paper I**).

It has been argued by Evrard *et al.* (2009) that there exists only one “true” and unique TPX2 ortholog per plant genome, sharing the functions described for animal TPX2. These authors also found that remaining TPX2-related proteins possess either a so-called Aurora-binding domain and/or one TPX2 MT-binding domain (MBD), where the latter can refer to either a centrally (PF12214) or C-terminal (PF06886) located domain of the TPX2 protein. Moreover, an important feature that distinguishes the WVD2/WDL clade from the rest in the phylogenetic tree is the presence of the conserved KLEEK motif within the TPX2 domain (Rajangam *et al.*, 2008a).

Binding of MAP20 to MTs was shown to be very strong *in vitro* and was also confirmed *in vivo* by transient expression of the labelled protein in *Arabidopsis* protoplasts (**Figure 3a–e, Paper I**). To determine the function of different AtMAP20 domains for MT interaction, labelled truncated versions of MAP20 was transiently expressed in tobacco epidermal leaf cells (**Figure 4a, Paper I**). First, it was observed that the decoration pattern of CMTs by the full-length protein differed, depending on the terminus tagged. N-terminal fusion gave fine, discontinues and intense labelling, whereas C-terminal fusion yielded a thick and continues labelling pattern (**Figure 4b–c, Paper I**). This suggests that the N- and/or C-terminus participates in defining AtMAP20 CMT-binding specificity. AtMAP20 was then divided into different truncated versions containing the N-terminal, C-terminal and TPX2 domain alone, or in different combinations, labelled at the C-terminal end. The N- or C-terminus alone resulted in ER accumulation, but no CMT decoration (**Figure 4d–e,**

Paper I), whereas TPX2 domain alone decorated CMTs in a dotted and strong pattern (**Figure 4g, Paper I**). This indicates that the TPX2 domain is required for physical binding to MTs. The N-terminus combined with TPX2 gave a thin but continuous labelling, whereas C-terminus combined with TPX2 resulted in a thick and short to punctuate CMT-labelling pattern (**Figure 4h–i, Paper I**). It is interesting to note that the labelling pattern obtained for the full-length construct fused with a marker at the N-terminus (**Figure 4c, Paper I**) could not be reproduced with any of the C-terminally fused truncated constructs, suggesting tag interference (*i.e.*, the position of the tag influences the labelling pattern). By co-expressing all full-length and truncated labelled AtMAP20 constructs with a labelled MAP4 MBD, fused with GFP, it was further confirmed that the labelling observed from the different MAP20 constructs originated from CMTs, and that the absence of labelling was not due to CMT destabilization (**Figure 5a–l, Paper I**). Taken together, the data shows that the TPX2 domain is important for interaction with CMTs, whereas the complete binding capacity of AtMAP20 depends on its N- and/or C-terminus. This is in contrast to other plant (Perrin *et al.*, 2007; Vos *et al.*, 2008) and animal (Brunet *et al.*, 2004) TPX2 family proteins, where full/partial protein function *in vivo* is impaired when C-terminal domain function is tagged/affected, but not the N-terminal domain.

The twisting, helicoidal phenotype of *Arabidopsis* plant organs observed for both PttMAP20- and AtMAP20-OE (Rajangam *et al.*, 2008a) (**Figure 6a, Paper I**) suggests an effect on the dynamic instability of MTs (Buschmann & Lloyd, 2008). Thus, to further evaluate AtMAP20 function on CMT organization *in planta*, WT seedlings and seedlings with ectopic OE of *AtMAP20* were grown horizontally on plates with medium containing suboptimal concentrations of different MT-interacting drugs; taxol, acting as a MT stabilizer, and oryzalin and propyzamide, acting as MT destabilizers (Furutani *et al.*, 2000; Buschmann *et al.*, 2009). When grown in the absence of drugs, AtMAP20-OE displayed shorter roots and a significantly increased root skewing angle, as compared to WT, mimicking the effect of the MT stabilizer taxol. Furthermore, AtMAP20-OE did not respond much when grown under increasing concentrations of taxol (**Figure 6b–c, Paper I**), implying saturation of a taxol-like effect on MTs. When grown on medium containing low concentrations of MT-destabilizing drugs, however, the AtMAP20-OE phenotype was reverted towards longer roots and lower root skewing angle, mimicking WT grown on control medium. WT seedlings did not respond to any large extent, indicating that they were less sensitive to this treatment. With higher concentrations of MT destabilizers, however, WT and AtMAP20-OE responded in a similar fashion with shorter roots and higher root skewing

angle. Together, these observations suggest that MAP20 acts as an MT stabilizer, inducing similar effects as taxol.

OE of *AtMAP20*, truncated in its N-terminus, did not give rise to the same root skewing phenotype as OE of the full-length construct (**Figure 6d–f, Paper I**). This supports the idea of the N-terminal variable domain as a regulating element in order for *AtMAP20* to interact properly with MTs *in planta*, as shown previously with transient expression in tobacco leaves (**Figure 4–5, Paper I**).

In conclusion, the proposed role of *AtMAP20* is to stabilize MTs. It is also concluded that proper MT binding of *AtMAP20* can only be achieved by the TPX2 domain, combined with the N- and/or C-terminal domain, highlighting the importance of these. Furthermore, CMT stabilization and MT-binding specificity *in vivo* appears to be dependent on accessibility to the N-terminal part; *i.e.*, *AtMAP20* requires an intact N-terminal domain to be functional.

4.1.2 *AtMAP20* Is Functioning in Secondary-Walled Cell Types and Required for Proper Cell Wall Composition and Structure (**Paper II**)

The function of *AtMAP20* in *Arabidopsis* was studied by characterizing GUS expression patterns *in planta*, driven by a native 2 kbp promoter sequence. In line with observations from hybrid aspen (Rajangam *et al.*, 2008a), *AtMAP20* was expressed in developing SX of the *Arabidopsis* hypocotyl (**Figure 1g, Paper II**). Expression was also noticed in vascular strands of stem, root and leaves. Expression was not consistent along the strands, however, but rather exhibited an irregular pattern (**Figure 1a–d, Paper II**). Expression was also seen in other secondary-walled cell types, such as phloem fibres, the gynoeceium of flowers and base and top part of siliques (**Figure 1e–g, Paper II**). Interestingly, expression in IFs of the basal stem was only observed sporadically (**Figure 1h, Paper II**). This was in contrast to *CESA7::GUS* plants (used as positive controls), where GUS staining was strong in IFs, but weak in the vascular bundles (**Figure 1h, Paper II**). Thus, it can be concluded that *AtMAP20* expression is confined to cell types with SCW, but not consistently expressed in all SCW cells of a certain type, as opposed to, *e.g.*, the SCW- and VE-specific TFs VND6/VND7 (Yamaguchi *et al.* 2008 and Ohashi–Ito *et al.* 2010). It can also be concluded that *AtMAP20* and *CESA7* is not necessarily co-regulated in the *Arabidopsis* inflorescence stem, as they showed discrepancies in their expression patterns.

For functional analysis, two T-DNA loss-of-function mutants were obtained, where *map20-2* was slightly leaky in its *AtMAP20* transcript, as compared to *map20-1*, which was considered a KO (**Figure 2, Paper II**). Both mutants grew normally; however, *map20-1* exhibited marginally slower growth

rate (**Figure 3, Paper II**). Interestingly, though, when seedlings were grown *in vitro* on agar plates in the dark, the etiolated hypocotyls of *map20* mutants were significantly longer, compared with WT (**Figure 4, Paper II**). A similar, but more pronounced, effect was observed for *irx3-4*, a T-DNA KO mutant in *CESA7* (Brown *et al.*, 2005) (**Figure 4, Paper II**). Both *AtMAP20* and *CESA7* (Gardiner *et al.*, 2003) are expressed in SCW cells only, and for the etiolated hypocotyl, expression will be active in the spiral-shaped and stretchable PXVs found in the stele. Thus, a longer hypocotyl indicates an effect on the SCW of PXVs and, consequently, on their mechanical abilities during primary growth. It is known that null mutations in *CESA7* impair the cellulose biosynthesis machinery and most likely give rise to a weakening in the SCW. It can therefore be suggested that a mechanical weakening in PXVs facilitates turgor-driven expansion of xylem cells, which in dark-grown hypocotyls could promote a general elongation of all adjacent cells. In analogy to this, longer hypocotyls in *map20* mutants could be the result of less rigid PXV SCWs, which thereby releases tissue tension, allowing for elongation. The nature of this novel concept remains to be described, but could be due to a defect in the patterning, or ultrastructure, of the CMFs themselves. Moreover, it was observed that XFs and VEs from short-day hypocotyls were significantly longer in the T-DNA mutants (**Table 1, Paper II**), implying either longer cambial cells and/or intrusive tip growth. If the crystalline structure of the cellulose polymer has, *de facto*, been compromised in *map20* mutants, it is tempting to speculate that this is somehow linked to an extended duration of the cell elongation/growth phase by some unknown mechanism. Though, considering that these mature plants initially germinated and grew in the dark, and that *AtMAP20* is postulated to act on the dynamic instability of CMTs, this can rather be due to secondary effects, yet to be defined.

Chemical analysis of the cell wall by Py-GC/MS, combined with OPLS-DA analysis, confirmed a modification (**Figure 5, Paper II**), but quantitative analysis of major cell wall polymers showed that this was minor (**Table 2, Paper II**), as well as any modification in monosaccharides released after trifluoroacetic acid (TFA) treatment (**Figure 6, Paper II**). This supports the notion that the mutation could cause improper patterning of CMFs; however, it could also imply a delayed and perhaps reduced deposition of CMFs, as the xylem cell growth phase could be prolonged (described earlier). Furthermore, microarray analysis of the KO mutant does not support significant changes in transcript abundance of any cell wall biosynthetic gene (**Table 3, Paper II**), except for the up-regulation of the SCW-related TF MYB63, known to activate the monolignol biosynthesis pathway (Zhou *et al.*, 2009).

In conclusion, *AtMAP20* expression analysis shows that it is only functional during SCW biosynthesis in various cell types. Characterization of loss-of-function T-DNA mutants did not reveal any major growth phenotypes or chemotypes, suggesting that *AtMAP20* function is redundant with other, perhaps stabilizing MAPs, not yet described. Putative candidates include TPX2 family proteins, such as *WDL3* (Liu *et al.*, 2013), and also other MAPs active during SCW/xylem biosynthesis. Although inconclusive, a modified chemotype, accompanied by longer hypocotyl and longer xylem cells, still suggests that *AtMAP20* is limiting proper SCW composition/structure of xylem cells. Furthermore, its MT-binding character, together with its putative impact on the dynamic instability of CMTs, implies that the primary target is related to CMF patterning and structure, which in effect are dependent on the organization of CMTs.

4.1.3 Exploring *AtMAP20* Function by an *Arabidopsis* Cell Culture System, Induced to Differentiate into Xylem Tracheary Elements

Unravelling gene function by analysing mutants/transgenes can be hampered by the fact that plant growth is in a constant homeostasis, and both external and internal cues impact on cell morphology. This prompted for functional analysis of *AtMAP20* by a cell biological approach, using *in vitro Arabidopsis* cell cultures, which copes with some of the problems associated with complex tissues. The establishment of a xylem TE differentiation system in *Arabidopsis* cell cultures constitutes a complementary tool to study gene function during SCW and TE formation (Pesquet *et al.*, 2010). These suspension cells can be induced to differentiate into TEs with up to 40% efficiency. In *Zinnia* TE cell cultures, this process involves SCW patterning, including non-cell-autonomous post-mortem lignification and PCD (Pesquet *et al.*, 2005, 2013). The remaining non-TE cells are still living, but are generally believed to neither undergo cell division nor SCW formation. Rather, they differentiate into a population resembling xylem parenchyma cells; though, further characterization is required to confirm this, depending on the criteria for defining SCW thickening. Nevertheless, the advantage of this system is that cell biological approaches can be applied to the molecular regulation of TE differentiation and SCW biosynthesis. This is more difficult *in planta* since vascular tissues are embedded in the plant body. Here, *AtMAP20* function was initiated in *Arabidopsis* TE cell cultures, and some preliminary results are presented.

First, the transcript profile of *AtMAP20* was monitored during TE differentiation in induced and uninduced basal (WT) cells. *CESA7* was used as a marker gene for the onset and progression of SCW formation in TEs. Transcript abundance of *AtMAP20* and *CESA7* increased in synchrony after

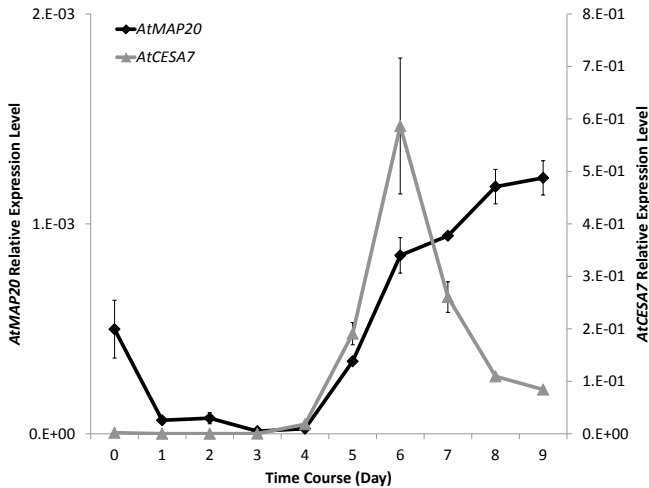


Figure 3. Transcript profiles of *AtMAP20* and *AtCESA7* in induced basal (WT) cell cultures. Experiment was repeated twice with similar results. Error bars are SD for $n =$ three technical replicates. Expression was normalized against that of *AtEF1- α* . No expression was observed in uninduced cultures.

four days when TEs started to differentiate. But, whereas *CESA7* showed a clear peak at day 6 and then decreased to low levels, transcripts of *AtMAP20* continued to accumulate until the end of the culture period at day 9 (**Figure 3**). As the induced cell culture is composed of a mixture of TEs

and of non-TEs, this result suggests that either *AtMAP20* is expressed in both cell types, or only in the living non-TEs. Taking into account, however, GUS expression from the *AtMAP20* promoter observed in VEs *in planta* (**Paper II**) and the possible presence of SCW thickening in non-TEs, it seems reasonable to believe that expression takes place in both cell types.

Second, to unravel the *in vivo* function of *AtMAP20* in TE cell cultures, transgenic lines exhibiting mis-regulation of *AtMAP20* were developed. Six RNAi and five OE lines were identified by qPCR screening and cultured for further analysis. The six RNAi lines were down-regulated in *AtMAP20*, ranging from 3–59% of WT transcript abundance level (data not shown). In all isolated RNAi lines, a fairly large population of cells in the cell culture developed bulky, globular cell phenotypes upon induction with no close resemblance to either TEs or non-TEs (**Figure 4**). Suppression of *AtMAP20* also completely inhibited the differentiation of TEs. It seems plausible that the large, globular cells observed in the cell cultures of RNAi lines were destined to differentiate into TEs, but failed because of unknown factors related to the suppression of *AtMAP20*. No apparent effect of *AtMAP20* down-regulation was observed among the population of non-TEs. The five OE lines were up-regulated in *AtMAP20* in a range from 10- to 40-fold of WT transcript abundance level (data not shown). In contrast to RNAi lines, no visible morphological phenotype was observed in OE lines (data not shown).

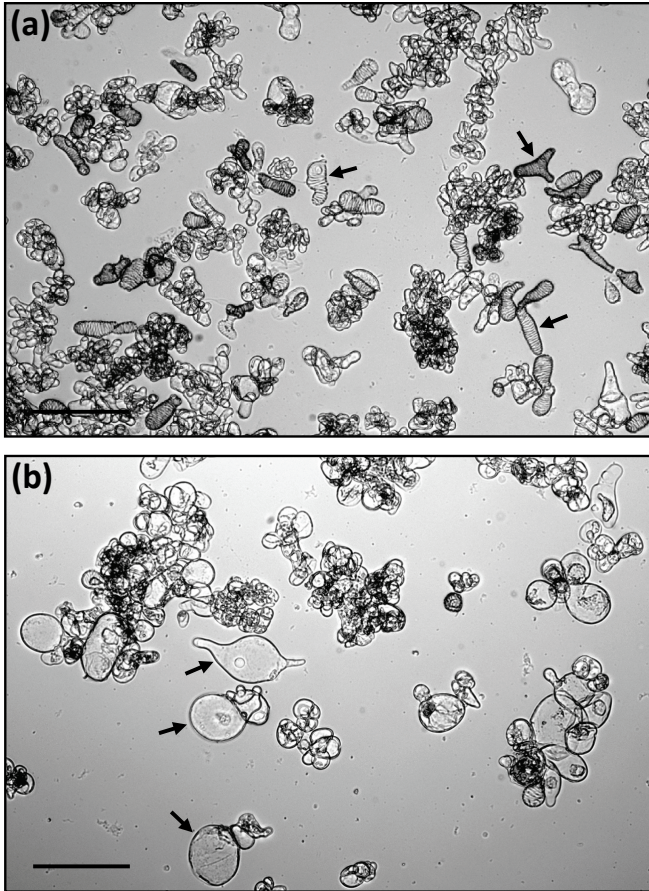


Figure 4. WT (a) and AtMAP20-RNAi (b) cell cultures at day 7. Arrows indicate tracheary elements (a) and undefined bulky globular cells (b), as a consequence of *AtMAP20* suppression. Scale bar = 200 μ m.

Taken together, since *AtMAP20* is implicated to bind strongly to MTs *in vitro* and stabilize MTs strongly *in vivo* (Paper I), it is tempting to speculate that *AtMAP20* down-regulation impairs CMT stabilization, and perhaps bundling, in cells normally destined to become TEs. This would favour a shift towards destabilization, rather than stabilization, of CMT; thus, resulting in an unorganized/rand

omized CMT array and, consequently, isotropic (uniform) cell expansion. Though, this phenotype is not observed *in planta* for the *map20* mutants (Paper II). The reason for this may be sought in the different nature of the experimental systems. The TE cell culture is out of the organism context, in which compensation mechanisms for loss of *AtMAP20* may take place that is absent in the isolated cell. Nevertheless, the cell culture system revealed that the stabilizing effect *AtMAP20* exerts on CMT organization during SCW formation is important for TE differentiation and, hence, SCW patterning.

4.1.4 Mis-Regulation of *PttMAP20* Suggests a Function in Cellulose Microfibril Angle and Xylem Cell Dimension in *Populus*

In addition to investigating the function of *AtMAP20* in *Arabidopsis* (**Paper I–II**), the role of *PttMAP20* in *Populus* was also studied. To visualize *PttMAP20* expression *in planta*, the promoter sequence, corresponding to a 2 kbp fragment upstream the start codon of *PtMAP20*, was cloned and fused with the *GUS* reporter gene. *GUS* staining was investigated in hybrid aspen explants grown *in vitro* and revealed expression in developing XFs and VEs, as well as in ray parenchyma cells (**Figure 5**). Staining was also observed in VC, and phloem cells. Though, more direct measurements of *PttMAP20* expression transcripts in tangential sections across wood forming tissues showed that transcript abundance is very low in these tissues (Rajangam *et al.*, 2008a).

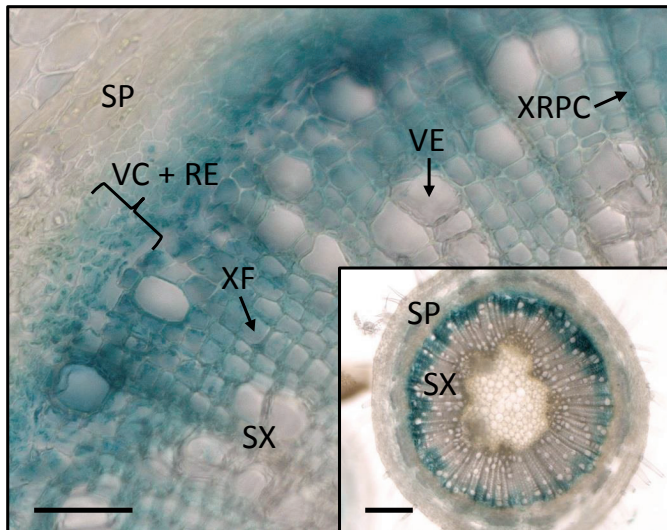


Figure 5. Promoter–*GUS* analysis on transverse freehand-sectioned basal stems of hybrid aspen explants grown *in vitro* for a 2 kbp fragment cloned upstream the start codon of *PtMAP20* (*Populus trichocarpa*). The staining pattern was reproduced in three independent lines. RE, radial expansion zone; SP, secondary phloem; SX, secondary xylem; VC, vascular cambium; VE, vessel element; XF, xylem fibre; XRPC, xylem ray parenchyma cell. Scale bars: large picture = 50 μm , inset picture = 200 μm .

Therefore, the *GUS* staining observed here in the VC and phloem is most likely an effect of diffusion of the *GUS* protein. Nevertheless, the *GUS* results suggest that *PttMAP20* is expressed in all xylem cell types in hybrid aspen.

To perform functional studies of *PttMAP20* in hybrid aspen, the native gene was cloned from a cDNA library into an RNAi and

OE construct under the constitutive 35S promoter. These were transformed into hybrid aspen WT (clone T89) trees. Three lines showing strong up-regulation (*PttMAP20*-OE), together with five down-regulated (*PttMAP20*-RNAi) lines, of *PttMAP20* were selected by qPCR screening (**Table 1**).

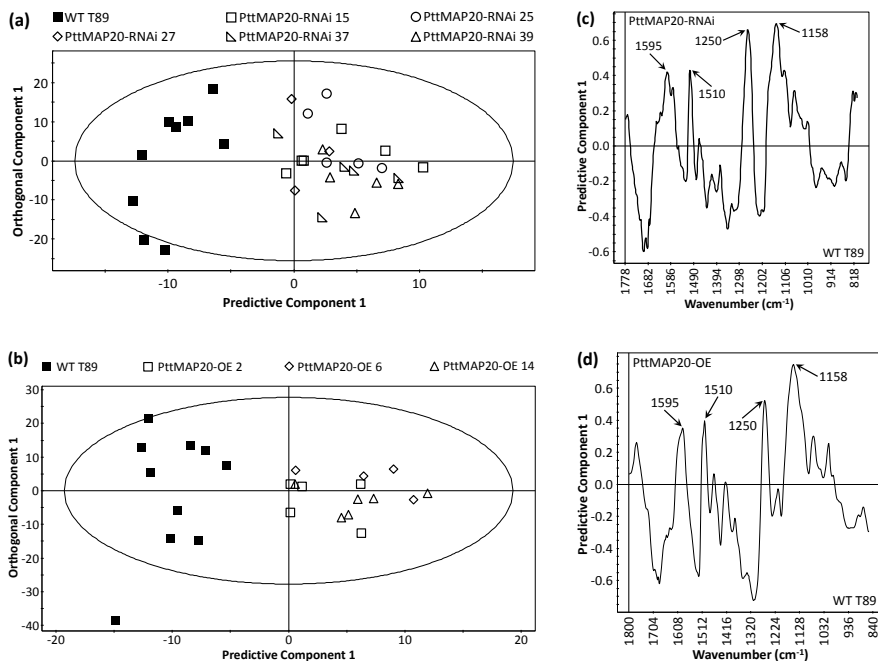


Figure 6. FT-IR microspectroscopic single element analysis on 20 μm transverse sections, sampled from a defined internode in stems of hybrid aspen explants grown *in vitro*. Spectra were acquired from 9–10 (WT) or 3–6 (RNAi/OE) plants per line with four independent spectra per plant. In order to obtain data from homogeneous tissue within the aperture, vessel elements and regions with spontaneously formed tension wood were avoided. OPLS-DA scores plots show the separation between WT and RNAi lines (a) and between WT and OE lines (b). Each symbol represents one plant. Corresponding loadings plots for the predictive component show factors separating WT from RNAi lines (c) and WT from OE lines (d). Arrows indicate cellulose/hemicellulose-related band (1158 cm^{-1}) and lignin-related bands (1250, 1510 and 1595 cm^{-1}), according to Gorzsás *et al.* (2011). Bands with positive loadings are more intense in RNAi/OE lines, whereas band with negative loadings are more intense in WT.

The selected transgenic lines of each construct were used for chemotyping of *in vitro* explants using FT-IR microspectroscopy, combined with OPLS-DA, on SX tissue from transverse sections. This showed a significant change in the chemotype of both OE and RNAi transgenes, compared with WT (**Figure 6**). The loadings plots suggested that the differences in PttMAP20-RNAi and PttMAP20-OE lines were similar. Bands assigned mainly to lignin and cellulose increased, whereas bands characteristic for hemicelluloses (possibly xylan) or unspecific carbohydrates decreased, in proportion to WT (**Figure 6**). Quantitative analysis of lignin by Py-GC/MS further confirmed an increase in OE lines, but not in RNAi lines (**Table 2**). No difference in S/G ratio was

observed. Crystalline cellulose was estimated by Updegraff method, but did not reveal any difference in the transgenic lines (**Table 2**). Furthermore, monosaccharides released after TFA treatment revealed small differences in the transgenic lines with an increase in rhamnose (**Figure 7**). From the chemical characterization, it can be concluded that mis-regulation of *PttMAP20* do affect the chemotype of xylem cell walls. This altered chemotype, however, as observed by FT-IR microspectroscopy combined with OPLS-DA, do not translate into any major quantitative differences of major cell wall polymers. Interestingly, though, in a genome-wide association-mapping study of wood characteristics in *Populus*, Porth *et al.* (2013) identified *PttMAP20* as a candidate gene linked to insoluble lignin content traits, as explained by SNPs (short for single nucleotide polymorphisms), which led the authors to suggest genetic interrelations between cellulose and

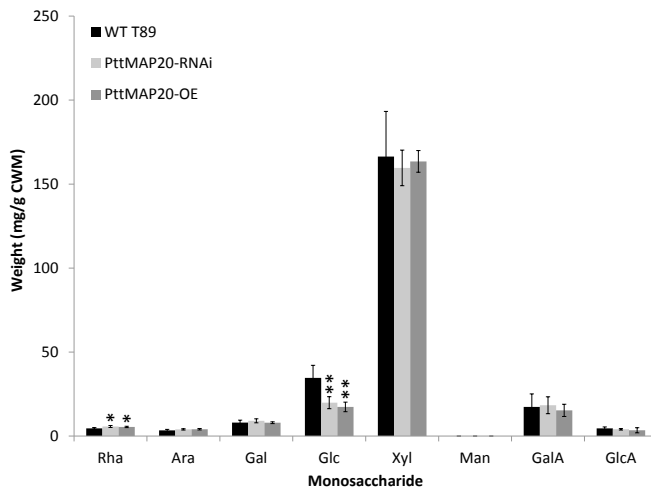


Figure 7. Monosaccharide composition of cell wall material (CWM) from stems of hybrid aspen explants grown *in vitro*. Rha, rhamnose; Ara, arabinose; Gal, galactose; Glc, glucose; Xyl, xylose; Man, mannose; GalA, galacturonic acid; GlcA, glucuronic acid. For WT, values are means \pm SD for $n =$ four biological replicates, each consisting of three pooled stems. For RNAi/OE, values are means \pm SD for $n =$ five (RNAi) or three (OE) biological replicates (one per line), each consisting of six pooled stems from the same line. * $P < 0.05$, ** $P < 0.01$ (Student's t test) for comparison with WT.

conditions, whereas expression of the homologous *PttWDL3A* and *PttWDL4A*, known to be highly expressed across developing SX in hybrid aspen (Rajangam *et al.*, 2008a), were not significantly different from WT (**Figure 8**). All transgenic lines grew normally. The OE trees, however, were slightly

lignin biosynthesis pathways.

Two lines each from RNAi and OE trees (PttMAP20-RNAi line 15 and 37 and PttMAP20-OE line 6 and 14) were grown in the greenhouse up to a height of about 1.8 m.

Mis-expression of *PttMAP20* in RNAi and OE lines were confirmed by qPCR analysis under these growth

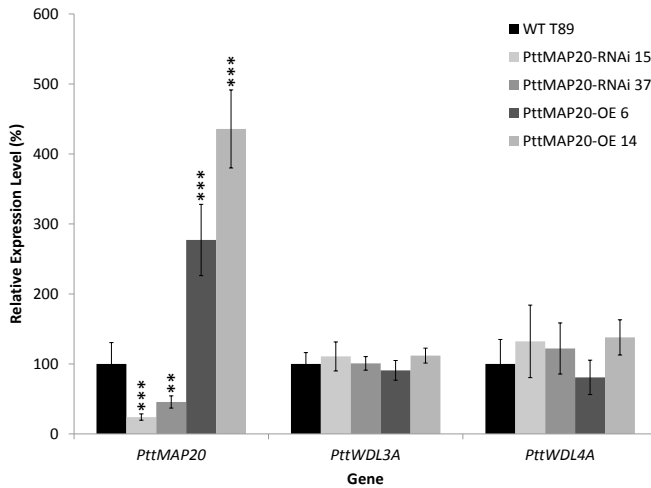


Figure 8. Quantitative PCR analysis of *PttMAP20*, *PttWDL3A* and *PttWDL4A* in developing secondary xylem, scraped from internode 31–40 of greenhouse-grown hybrid aspen trees. Values are means \pm SD for n = eight (WT) or six (RNAi/OE) biological replicates. $**P < 0.01$, $***P < 0.001$ (Student's t test) for comparison with WT.

FT-IR spectroscopy. As opposed to *in vitro* grown explants, the OPLS-DA analysis did not show any differences between transgenic and WT trees (data not shown). A major difference between these two sample types is that SX of explants grown *in vitro* consists of developing (living) XFs, whereas that of greenhouse-grown trees consists mainly of mature (dead) XFs. Thus, developing SX from transverse sections of greenhouse-grown trees were analysed with FT-IR microspectroscopy at different radial distances (*i.e.*, at 400 and 1000 μm) from the VC. Indeed, a difference in chemotype was observed across developing SX when measured at a radial distance of 400 μm from the VC, as depicted from OPLS-DA scores plots (Figure 9). This is in agreement with hybrid aspen explants grown *in vitro*. No difference in chemotype was observed in mature SX, 1000 μm from the VC (data not shown). It can therefore be concluded that the chemotype observed in developing SX is not maintained in mature SX. The exact components underlying the difference in developing SX remains obscure.

Measurements of XF and VE dimensions showed a consistent difference from WT only for OE line 14; *i.e.*, the line with highest OE of *PttMAP20* (Table 4). It had significantly longer and wider XFs and VEs, whereas OE line 6 only had wider XFs. The RNAi lines were not different from WT, although a trend for longer XFs and VEs was observed in line 15, the strongest RNAi line. Increased length of both VEs and XFs in OE line 14, with a larger increase in

smaller in height and leaf size, and line 14 also in stem diameter (Table 3). No obvious abnormalities in stem anatomy could be observed under the microscopy in any of the transgenic lines.

Wood powders from greenhouse-grown trees were chemotyped with

FT-IR

XFs, is reminiscent of the *Arabidopsis map20-1* T-DNA KO mutant (**Paper II**). The increase in VEs, as well as XFs, could be explained by longer cambial initial cells, whereas the proportionally longer XFs indicate an effect on intrusive tip growth (Evert, 2006; Fromm, 2013).

To study any effect on CMF orientation, the MFA of transgenic trees was measured using XRD analysis. Again, the highest OE line 14 was significantly

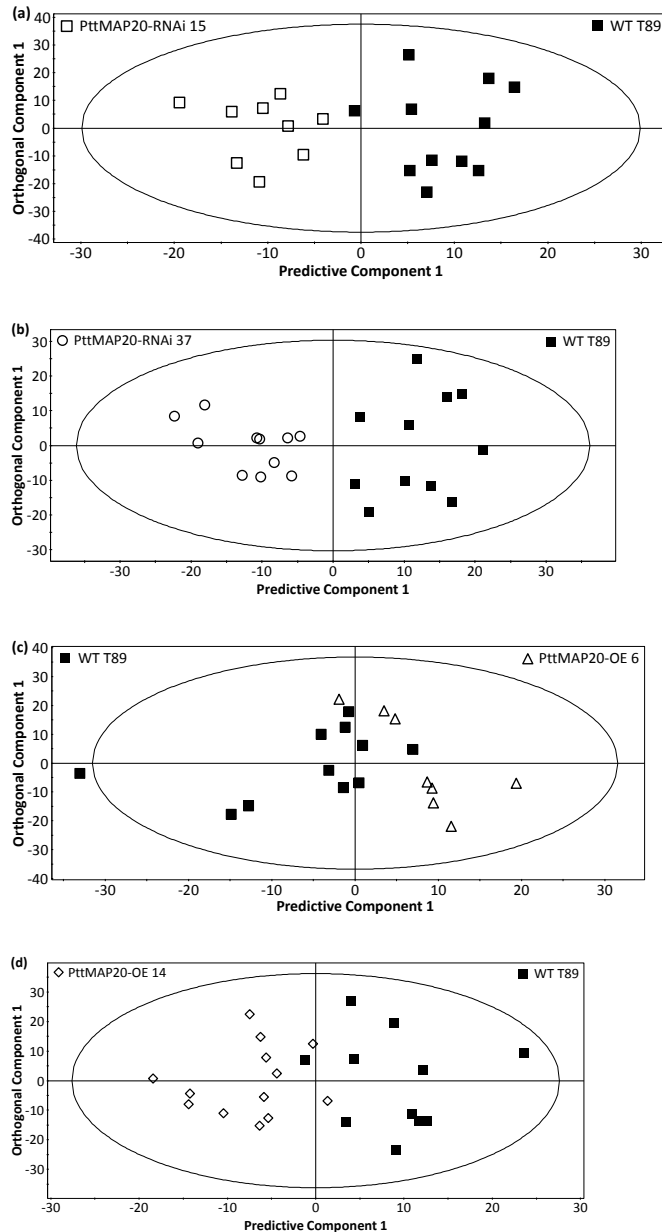
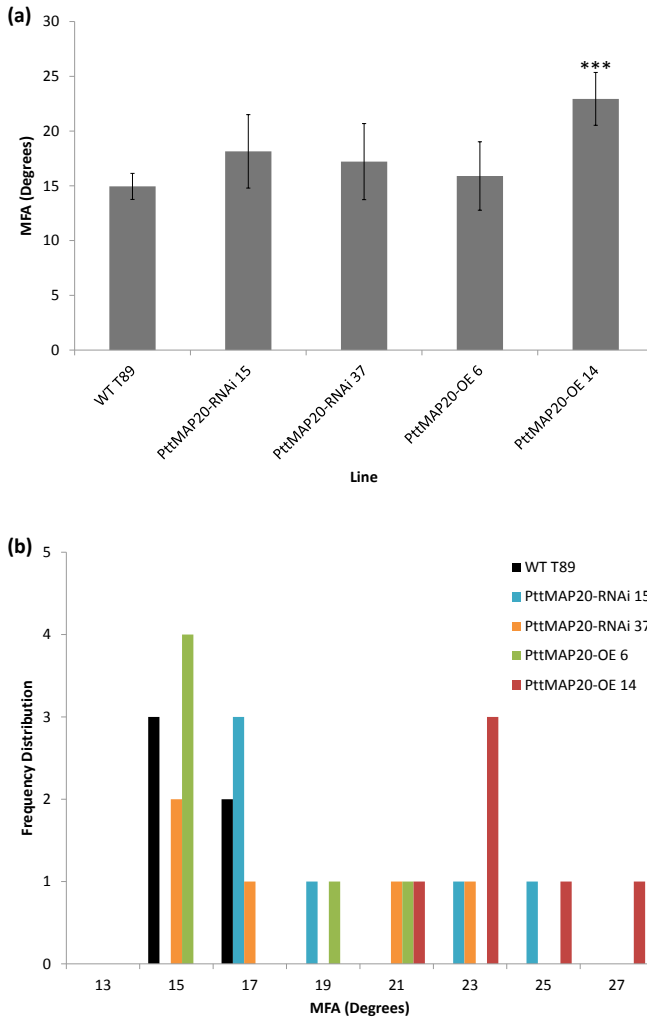


Figure 9. FT-IR microspectroscopic single element analysis on 20 μm transverse sections, sampled from internode 43 in stems of green-house grown hybrid aspen trees. Spectra were acquired at a radial distance of 400 μm from the vascular cambium in 7 (WT) or 5–6 (RNAi/OE) trees per line with 1–3 spectra per tree. In order to obtain data from homogeneous tissue within the aperture, vessel elements and regions with spontaneously formed tension wood, were avoided. OPLS-DA scores plots (a–d) show the separation between WT and RNAi/OE lines. Each symbol represents one spectrum, irrespective of tree. Details on model reliability (quality): (a), $Q^2(\text{cum}) = 0.74$; (b), $Q^2(\text{cum}) = 0.75$; (c), $Q^2(\text{cum}) = -0.05$ and (d), $Q^2(\text{cum}) = 0.56$.

different from WT, exhibiting an increased MFA (**Figure 10a**). Though, whereas WT and OE line 14 displayed a normal distribution pattern of MFA between the replicate trees, the remaining PttMAP20-RNAi and PttMAP20-OE lines showed an irregular distribution pattern (**Figure 10b**). Half of the individuals were similar to WT, and the other half showed significantly higher MFA. These phenomena could be the result of inconsistent down-regulation of *PttMAP20* along the stem in RNAi trees, giving rise to a mosaic effect on the phenotype. This would be revealed by MFA measurements that are made at a very limited SX area, but not by the chemical measurements or XF and VE measurements that includes a homogenized sample of the whole stem. Indeed, mosaic patterns of a lignin phenotype were observed in *Populus* greenhouse-grown trees down-regulated in *CCR* (Leple *et al.*, 2007). Since the lignin modified by *CCR* down-regulation was marked by an orange–brown colour, this effect was visible and therefore easily scored.

Transcriptome analysis was performed on greenhouse-grown trees, representing the two *PttMAP20* down-regulated lines. Although the strongest phenotype was observed in PttMAP20-OE trees, the RNAi lines were selected for this microarray analysis to better reveal endogenous *PttMAP20* function. The down-regulation of *PttMAP20* was confirmed in both transgenic lines, as supported by qPCR data (**Figure 8**). After applying a set of filter criteria, (signal > 50, mis-regulation > 1.2-fold) 354 significant (Student's *t*-test, $P < 0.05$) genes were found to be regulated in a similar fashion in both RNAi lines, compared with WT; 269 of these were down-regulated and 85 were up-regulated (**Table 5**). The microarray data set revealed significant mis-regulation in a number of genes involved in carbohydrate metabolism, along with some recognized TFs, signalling, transport and cell wall related genes. Interestingly, 26 of these (**Table 6**) overlapped with genes mis-regulated by > 1.2-fold in a microarray experiment conducted on basal stem segments from the *map20-1* T-DNA KO mutant in *Arabidopsis* (**Paper II**). Among these overlapping genes, one striking observation was the up-regulation of *IRX8* (*GAUT12*), a gene known to be important for glucuronoxylan biosynthesis (Persson *et al.*, 2007). This is in contrast to the data obtained from FT-IR microspectroscopy and wet chemistry, which rather suggested a decrease in xylan/hemicelluloses. Alternatively, up-regulation of a gene associated with xylan biosynthesis could also indicate a response to compensate for a putatively lower amount of this hemicellulosic polymer.

Taken together, it can be concluded that mis-regulation of *PttMAP20* in *Populus* does affect certain aspects of SX development; however, its function could be redundant with that of other TPX2 family proteins. Considering its role as a CMT stabilizer (**Paper I**), the primary effect is most likely exerted on



the dynamic instability of MT arrays. Although data are not conclusive, due to large between-tree variations, it can be suggested that the altered MFA in *PttMAP20* mis-regulated trees is caused by altered MT dynamics. The observed phenotypes in cell wall chemistry and xylem cell morphology may well be secondary effects from this function.

Figure 10. Microfibril angle (MFA) analysis on radial 80 μm sections of basal stem segments from greenhouse-grown hybrid aspen trees. Values in (a) are means \pm SD for $n = 5$ (WT) or 5–6 (RNAi/OE) trees. *** $P < 0.001$ (Student's t test) for comparison with WT. A frequency distribution plot over measured MFAs in (a) is displayed in (b).

Table 1. *Quantitative PCR analysis of PttMAP20 from a defined internode in stems of WT, RNAi and OE hybrid aspen explants grown in vitro.*

Line	Relative Expression Level (Fold Change)
WT T89	1.00 ± 0.10
PttMAP20-RNAi 15	0.14 ± 0.01
PttMAP20-RNAi 25	0.14 ± 0.05
PttMAP20-RNAi 27	0.11 ± 0.05
PttMAP20-RNAi 37	0.11 ± 0.00
PttMAP20-RNAi 39	0.18 ± 0.03
PttMAP20-OE 2	12.76 ± 0.66
PttMAP20-OE 6	21.41 ± 0.26
PttMAP20-OE 14	37.62 ± 3.62

Values are means ± SD for $n = 3$ technical replicates, each consisting of 12 (WT) or 6 (RNAi/OE) pooled biological replicates.

Table 2. *Lignin and cellulose content from stem cell wall material of WT, RNAi and OE hybrid aspen explants grown in vitro.*

Line	S (%)	G (%)	S/G (Ratio)	S + G (%)	Updegraff Cellulose (mg/g CWM)
WT T89	4.1 ± 0.3	6.3 ± 0.4	0.66 ± 0.04	10.4 ± 0.7	189 ± 22
PttMAP20-RNAi	4.0 ± 0.3	6.3 ± 0.3	0.64 ± 0.06	10.3 ± 0.4	196 ± 18
PttMAP20-OE	4.5 ± 0.4*	6.5 ± 0.2*	0.69 ± 0.05	11.0 ± 0.5*	179 ± 16

Syringyl (S) and guaiacyl (G) lignin units were estimated using Py-GC/MS and are expressed as percentages of total ion counts. For WT, values are means ± SD for $n =$ four biological replicates, each consisting of three pooled stems. For RNAi/OE, values are means ± SD for $n =$ five (RNAi) or three (OE) biological replicates (one per line), each consisting of six pooled stems from the same line. * $P < 0.05$ (Student's t test) for comparison with WT. CWM, cell wall material.

Table 3. *Growth analysis of 10-week-old greenhouse-grown WT, RNAi and OE hybrid aspen trees.*

Line	Plant Height – Final (cm)	Stem Diameter – Final (mm)	Internode Length (cm)	Leaf Length (cm)	Leaf Width (cm)
WT T89	170 ± 14	11.4 ± 1.0	2.4 ± 0.3	16.4 ± 1.1	13.5 ± 1.1
PttMAP20-RNAi 15	168 ± 6	10.9 ± 0.9	2.7 ± 0.1**	16.1 ± 1.1	14.3 ± 1.4
PttMAP20-RNAi 37	159 ± 8	11.2 ± 0.6	2.3 ± 0.1	14.8 ± 2.5	12.6 ± 1.8
PttMAP20-OE 6	156 ± 4*	10.4 ± 0.6*	2.3 ± 0.1	15.1 ± 0.7*	11.8 ± 1.1**
PttMAP20-OE 14	156 ± 7*	11.0 ± 0.5	2.1 ± 0.1*	14.4 ± 0.8**	11.8 ± 0.7*

Plant height was measured twice a week during the entire growth period, along with stem diameter, to estimate the growth rate of stem length and width. In addition, internode length, leaf length and width and final height and width of the stem were measured at the day of harvest. Values are means \pm SD for $n = 10$ (WT) or 8 (RNAi/OE) biological replicates. * $P < 0.05$, ** $P < 0.01$ (Student's t test) for comparison with WT.

Table 4. *Xylem fibre and vessel element morphology of greenhouse-grown WT, RNAi and OE hybrid aspen trees.*

Line	Fibre Length (μm)	Fibre Width (μm)	Vessel Element Length (Tail to Tail) (μm)	Vessel Element Length (μm)	Vessel Element Width (μm)
WT T89	443 \pm 29	21.5 \pm 1.2	326 \pm 17	247 \pm 12	60.5 \pm 4.3
PttMAP20-RNAi 15	473 \pm 27	21.2 \pm 1.2	340 \pm 25	264 \pm 17	59.3 \pm 4.4
PttMAP20-RNAi 37	440 \pm 9	21.8 \pm 0.6	335 \pm 8	258 \pm 11	58.9 \pm 4.1
PttMAP20-OE 6	464 \pm 17	22.8 \pm 0.9*	333 \pm 17	260 \pm 7	60.9 \pm 1.5
PttMAP20-OE 14	494 \pm 26**	23.6 \pm 0.9**	356 \pm 17**	272 \pm 9**	64.9 \pm 1.5*

Cell dimensions for some common xylem cell types were assessed on macerated wood from internode 43. For each tree, 50 fibres and 25 vessel elements were measured. Values are means \pm SD for $n =$ eight (WT) or six (RNAi/OE) biological replicates. * $P < 0.05$, ** $P < 0.01$ (Student's t test) for comparison with WT.

Table 5. *Distribution of genes from microarray data of PttMAP20-RNAi line 15 and 37, and that from a knockout mutant of AtMAP20 in Arabidopsis, described in Paper II, into different functional categories.*

Category ID	Category Name	PttMAP20-RNAi Down-Regulated Genes (Frequency)	PttMAP20-RNAi Up-Regulated Genes (Frequency)	<i>map20-1</i> Down-Regulated Genes (Frequency)	<i>map20-1</i> Up-Regulated Genes (Frequency)
B01	Photosynthesis	0	0	33	3
B02	Major CHO Metabolism	0	0	7	2
B03	Minor CHO Metabolism	3	3	1	3
B04	Glycolysis	0	0	3	5
B05	Fermentation	0	0	0	0
B06	Gluconeogenesis	1	0	2	1
B07	OPP	0	0	2	1
B08	TCA	0	0	1	1
B09	Mitochondrial Electron Transport	0	0	3	1
B10	Cell Wall	2	0	6	12
B11	Lipid Metabolism	1	1	5	10
B12	N-Metabolism	2	0	1	2
B13	Amino Acid Metabolism	2	1	3	14
B14	S-Assimilation	0	0	1	0

B15	Metal Handling	1	0	1	1
B16	Secondary Metabolism	2	1	15	8
B17	Hormone Metabolism	5	3	10	10
B18	Co-Factor and Vitamine Metabolism	1	0	1	5
B19	Tetrapyrrole Synthesis	0	0	5	0
B20	Stress	23	9	9	11
B21	Redox	1	0	12	6
B22	Polyamine Metabolism	0	0	0	1
B23	Nucleotide Metabolism	0	0	1	9
B24	Biodegradation of Xenobiotics	0	0	0	1
B25	C1-Metabolism	0	0	1	0
B26	Miscellaneous	13	6	24	42
B27	RNA	43	6	56	57
B28	DNA	3	1	17	12
B29	Protein	20	7	74	79
B30	Signalling	18	4	22	28
B31	Cell	5	3	7	16
B32	microRNA	0	0	0	0
B33	Development	8	1	12	13
B34	Transport	21	4	27	18
B35	Not Assigned	66	15	199	175
N/A	N/A	10	8	34	48
Σ	Total	269	85	595	595

Frequencies are based on *Populus* and *Arabidopsis* (**Paper II**) genes significantly (Student's *t* test, $P < 0.05$) mis-regulated by more than 1.2-fold, in comparison with respective WT, with signal intensity values > 50 . N/A, not available.

Table 6. *Microarray data showing mis-regulated genes for PttMAP20-RNAi line 15 and 37, in comparison with WT T89, that were in common with that from a knockout mutant of AtMAP20 in Arabidopsis, described in Paper II.*

POPTR ID v2.2	Regu- lation	AGI ID	At Symbol	TAIR9 Annotation
POPTR_0009s01380	Down	At2g28070		ABC transporter family protein
POPTR_0016s04240	Down	At2g41560	ACA4	ACA4 (AUTO-INHIBITED CA(2+)-ATPASE, ISOFORM 4); calcium-transporting ATPase/ calmodulin binding
POPTR_0005s00460	Down	At1g11910		aspartyl protease family protein
POPTR_0016s13620	Down	At5g03570	ATIREG2	ATIREG2 (IRON-REGULATED PROTEIN 2); nickel ion transmembrane transporter

POPTR_0044s00270	Down	At4g27290		ATP binding / protein kinase/ protein serine/threonine kinase/ protein tyrosine kinase/ sugar binding
POPTR_0004s01880	Down	At4g21760	BGLU47	BGLU47 (Beta-glucosidase 47); catalytic/ cation binding / hydrolase, hydrolyzing O-glycosyl compounds
POPTR_0011s02840	Down	At1g29810		dehydratase family
POPTR_0010s04860	Down	At1g70000		DNA-binding family protein
POPTR_0004s04670	Down	At1g28330	DRM1, DYL1	DYL1 (DORMANCY-ASSOCIATED PROTEIN-LIKE 1)
POPTR_0012s14200	Down	At5g62200		embryo-specific protein-related
POPTR_0003s17500	Down	At1g32550		ferredoxin family protein
POPTR_0011s13600	Up	At5g54690	GAUT12, LGT6, IRX8	GAUT12 (GALACTURONOSYLTRANSFERASE E 12); polygalacturonate 4-alpha-galacturonosyltransferase/ transferase, transferring glycosyl groups / transferase, transferring hexosyl groups
POPTR_0014s18240	Up	At5g63230		glycosyl hydrolase family protein 17
POPTR_0006s21140	Down	At1g15670		kelch repeat-containing F-box family protein
POPTR_0004s24010	Down	At5g49760		leucine-rich repeat family protein / protein kinase family protein
POPTR_0015s07270	Down	At1g74360		leucine-rich repeat transmembrane protein kinase, putative
POPTR_0009s10980	Down	At2g03500		myb family transcription factor
POPTR_0014s12480	Down	At1g02860	NLA, BAH1	NLA (nitrogen limitation adaptation); ubiquitin-protein ligase
POPTR_0017s07600	Down	At2g36690		oxidoreductase, 2OG-Fe(II) oxygenase family protein
POPTR_0001s14620	Down	At1g15520	PDR12, ATPDR12	PDR12 (PLEIOTROPIC DRUG RESISTANCE 12); ATPase, coupled to transmembrane movement of substances
POPTR_0015s09150	Down	At1g17100		SOUL heme-binding family protein
POPTR_0005s08370	Down	At5g65210	TGA1	TGA1; DNA binding / calmodulin binding / transcription factor
POPTR_0002s20100	Down	At3g62650		unknown protein
POPTR_0004s04420	Down	At4g32480		unknown protein
POPTR_0005s07420	Down	At1g17840	WBC11, ABCG11, DSO, COF1, ATWBC11	WBC11 (WHITE-BROWN COMPLEX HOMOLOG PROTEIN 11); ATPase, coupled to transmembrane movement of substances / fatty acid transporter
POPTR_0004s08240	Down	At1g66140	ZFP4	ZFP4 (ZINC FINGER PROTEIN 4); nucleic acid binding / transcription

Populus genes listed are mis-regulated by more than 1.2-fold in either RNAi line with signal intensity values > 50. Three biological replicates, each consisting of two pooled greenhouse-grown hybrid aspen trees, were assessed. The expression (up/down) for each gene listed was significantly different from WT (Student's *t* test, $P < 0.05$). *Arabidopsis* genes listed were mis-regulated by more than 2-fold in *map20-1*, compared with WT (Col-0), as described in **Paper II**.

4.1.5 Summary of *MAP20* Function in *Arabidopsis* and *Populus*

PttMAP20 was first recognized by Rajangam *et al.* (2008a) as a highly expressed MAP in SX-forming tissues of hybrid aspen. It contains a TPX2 MT-binding domain and belongs to the family of TPX2-related proteins that are all predicted to have MT-binding capacities (Evrard *et al.*, 2009). As demonstrated in this thesis, *AtMAP20* is generally expressed during SCW formation of different tissues and cell types in *Arabidopsis*, whereas no significant expression was observed in cells with PCWs only (**Paper II**). Thus, MAP20 belongs to the increasing family of SCW MAPs, including MAP65s (*e.g.*, MAP65-8), MAP70-1, MAP70-5, MIDD1, FRA1 and FRA2. Whereas *MAP20* expression appears to be confined only to SCW-forming cell types, literature is scarce for similar specificity in expression concerning other SCW MAPs. Because *AtMAP20* is not consistently expressed in all cell types where SCW formation is taking place (**Paper II**), MAP20 function is likely to be redundant with other SCW MAPs. Likely candidates include some of the already identified MAPs, or other yet to be described MAPs (*e.g.*, other TPX2 domain containing proteins fall into this category).

The redundancy of MAP20 becomes obvious when studying KO mutants of *AtMAP20* in *Arabidopsis* (**Paper II**) and is also suggested from transgenes down-regulated in *PttMAP20* in hybrid aspen (**Section 4.1.4, this thesis**). In both cases, only weak growth phenotypes and chemotypes could be observed. Considering the general function of MAPs in organizing the CMT network, and the importance of CMTs for the patterning and ordered deposition of CMFs in the cell wall, it can be expected that a primary effect from *map20* mutants would be on cellulose ultrastructure and patterning. For SCW-specific MAPs, such as MAP20, this would in turn be reflected on mechanical strength/stiffness in stems and roots. Results from *PttMAP20*-RNAi trees in hybrid aspen, described in this thesis, indicate a small effect on MFA of XFs. Furthermore, KO mutants of *AtMAP20* in etiolated *Arabidopsis* seedlings exhibit longer hypocotyls, an observation that can be related to a weaker mechanical strength of the PXVs (**Paper II**). Though, due to inconsistent results between replicate trees in hybrid aspen, and a lack of direct measurements on mechanical properties and cellulose MFA in *Arabidopsis* plants, further confirmatory data is required to conclusively establish a role for

MAP20 in CMF deposition of SCWs. Although PttMAP20-OE does not reveal the endogenous function of the protein, one of the phenotypes in these trees suggests a role in determining cellulose MFA of XFs. Minor, but significant, effects were also observed in cell wall chemistry and xylem cell morphology in *MAP20* mis-regulated hybrid aspen trees and loss-of-function *Arabidopsis* mutants. Though, these are likely to be secondary effects to a presumed altered integrity of the cellulose polymer structure.

A much more dramatic phenotype was observed when *AtMAP20* was down-regulated in *Arabidopsis* TE cell cultures (**Section 4.1.3, this thesis**). This was manifested by a complete loss of TE differentiation and the emergence of a large and globular cell type population. Intuitively, these results suggest that TE differentiation is perturbed by down-regulation of *AtMAP20*, and that anisotropic expansion takes place due to an aberrant structure of CMFs. Considering that the observed phenotype is unique to TE cell cultures, and not observed *in planta*, it can be inferred that the TE cell culture system is missing some component(s) present in the whole plant context. Further studies are still required to understand the phenotype occurring in the TE system, which might provide key information about MAP20 function and its effect on the dynamic instability of CMTs.

Biochemical and genetic studies were conducted to reveal the cellular function of AtMAP20 on CMT organization (**Paper I**). AtMAP20 binds with high affinity to MTs *in vitro*. Further, domain-mapping experiments showed that the central TPX2 domain is required for direct binding to MTs *in vivo*, whereas full MT-binding capacity also relies on accessibility to the N- and/or C-terminal end. The right-handed twisting of AtMAP20-OE plants, together with shorter, skewing roots, indicates that AtMAP20 is acting as an MT stabilizer, mimicking a phenotype induced by the MT-stabilizing drug taxol. As increasing concentrations of this drug did not add any substantial effect to the root phenotype, AtMAP20-OE is expected to stabilize MTs strongly *in vivo*. Finally, truncation of the N-terminal domain concluded that the MT stabilization function *in planta* is dependent on the full sequence of this end.

Taken together, the results presented in this thesis suggest that MAP20 functions in stabilizing MTs and, hence, has a role in CMF alignment/structure in SCWs. In comparison, other plant TPX2 family proteins have widely different functions. The TPX2 protein itself is a nucleus-located MAP, crucial for mitotic spindle assembly during cytokinesis (Vos *et al.*, 2008). WDL3 is associated with anisotropic cell expansion in *Arabidopsis* roots and shoots (hypocotyls) (Liu *et al.*, 2013). Further, it was found that mis-regulation of *WVD2* and *WDL1* in *Arabidopsis* led to root skewing and organ handedness Yuen *et al.* (2003), and *WVD2* was shown to localize to CMTs and bundle

MTs *in vitro* (Perrin *et al.* (2007), consistent with a putative function in CMT array organization. PttMAP20 was previously demonstrated *in vitro* to bind to the cellulose inhibitor DCB, and therefore suggested to directly or indirectly interact with the cellulose biosynthesis machinery, as binding to DCB did not affect PttMAP20 binding to MTs (Rajangam *et al.*, 2008a). Even if such a function still remains a possibility, the findings accounted for in this thesis do not directly support such a model. Rather, considering its stabilizing function, there is a possibility for MAP20 in *Populus* and *Arabidopsis* to also bundle CMTs, perhaps in association with other redundant MAPs; thus, facilitating biosynthesis of a multi-layered SCW with differing MFAs. Further research is, however, required to define MAP20 regulatory function on CMT dynamics.

4.2 MYB103 Is Required for Syringyl Lignin Biosynthesis in *Arabidopsis* Inflorescence Stems (**Paper III**)

The TF *MYB103* (At1g63910) was initially identified by Zhong *et al.* (2008) as a member of the transcriptional network regulating SCW biosynthesis in *Arabidopsis*. They observed that MYB103 was strongly down-regulated in SND1-/NST1-RNAi plants and showed that it was a direct target of the SWN master switches SND1/NST1, NST2 and VND6/VND7, by promoter transactivation analysis in *Arabidopsis* leaf protoplasts. Promoter-GUS analysis visualized MYB103 expression in developing IFs, XFs and VEs in stems and in developing secondary XFs in roots. They further showed that protoplasts transfected with a MYB103-OE construct induced expression of a GUS reporter gene, driven by the *CESA8* promoter, and hypothesized that MYB103 was important for cellulose biosynthesis. Whereas RNAi inhibition did not cause any visible growth phenotype, probably due to functional redundancy with other protein(s), DR caused a severe reduction in SCW thickening in IFs and XFs. The authors further observed that OE resulted in an increase in SCW thickening in the same cell types.

The closest *Arabidopsis* homologs to *MYB103* are *MYB26* (At3g13890) and *MYB67* (At3g12720). MYB26 is required for SCW deposition in stamen/anther development (endothecium) (Yang *et al.*, 2007). In the same clade (Stracke *et al.*, 2001; Dubos *et al.*, 2010), more distantly related genes are *MYB86* (At5g26660), *MYB55* (At4g01680), *MYB50* (At1g57560) and *MYB61* (At1g09540), where mutations in *MYB61* results in pleiotropic effects influencing lignin deposition (Newman *et al.*, 2004), mucilage production (Penfield *et al.*, 2001) and closure of stomatal aperture (Liang *et al.*, 2005). It has been suggested that MYB61 plays a role in carbon allocation upstream of these phenomena (Dubos *et al.*, 2010).

There are two orthologs of MYB103 in *Populus* (JGI, v1.1, http://genome.jgi-psf.org/Poptr1_1/Poptr1_1.home.html); *PtrMYB10* (grail3.0008045101) and *PtrMYB128* (grail3.0018034201), which functions remains unknown (Wilkins *et al.*, 2009). Furthermore, a whole-genome BLASTx tool, described in Sjödin *et al.* (2009) and implemented at PopGenIE (<http://popgenie.org/>) of *P. trichocarpa* v2.2 genes downloaded from Phytozome (Tuskan *et al.*, 2006), against *Arabidopsis* (TAIR10 release) genes identified two new gene models in *Populus* (POPTR_0001s09810 and POPTR_0003s13190, respectively), rejecting the old ones. Obviously, new releases of the *P. trichocarpa* genome assembly require revisits and updates on gene models and phylogenetic relationship with *Arabidopsis* homologs and orthologs. From the recent advances in gene annotation (*Populus trichocarpa* v3.0, DOE-JGI, Phytozome), *PtrMYB10* and *PtrMYB128* are now annotated as Potri.001G099800 and Potri.003G132000, respectively.

The suggested function of *MYB103* as a regulator of SCW formation by Zhong *et al.* (2008) was an important foundation for the work in **Paper III**. Homozygous seeds of two T-DNA mutants (*myb103-1* and *myb103-2*, respectively) were isolated by genotyping. *myb103-1* turned out to be a null mutant, whereas *myb103-2* had about 100% of WT transcript level (**Figure 1b, Paper III**). *myb103-2* transcript was not functional, however, as phenotyping data on both mutants was coherent, described in detail later. No visible morphological or anatomical growth phenotype could be observed when compared with WT (**Figure S2, Paper III**). Though, when basal stem segments were analysed with Py-GC/MS, combined with OPLS-DA, both mutants exhibited a strongly reduced S/G lignin ratio and separated clearly from WT on a scores plot (**Table 1 & Figure S3, Paper III**). The amount of S lignin was reduced by 70–75%, compared with WT, and this was accompanied by an equivalent increase in G lignin, leaving the total lignin amount unaltered. Thus, the decrease in S lignin was compensated for by a concomitant increase in G lignin. The reduced S/G lignin ratio in basal stem segments was confirmed by 2D NMR analysis, combined with OPLS-DA, where the main loadings were related to S and G lignin (**Figure 2, Paper III**). Nevertheless, minor loadings also revealed other cell wall modifications, compared with WT; glucomannan and cellulose were decreased in both mutants, whereas xylan was increased (**Figure S4, Paper III**). The same material was further analysed for Klason lignin, Updegraff (crystalline) cellulose and monosaccharides (**Table 1–2, Paper III**), which largely supported results obtained from Py-GC/MS and 2D NMR.

The S/G lignin ratio displays large variation, not only between different plant taxa, but also between different xylem cell types within the same plant

(Boerjan *et al.*, 2003). In *Arabidopsis* inflorescence stems, the IFs are rich in S lignin, in contrast to VEs and XFs in the vascular bundle, as demonstrated by Meyer *et al.* (1998) and Patten *et al.* (2010). To specifically assess chemical modifications in different cell types (*i.e.*, VEs, XFs and IFs) in the *myb103-1* mutant, transverse sections of the basal inflorescence stem (**Figure 3a, Paper III**) were analysed by FT-IR microspectroscopy, coupled with an FPA detector, and combined with OPLS-DA. Prior to comparing mutants with WT, the chemotype of these three cell types were first evaluated in WT plants. On a scores plot, they all separated from each other (**Figure 3b, S5, Paper III**) and pairwise comparison from OPLS-DA loadings plots indicated higher proportion of S lignin in IFs and higher proportion of G lignin in VEs and XFs (**Figure 3c–e, Paper III**). A higher relative lignin amount in VEs, compared with XFs, could also be concluded, as could a potentially higher relative amount of hemicellulose in XFs. *myb103-1* displayed a clear separation from WT on an OPLS-DA scores plot for all cell types (**Figure 4a–c, Paper III**). A similar pattern of bands on the corresponding loadings plots contributed to the separation (**Figure 4d–f, Paper III**), suggesting similar chemical modification in their cell walls. This is in line with previous observations that MYB103 is indeed expressed in all three cell types (Zhong *et al.*, 2008). The set of bands that were more intense in mutants have all been related to G lignin (Faix, 1991). Thus, cell-specific FT-IR microspectroscopy shows that MYB103 is acting in all xylem cell types in the basal stem to stimulate S lignin biosynthesis.

In the phenylpropanoid pathway, F5H has been identified as a key enzyme that determines the composition of S and G lignin monomers and, hence, the S/G lignin ratio in the polymer in xylem cells of angiosperms (Chapple *et al.*, 1992; Meyer *et al.*, 1996, 1998; Marita *et al.*, 1999; Ruegger *et al.*, 1999; Franke *et al.*, 2000). Its expression is required for diverting the production of monolignols away from G lignin and instead steering it towards S lignin and sinapic acid biosynthesis. As anticipated, *F5H* was indeed down-regulated by about 75% in both *myb103* mutants (**Figure 5, Paper III**), verifying that this is a key target of MYB103. Furthermore, allelic complementation of the two *myb103* mutants by reciprocal crossing generated F₁ heterozygous offspring that were modulated in a similar fashion as their homozygous parental lines, with respect to S and G lignin composition and *F5H* transcript level (**Figure S1g–i, Paper III**). To compare the effects of *MYB103* KO with that of a KO mutant in *F5H* (*f5h1*), their metabolomes were analysed. Whereas their metabolic profile differed from WT, they also differed from each other (**Figure 6a, Paper III**). The main variable separating *myb103-1* from *f5h1-4* is the absence of sinapoyl malate in the latter (**Figure S6, Paper III**). Because

sinapoyl malate is produced predominantly in epidermal tissue (Li *et al.*, 2010), it is plausible that *myb103-1* exhibits normal transcript levels of *F5H* in epidermal cells, since *MYB103* is not expressed there. When only metabolites derived from the oxidative coupling of G and S alcohols are considered, *f5h1-4* and *myb103-1* do display highly overlapping metabolic profiles. Both mutants exhibit increased levels of only G-containing oligolignols (**Figure 6b, Paper III**) and decreased levels of S-containing oligolignols (**Figure 6c, Paper III**), but to different levels since S lignin biosynthesis is not completely blocked in *myb103-1* due to the presence of smaller amounts of *F5H* transcripts.

A microarray experiment was conducted to provide insight into transcriptome changes in both *myb103* mutant lines. Genes mis-regulated by > 2-fold, compared with WT, and with a signal strength of > 50 were considered (**Table 3, Paper III**). Most of the mis-regulated genes were down-regulated and responded in a similar manner in both mutant lines. The down-regulation of *F5H* was confirmed, and it was one of the most down-regulated genes. In addition, the transcriptome analysis also revealed mis-expression of several recognized SCW-related TFs and biosynthesis genes, such as *MYB20*, *MYB63*, *MYB69*, *SND2* and *SND3* (Wang & Dixon, 2011; Hussey *et al.*, 2013). Among the down-regulated cell wall related genes were two that encode MT-binding proteins (MAP65-8 and MAP70-5), thought to influence SCW formation (Mao *et al.*, 2006; Smertenko *et al.*, 2008; Pesquet *et al.*, 2010); LAC17, which has been shown to be important for lignification (Berthet *et al.*, 2011) and CSLA9, which is thought to be involved in mannan biosynthesis (Goubet *et al.*, 2009; Davis *et al.*, 2010). Remarkably, neither of the SCW master switches were significantly mis-regulated, nor were any of the SCW *CESA* genes, despite the fact that MYB103 can potentially induce the expression of *CESA8 in vitro*, as demonstrated by Zhong *et al.* (2008). Though, expression analysis of the three SCW *CESAs* by qPCR showed a small, but significant, down-regulation of *CESA4* in *myb103-2* (**Figure 5, Paper III**). This is in accordance with a small decrease in cellulose in *myb103* plants, implicated by 2D NMR analysis (**Figure S4, Paper III**). Thus, a role for MYB103 in cellulose biosynthesis cannot be entirely excluded.

The mis-regulation of some recognized TFs was intriguing; possibly, these are direct/indirect downstream targets of MYB103. When MYB103 and some other selected NAC and MYB TFs were tested for interaction with the promoters of some of the early genes in the phenylpropanoid pathway, only *SND2* had a small positive effect, whereas MYB69 had a small negative effect, in transactivating the *F5H* promoter (**Table 4, Paper III**). The most striking observations were the positive transactivation of some other monolignol promoters, mediated by MYB20 and MYB63. For the latter, this is in line with

its postulated role as a positive and specific inducer of genes in the monolignol biosynthesis pathway, and that this transcriptional activation is mediated through interaction with the AC element in their promoters (Zhou *et al.*, 2009). Surprisingly, no activation of the *F5H* promoter by SND1 was observed, in contrast to previous reports by Zhao *et al.* (2010). In their study, however, *Arabidopsis* *SND1* gene was used as an effector and *Medicago* *F5H* promoter as a reporter, making a direct comparison somewhat problematic and even misleading, as also verified in **Figure S7b, Paper III**. The activation is most likely due to the fact that the *MtF5H* promoter sequence contains several MYB1AT motifs (a type of MYB-binding AC element), which are lacking in the *AtF5H* promoter (**Table S1 & Figure S7a, Paper III**). In addition, *AtF5H* was neither a direct target of AtSND1, in a global protoplast transactivation study (Zhong *et al.*, 2010c), nor of AtVND7, in an *in vitro* TE transdifferentiation study (Yamaguchi *et al.*, 2011). Thus, interaction with *MtF5H* by AtSND1 might not reflect a true direct activation universal for angiosperms and should, hence, be viewed with caution. Even transient expression analysis *in vitro* should be viewed with caution, since effectors (TFs) might need additional co-factor(s) to bind to their reporter targets (promoters) for their true function *in planta*.

In conclusion, the specific mode of action of MYB103 cannot be provided, nor can the specific molecular mechanism regulating *F5H* expression and S/G lignin ratio in developing SCWs. In fact, it has been suggested (Zhao & Dixon, 2011) that regulation of SCW biosynthesis is far more complex than the linear feed-forward loops, often depicted in transcriptional network overviews. Nevertheless, the study in **Paper III** clearly demonstrates that a loss-of-function of *MYB103* triggers a strong decrease in *F5H* expression and therefore causes a large reduction in S lignin and S/G lignin ratio in *Arabidopsis* stems. Taken together, *MYB103* is required for *F5H* expression.

4.3 Analytical Pyrolysis, Coupled with Gas Chromatographic / Mass Spectrometric Separation, as a High-Throughput Method for Chemical Characterization of Lignocellulosic Plant Material (**Paper IV**)

Py-GC/MS has the potential to be used as a high-throughput analytical platform for lignocellulosic (*i.e.*, cell wall material, CWM) samples. It has the advantage of being relatively fast and can handle small sample amounts. Moreover, the complete CWM can be analysed without prior separation of individual cell wall components, providing a chemical fingerprint of the sample. A major bottleneck for its use as a high-throughput tool has been the

lack of efficient data processing tools. This was recently solved, however, by applying MCR-AR to Py-GC/MS data handling (Gerber *et al.*, 2012).

In **Paper IV**, two applications for high-throughput chemotyping of plant material, using PY-GC/MS, was demonstrated. First, its use as a screening tool for analysing putative *Arabidopsis* SCW mutants. Second, its use as a microanalytical tool on cryo-sectioned samples for analysing the lignin content and composition across SX-forming tissues in *Populus*. The setup used in these studies allowed for 300 samples to be analysed in less than 7 days, and samples down to 1 µg could be analysed with high reliability.

For the first application, 31 genotypes with either the Columbia or Wassilewskija ecotype background (**Table S1, Paper IV**) were classified with hierarchical clustering, according to their chemotype. Based on previous work by Pesquet *et al.* (2005), these mutants were all hypothesized to be important for SCW formation, because homologous genes in *Zinnia* were all up-regulated upon induction of xylem TE differentiation in cell cultures. Positive controls of previously characterized mutants related to major wall polymers (*i.e.*, cellulose, hemicelluloses and lignin) were also included for comparison and method evaluation. Furthermore, a surplus of WT plants provided a large coverage for the natural variation within each ecotype used. The whole experiment included 305 samples that were run in 1 experiment. Spectra were processed, analysed by OPLS-DA and hierarchical clustering performed on the loadings vectors from bootstrapped, class-balanced OPLS-DA models between one mutant genotype and WT samples. This approach removes systematic variation (in this case, the use of two different ecotypes) and therefore allows for comparison of all samples. The resulting heat map (**Figure 1, Paper IV**) showed that the positive controls, deficient in lignin and carbohydrates, made two different clusters. Other mutants with a chemotype different from WT could be identified according to the number of misclassifications in the bootstrapping. From the genotypes analysed here, six mutants with strong modification in their chemotype, not previously described, were identified. The samples used were not extracted; *i.e.*, soluble compounds, such as sugars, secondary metabolites, *etc.*, were not removed from the plant material, prior to analysis. Thus, any mutant chemotype could reflect changes in both soluble and insoluble CWM fractions. Nevertheless, the method described here can also be applied to extracted CWM alone.

For the second application, microanalysis of cryo-dissected longitudinal tangential sections (10 µm thick) from field-grown *Populus* trees was carried out to study the succession of lignification from the phloem, across the SX and to the first annual ring. The typical spatio-temporal relationship between S, G and H lignin monomers, obtained from non-extracted CWM, is illustrated in

Figure 2–3, Paper IV. The data shows that both S and G lignin increase in parallel. This is of interest, since there is a variation in the spatio-temporal regulation of S/G lignin ratio *in planta* (Donaldson, 2001). Thus, the data analysed in **Paper IV** suggest that this is not due to an unequal presence of these two monomers; rather, their spatial distribution might be different in the symplasm vs the apoplasm.

In conclusion, assessing the currently established Py-GC/MS platform, described in **Paper IV**, offers an overall advantage as an unambiguous, high-throughput chemical analysis tool in addressing a biological problem. This was mainly manifested by, first, the flexibility in lignocellulosic sample type (*e.g.*, herbs, trees, *etc*), second, the low sample amount required (> 1 µg) and, third, a suitable complement to alternative techniques (*e.g.*, FT-IR, NIR and Raman). Though, if the desire is to analyse the composition of cell walls only, applying non-extracted CWM could lead towards bias and, hence, misinterpretations; a potential drawback. Nevertheless, this can be overcome by using extract-free CWM, obtained by a wet chemistry approach, which includes only an additional downstream step; albeit, rather time-consuming.

5 Conclusions and Future Perspectives

5.1 Main Conclusions

Plant SCWs feature complex structures that are built according to instructions from TFs with a role to coordinate a cascade of downstream gene expression. TFs are, in their turn, regulated by upstream influences of different plant hormones, environmental stimuli and other signalling mechanisms. Downstream the TF regulating network, MAPs along with cell wall biosynthesis genes are important contributors to the biosynthesis of SCW-forming cells, including xylem cells.

This thesis emphasizes the function of the TF MYB103 in SCW biosynthesis. In **Paper III**, MYB103 was demonstrated to be required for S lignin biosynthesis and therefore an important determinant in S/G lignin ratio of xylem cell walls. MYB103 acts upstream the expression of *F5H*, which codes for an essential enzyme in the S lignin biosynthesis pathway in angiosperms. In *Arabidopsis myb103* loss-of-function mutants, *F5H* was down-regulated in proportion to the lowered S lignin content. The direct downstream target(s) of MYB103, however, remains to be established.

In **Paper I–II**, the role of *AtMAP20* was studied and demonstrated to be specifically expressed in SCW-forming cell types. *AtMAP20* binds strongly to MTs *in vitro* and stabilizes them strongly *in vivo*. This binding specificity was shown to be dependent on an intact N-terminal sequence. Further, the centrally located TPX2 domain, in combination with the N- and/or C-terminal domain, was required for full MT-binding capacity. Loss-of-function *map20* mutants in *Arabidopsis* exhibited longer hypocotyls in dark-grown seedlings, hypothesized to be due to affected cellulose structure and impaired PXV walls. Mis-expression of *PttMAP20* in transgenic *Populus* trees caused an effect on cellulose MFA (**Section 4.1.4, this thesis**), which is important for mechanical properties. At the cellular level, *AtMAP20* was implicated in regulating the

dynamic instability of MTs; OE mimicked the stabilizing effect of the drug taxol. Thus, it can be concluded that AtMAP20 functions as an MT stabilizer. Taken together, MAP20 is proposed to be important for the dynamic instability of MTs during SCW formation and indirectly impact on the proper patterning of CMFs in the multi-layered SCW. This will in turn influence the mechanical properties of wood.

5.2 Outlooks and Future Research Directions

From the work of this thesis, it is clear that the transcriptional regulation of SCW biosynthesis is far more complex than originally suggested. Concerning MYB103, future research should be directed towards identifying its direct targets, *e.g.*, by an estradiol- or glucocorticoid-inducible system, combined with CHX treatment and microarray analysis. To demonstrate physical interaction of TF to promoter elements, ChIP analysis can be used; to identify the DNA binding site(s), EMSA analysis would be required. Not only could this reveal the link between MYB103 and F5H, but also if/how MYB103 is involved in other regulatory loops, putatively important for synthesizing other cell wall polymers.

Addressing a more complete understanding function of MAP20 requires complementary research to be carried out. Further genetic analysis will be appropriate to unequivocally conclude about its role in regulating the dynamic instability of MTs. Such experiments would include crossing AtMAP20-OE plants with an EB1-OE and/or TUB6-OE GFP fluorescent marker line and study MT dynamics (*i.e.*, confirm the MT-stabilizing effect of AtMAP20 *in situ*) of epidermal hypocotyl cells in *Arabidopsis* seedlings under a confocal microscope. To better understand the downstream function of MAP20 on cellulose structure, measurements of MFA and mechanical analysis of mutant plants will be required. The minor effect observed in KO mutant plants suggests that other MAPs have redundant functions with MAP20; the identification of these MAPs, in combination with multiple KO mutants, will facilitate studies on MAP20 function in relation to cell wall formation.

Further exploiting the TE inducible *Arabidopsis* cell culture system (**Section 4.1.3, this thesis**) will provide insight into the function of MAP20. By expressing tagged versions of MAP20, its cellular localization can be revealed, as well as its expression in different cell types. These approaches will help to better understand the globular cell population observed in the RNAi lines. Expressing His-labelled MAP20 could facilitate Co-IP to identify potential binding partners of MAP20. Then, a model can be built on how MAP20 (and potential partner proteins) binds to MTs and affects SCW patterning *in vivo*.

References

- Abe, T. & Hashimoto, T. (2005). Altered microtubule dynamics by expression of modified α -tubulin protein causes right-handed helical growth in transgenic Arabidopsis plants. *The Plant Journal*, 43(2), pp. 191-204.
- Albersheim, P., Darvill, A., Roberts, K., Sederoff, R. & Staehelin, A. (2011). *Plant Cell Walls: From Chemistry to Biology*. First. ed: Garland Science, Taylor & Francis Group, LLC. Available from: <http://books.google.com/books?id=JFPQGWAACAAJ>.
- Amor, Y., Haigler, C.H., Johnson, S., Wainscott, M. & Delmer, D.P. (1995). A membrane-associated form of sucrose synthase and its potential role in synthesis of cellulose and callose in plants. *Proceedings of the National Academy of Sciences*, 92(20), pp. 9353-9357.
- Anderson, C.T., Carroll, A., Akhmetova, L. & Somerville, C. (2010). Real-Time Imaging of Cellulose Reorientation during Cell Wall Expansion in Arabidopsis Roots. *Plant Physiol.*, 152(2), pp. 787-796.
- Antizar-Ladislao, B. & Turrión-Gómez, J.L. (2008). Second-generation biofuels and local bioenergy systems. *Biofuels, Bioproducts and Biorefining*, 2(5), pp. 455-469.
- Arato, C., Pye, E.K. & Gjennestad, G. (2005). The lignol approach to biorefining of woody biomass to produce ethanol and chemicals. *Applied Biochemistry and Biotechnology*, 123(1-3), pp. 871-882.
- Arioli, T., Peng, L.C., Betzner, A.S., Burn, J., Wittke, W., Herth, W., Camilleri, C., Hofte, H., Plazinski, J., Birch, R., Cork, A., Glover, J., Redmond, J. & Williamson, R.E. (1998). Molecular analysis of cellulose biosynthesis in Arabidopsis. *Science*, 279(5351), pp. 717-720.
- Atanassov, I.I., Pittman, J.K. & Turner, S.R. (2009). Elucidating the Mechanisms of Assembly and Subunit Interaction of the Cellulose Synthase Complex of Arabidopsis Secondary Cell Walls. *J. Biol. Chem.*, 284(6), pp. 3833-3841.
- Barnett, J.R. & Victoria, A.B. (2004). Cellulose microfibril angle in the cell wall of wood fibres. *Biological Reviews*, 79(2), pp. 461-472.
- Bashline, L., Lei, L., Li, S. & Gu, Y. (2014). Cell Wall, Cytoskeleton, and Cell Expansion in Higher Plants. *Molecular Plant*, 7(4), pp. 586-600.
- Baskin, T.I. (2001). On the alignment of cellulose microfibrils by cortical microtubules: A review and a model. *Protoplasma*, 215(1), pp. 150-171.
- Baskin, T.I. (2005). ANISOTROPIC EXPANSION OF THE PLANT CELL WALL. *Annual Review of Cell and Developmental Biology*, 21(1), pp. 203-222.

- Baskin, T.I., Beemster, G.T.S., Judy-March, J.E. & Marga, F. (2004). Disorganization of Cortical Microtubules Stimulates Tangential Expansion and Reduces the Uniformity of Cellulose Microfibril Alignment among Cells in the Root of Arabidopsis. *Plant Physiol.*, 135(4), pp. 2279-2290.
- Baskin, T.I., Meekes, H.T.H.M., Liang, B.M. & Sharp, R.E. (1999). Regulation of Growth Anisotropy in Well-Watered and Water-Stressed Maize Roots. II. Role of Cortical Microtubules and Cellulose Microfibrils. *Plant Physiol.*, 119(2), pp. 681-692.
- Berthet, S., Demont-Caulet, N., Pollet, B., Bidzinski, P., Cézard, L., Le Bris, P., Borrega, N., Hervé, J., Blondet, E., Balzergue, S., Lapierre, C. & Jouanin, L. (2011). Disruption of LACCASE4 and 17 Results in Tissue-Specific Alterations to Lignification of Arabidopsis thaliana Stems. *The Plant Cell Online*, 23(3), pp. 1124-1137.
- Bhargava, A., Ahad, A., Wang, S., Mansfield, S., Haughn, G., Douglas, C. & Ellis, B. (2013). The interacting MYB75 and KNAT7 transcription factors modulate secondary cell wall deposition both in stems and seed coat in Arabidopsis. *Planta*, 237(5), pp. 1199-1211.
- Bhargava, A., Mansfield, S.D., Hall, H.C., Douglas, C.J. & Ellis, B.E. (2010). MYB75 Functions in Regulation of Secondary Cell Wall Formation in the Arabidopsis Inflorescence Stem. *Plant Physiol.*, 154(3), pp. 1428-1438.
- Birnbaum, K., Shasha, D.E., Wang, J.Y., Jung, J.W., Lambert, G.M., Galbraith, D.W. & Benfey, P.N. (2003). A Gene Expression Map of the Arabidopsis Root. *Science*, 302(5652), pp. 1956-1960.
- Bjurhager, I., Olsson, A.-M., Zhang, B., Gerber, L., Kumar, M., Berglund, L.A., Burgert, I., Sundberg, B. & Salmén, L. (2010). Ultrastructure and Mechanical Properties of Populus Wood with Reduced Lignin Content Caused by Transgenic Down-Regulation of Cinnamate 4-Hydroxylase. *Biomacromolecules*, 11(9), pp. 2359-2365.
- Boerjan, W., Ralph, J. & Baucher, M. (2003). Lignin biosynthesis. *Annual Review of Plant Biology*, 54, pp. 519-546.
- Bollhöner, B., Prestele, J. & Tuominen, H. (2012). Xylem cell death: emerging understanding of regulation and function. *Journal of Experimental Botany*.
- Borevitz, J.O., Xia, Y., Blount, J., Dixon, R.A. & Lamb, C. (2000). Activation Tagging Identifies a Conserved MYB Regulator of Phenylpropanoid Biosynthesis. *The Plant Cell Online*, 12(12), pp. 2383-2393.
- Bowling, A.J. & Brown, R.M. (2008). The cytoplasmic domain of the cellulose-synthesizing complex in vascular plants. *Protoplasma*, 233(1), pp. 115-127.
- Bringmann, M., Landrein, B., Schudoma, C., Hamant, O., Hauser, M.-T. & Persson, S. (2012a). Cracking the elusive alignment hypothesis: the microtubule–cellulose synthase nexus unraveled. *Trends in Plant Science*, 17(11), pp. 666-674.
- Bringmann, M., Li, E., Sampathkumar, A., Kocabek, T., Hauser, M.-T. & Persson, S. (2012b). POM-POM2/CELLULOSE SYNTHASE INTERACTING1 Is Essential for the Functional Association of Cellulose Synthase and Microtubules in Arabidopsis. *The Plant Cell Online*, 24(1), pp. 163-177.
- Brown, D.M., Zeef, L.A.H., Ellis, J., Goodacre, R. & Turner, S.R. (2005). Identification of novel genes in Arabidopsis involved in secondary cell wall formation using expression profiling and reverse genetics. *Plant Cell*, 17(8), pp. 2281-2295.

- Burgert, I. (2006). Exploring the micromechanical design of plant cell walls. *American Journal of Botany*, 93(10), pp. 1391-1401.
- Burgert, I. & Keplinger, T. (2013). Plant micro- and nanomechanics: experimental techniques for plant cell-wall analysis. *Journal of Experimental Botany*, 64(15), pp. 4635-4649.
- Burk, D.H., Liu, B., Zhong, R., Morrison, W.H. & Ye, Z.-H. (2001). A Katanin-like Protein Regulates Normal Cell Wall Biosynthesis and Cell Elongation. *Plant Cell*, 13(4), pp. 807-828.
- Burk, D.H. & Ye, Z.H. (2002). Alteration of oriented deposition of cellulose microfibrils by mutation of a katanin-like microtubule-severing protein. *Plant Cell*, 14(9), pp. 2145-2160.
- Burk, D.H., Zhong, R. & Ye, Z.-H. (2007). The Katanin Microtubule Severing Protein in Plants. *Journal of Integrative Plant Biology*, 49(8), pp. 1174-1182.
- Burn, J.E., Hocart, C.H., Birch, R.J., Cork, A.C. & Williamson, R.E. (2002). Functional analysis of the cellulose synthase genes Cesa1, Cesa2, and Cesa3 in Arabidopsis. *Plant Physiology*, 129(2), pp. 797-807.
- Buschmann, H., Hauptmann, M., Niessing, D., Lloyd, C.W. & Schäffner, A.R. (2009). Helical Growth of the Arabidopsis Mutant *tortifolia2* Does Not Depend on Cell Division Patterns but Involves Handed Twisting of Isolated Cells. *The Plant Cell Online*, 21(7), pp. 2090-2106.
- Buschmann, H. & Lloyd, C.W. (2008). Arabidopsis Mutants and the Network of Microtubule-Associated Functions. *Mol Plant*, 1(6), pp. 888-898.
- Cao, L., Wang, L., Zheng, M., Cao, H., Ding, L., Zhang, X. & Fu, Y. (2013). Arabidopsis AUGMIN Subunit8 Is a Microtubule Plus-End Binding Protein That Promotes Microtubule Reorientation in Hypocotyls. *The Plant Cell Online*, 25(6), pp. 2187-2201.
- Carroll, A., Mansoori, N., Li, S., Lei, L., Vernhettes, S., Visser, R.G.F., Somerville, C., Gu, Y. & Trindade, L.M. (2012). Complexes with Mixed Primary and Secondary Cellulose Synthases Are Functional in Arabidopsis Plants. *Plant Physiology*, 160(2), pp. 726-737.
- Cassan-Wang, H., Goué, N., SAIDI, M.N., Legay, S., Sivadon, P., Goffner, D. & Grima-Pettenati, J. (2013). Identification of novel transcription factors regulating secondary cell wall formation in Arabidopsis. *Frontiers in Plant Science*, 4.
- Chabannes, M., Ruel, K., Yoshinaga, A., Chabbert, B., Jauneau, A., Joseleau, J.-P. & Boudet, A.-M. (2001). In situ analysis of lignins in transgenic tobacco reveals a differential impact of individual transformations on the spatial patterns of lignin deposition at the cellular and subcellular levels. *The Plant Journal*, 28(3), pp. 271-282.
- Chaffey, N. (2002). Why is there so little research into the cell biology of the secondary vascular system of trees? *New Phytologist*, 153(2), pp. 213-223.
- Chaffey, N., Cholewa, E., Regan, S. & Sundberg, B. (2002). Secondary xylem development in Arabidopsis: a model for wood formation. *Physiologia Plantarum*, 114(4), pp. 594-600.
- Chan, J., Calder, G., Fox, S. & Lloyd, C. (2007). Cortical microtubule arrays undergo rotary movements in Arabidopsis hypocotyl epidermal cells. *Nat Cell Biol*, 9(2), pp. 171-175.
- Chan, J., Crowell, E., Eder, M., Calder, G., Bunnewell, S., Findlay, K., Vernhettes, S., Höfte, H. & Lloyd, C. (2010). The rotation of cellulose synthase trajectories is microtubule dependent and influences the texture of epidermal cell walls in Arabidopsis hypocotyls. *Journal of Cell Science*, 123(20), pp. 3490-3495.

- Chan, J., Eder, M., Crowell, E.F., Hampson, J., Calder, G. & Lloyd, C. (2011). Microtubules and CESA tracks at the inner epidermal wall align independently of those on the outer wall of light-grown *Arabidopsis* hypocotyls. *Journal of Cell Science*, 124(7), pp. 1088-1094.
- Chan, J., Jensen, C.G., Jensen, L.C.W., Bush, M. & Lloyd, C.W. (1999). The 65-kDa carrot microtubule-associated protein forms regularly arranged filamentous cross-bridges between microtubules. *Proceedings of the National Academy of Sciences*, 96(26), pp. 14931-14936.
- Chapple, C., Vogt, T., Ellis, B.E. & Somerville, C.R. (1992). An *Arabidopsis* Mutant Defective in the General Phenylpropanoid Pathway. *The Plant Cell Online*, 4(11), pp. 1413-1424.
- Clair, B., Alm eras, T., Pilate, G., Jullien, D., Sugiyama, J. & Riekel, C. (2011). Maturation Stress Generation in Poplar Tension Wood Studied by Synchrotron Radiation Microdiffraction. *Plant Physiology*, 155(1), pp. 562-570.
- Cosgrove, D. & Jarvis, m. (2012). Comparative structure and biomechanics of plant primary and secondary cell walls. *Frontiers in Plant Science*, 3.
- Cosgrove, D.J. (2005). Growth of the plant cell wall. *Nature Reviews Molecular Cell Biology*, 6(11), pp. 850-861.
- Crowell, E.F., Bischoff, V., Desprez, T., Rolland, A., Stierhof, Y.-D., Schumacher, K., Gonneau, M., Hofte, H. & Vernhettes, S. (2009). Pausing of Golgi Bodies on Microtubules Regulates Secretion of Cellulose Synthase Complexes in *Arabidopsis*. *Plant Cell*, 21(4), pp. 1141-1154.
- Crowell, E.F., Gonneau, M., Stierhof, Y.D., H fte, H. & Vernhettes, S. (2010a). Regulated trafficking of cellulose synthases. *Current Opinion in Plant Biology*, 13(6), pp. 700-705.
- Crowell, E.F., Gonneau, M., Vernhettes, S. & H fte, H. (2010b). Regulation of anisotropic cell expansion in higher plants. *Comptes Rendus Biologies*, 333(4), pp. 320-324.
- Davis, J., Brandizzi, F., Liepman, A.H. & Keegstra, K. (2010). *Arabidopsis* mannan synthase CSLA9 and glucan synthase CSLC4 have opposite orientations in the Golgi membrane. *The Plant Journal*, 64(6), pp. 1028-1037.
- DeBolt, S., Gutierrez, R., Ehrhardt, D.W., Melo, C.V., Ross, L., Cutler, S.R., Somerville, C. & Bonetta, D. (2007a). Morlin, an inhibitor of cortical microtubule dynamics and cellulose synthase movement. *Proceedings of the National Academy of Sciences*, 104(14), pp. 5854-5859.
- DeBolt, S., Gutierrez, R., Ehrhardt, D.W. & Somerville, C. (2007b). Nonmotile Cellulose Synthase Subunits Repeatedly Accumulate within Localized Regions at the Plasma Membrane in *Arabidopsis* Hypocotyl Cells following 2,6-Dichlorobenzonitrile Treatment. *Plant Physiol.*, 145(2), pp. 334-338.
- D jardin, A., Laurans, F., Arnaud, D., Breton, C., Pilate, G. & Lepl , J.-C. (2010). Wood formation in Angiosperms. *Comptes Rendus Biologies*, 333(4), pp. 325-334.
- Delmer, D.P. (1999). Cellulose biosynthesis: Exciting times for a difficult field of study. *Annual Review of Plant Physiology and Plant Molecular Biology*, 50, pp. 245-276.
- Demura, T. & Ye, Z.-H. (2010). Regulation of plant biomass production. *Current Opinion in Plant Biology*, 13(3), pp. 298-303.
- Desprez, T., Juraniec, M., Crowell, E.F., Jouy, H., Pochylova, Z., Parcy, F., Hofte, H., Gonneau, M. & Vernhettes, S. (2007). Organization of cellulose synthase complexes involved in primary cell wall synthesis in *Arabidopsis thaliana*. *Proceedings of the National Academy of Sciences*, 104(39), pp. 15572-15577.

- Dixit, R. & Cyr, R. (2004a). The Cortical Microtubule Array: From Dynamics to Organization. *Plant Cell*, 16(10), pp. 2546-2552.
- Dixit, R. & Cyr, R. (2004b). Encounters between Dynamic Cortical Microtubules Promote Ordering of the Cortical Array through Angle-Dependent Modifications of Microtubule Behavior. *Plant Cell*, 16(12), pp. 3274-3284.
- Djerbi, S., Lindskog, M., Arvestad, L., Sterky, F. & Teeri, T.T. (2005). The genome sequence of black cottonwood (*Populus trichocarpa*) reveals 18 conserved cellulose synthase (CesA) genes. *Planta*, 221(5), pp. 739-746.
- Doblin, M.S., Kurek, I., Jacob-Wilk, D. & Delmer, D.P. (2002). Cellulose biosynthesis in plants: from genes to rosettes. *Plant and Cell Physiology*, 43(12), pp. 1407-1420.
- Donaldson, L.A. (2001). Lignification and lignin topochemistry — an ultrastructural view. *Phytochemistry*, 57(6), pp. 859-873.
- Dubos, C., Stracke, R., Grotewold, E., Weisshaar, B., Martin, C. & Lepiniec, L. (2010). MYB transcription factors in Arabidopsis. *Trends in Plant Science*, 15(10), pp. 573-581.
- Ehltig, J., Matheus, N., Aeschliman, D.S., Li, E., Hamberger, B., Cullis, I.F., Zhuang, J., Kaneda, M., Mansfield, S.D., Samuels, L., Ritland, K., Ellis, B.E., Bohlmann, J. & Douglas, C.J. (2005). Global transcript profiling of primary stems from *Arabidopsis thaliana* identifies candidate genes for missing links in lignin biosynthesis and transcriptional regulators of fiber differentiation. *The Plant Journal*, 42(5), pp. 618-640.
- Ehrhardt, D.W. (2008). Straighten up and fly right—microtubule dynamics and organization of non-centrosomal arrays in higher plants. *Current Opinion in Cell Biology*, 20(1), pp. 107-116.
- Ehrhardt, D.W. & Shaw, S.L. (2006). MICROTUBULE DYNAMICS AND ORGANIZATION IN THE PLANT CORTICAL ARRAY. *Annual Review of Plant Biology*, 57(1), pp. 859-875.
- Emons, A. (1982). Microtubules do not control microfibril orientation in a helicoidal cell wall. *Protoplasma*, 113(1), pp. 85-87.
- Emons, A.M.C. (1994). Winding threads around plant cells: a geometrical model for microfibril deposition. *Plant, Cell & Environment*, 17(1), pp. 3-14.
- Emons, A.M.C., Höfte, H. & Mulder, B.M. (2007). Microtubules and cellulose microfibrils: how intimate is their relationship? *Trends in Plant Science*, 12(7), pp. 279-281.
- Emons, A.M.C. & Mulder, B.M. (1998). The making of the architecture of the plant cell wall: How cells exploit geometry. *Proceedings of the National Academy of Sciences*, 95(12), pp. 7215-7219.
- Emons, A.M.C. & Mulder, B.M. (2000). How the deposition of cellulose microfibrils builds cell wall architecture. *Trends in Plant Science*, 5(1), pp. 35-40.
- Emons, A.M.C., Schel, J.H.N. & Mulder, B.M. (2002). The Geometrical Model for Microfibril Deposition and the Influence of the Cell Wall Matrix. *Plant Biology*, 4(1), pp. 22-26.
- Endler, A. & Persson, S. (2011). Cellulose Synthases and Synthesis in Arabidopsis. *Molecular Plant*, 4(2), pp. 199-211.
- Endo, S., Pesquet, E., Yamaguchi, M., Tashiro, G., Sato, M., Toyooka, K., Nishikubo, N., Udagawa-Motose, M., Kubo, M., Fukuda, H. & Demura, T. (2009). Identifying New Components Participating in the Secondary Cell Wall Formation of Vessel Elements in *Zinnia* and Arabidopsis. *Plant Cell*, 21(4), pp. 1155-1165.

- Evert, R.F. (2006). *Esau's Plant Anatomy: Meristems, Cells, and Tissues of the Plant Body: Their Structure, Function, and Development*. Third. ed: John Wiley & Sons, Inc. Available from: <http://books.google.se/books?id=0DhEBA5xgbkC>.
- Evrard, J.-L., Pieuchot, L., Vos, J.W., Vernos, I. & Schmit, A.-C. (2009). Plant TPX2 and related proteins. *Plant Signaling & Behavior*, 4(1), pp. 69-72.
- Faix, O. (1991). Classification of Lignins from Different Botanical Origins by FT-IR Spectroscopy. *Holzforschung*, 45(s1), pp. 21-28.
- Fellows, C.M., Brown, T.C. & Doherty, W.O.S. (2011). Lignocellulosics as a Renewable Feedstock for Chemical Industry: Chemicals from Lignin. In: *Green Chemistry for Environmental Remediation* John Wiley & Sons, Inc., pp. 561-610. Available from: <http://dx.doi.org/10.1002/9781118287705.ch18>.
- Fernandes, A.N., Thomas, L.H., Altaner, C.M., Callow, P., Forsyth, V.T., Apperley, D.C., Kennedy, C.J. & Jarvis, M.C. (2011). Nanostructure of cellulose microfibrils in spruce wood. *Proceedings of the National Academy of Sciences*, 108(47), pp. E1195-E1203.
- Fisher, D.D. & Cyr, R.J. (1998). Extending the Microtubule/Microfibril Paradigm . Cellulose Synthesis Is Required for Normal Cortical Microtubule Alignment in Elongating Cells. *Plant Physiol.*, 116(3), pp. 1043-1051.
- Franke, R., McMichael, C.M., Meyer, K., Shirley, A.M., Cusumano, J.C. & Chapple, C. (2000). Modified lignin in tobacco and poplar plants over-expressing the Arabidopsis gene encoding ferulate 5-hydroxylase. *Plant Journal*, 22(3), pp. 223-234.
- Fromm, J. (2013). Xylem Development in Trees: From Cambial Divisions to Mature Wood Cells. In: Fromm, J. (ed. *Cellular Aspects of Wood Formation*. (Plant Cell Monographs, 20) Springer Berlin Heidelberg, pp. 3-39. Available from: http://dx.doi.org/10.1007/978-3-642-36491-4_1.
- Fujii, S., Hayashi, T. & Mizuno, K. (2010). Sucrose Synthase is an Integral Component of the Cellulose Synthesis Machinery. *Plant Cell Physiol.*, 51(2), pp. 294-301.
- Fujita, M., Himmelspach, R., Hocart, C.H., Williamson, R.E., Mansfield, S.D. & Wasteneys, G.O. (2011). Cortical microtubules optimize cell-wall crystallinity to drive unidirectional growth in Arabidopsis. *The Plant Journal*, 66(6), pp. 915-928.
- Furutani, I., Watanabe, Y., Prieto, R., Masukawa, M., Suzuki, K., Naoi, K., Thitamadee, S., Shikanai, T. & Hashimoto, T. (2000). The SPIRAL genes are required for directional control of cell elongation in Arabidopsis thaliana. *Development*, 127(20), pp. 4443-4453.
- Gardiner, J.C., Taylor, N.G. & Turner, S.R. (2003). Control of Cellulose Synthase Complex Localization in Developing Xylem. *Plant Cell*, 15(8), pp. 1740-1748.
- Gardner, M.K., Zanic, M. & Howard, J. (2013). Microtubule catastrophe and rescue. *Current Opinion in Cell Biology*, 25(1), pp. 14-22.
- Geitmann, A. (2010). Mechanical modeling and structural analysis of the primary plant cell wall. *Current Opinion in Plant Biology*, 13(6), pp. 693-699.
- Gerber, L., Eliasson, M., Trygg, J., Moritz, T. & Sundberg, B. (2012). Multivariate curve resolution provides a high-throughput data processing pipeline for pyrolysis-gas chromatography/mass spectrometry. *Journal of Analytical and Applied Pyrolysis*, 95(0), pp. 95-100.

- Giddings, T.H. & Staehelin, L.A. (1991). Microtubule-Mediated Control of Microfibril Deposition: A Re-Examination of the Hypothesis. In: Lloyd, C.W. (ed. *The Cytoskeletal Basis of Plant Growth and Form*. First. ed. London: Academic Press, pp. 85-100.
- Gorzás, A., Stenlund, H., Persson, P., Trygg, J. & Sundberg, B. (2011). Cell-specific chemotyping and multivariate imaging by combined FT-IR microspectroscopy and orthogonal projections to latent structures (OPLS) analysis reveals the chemical landscape of secondary xylem. *The Plant Journal*, 66(5), pp. 903-914.
- Gorzás, A. & Sundberg, B. (2014). Chemical Fingerprinting of Arabidopsis Using Fourier Transform Infrared (FT-IR) Spectroscopic Approaches. In: Sanchez-Serrano, J.J. & Salinas, J. (eds) *Arabidopsis Protocols*. (Methods in Molecular Biology, 1062) Humana Press, pp. 317-352. Available from: http://dx.doi.org/10.1007/978-1-62703-580-4_18.
- Goshima, G. (2011). Identification of a TPX2-Like Microtubule-Associated Protein in *Drosophila*. *PLoS ONE*, 6(11), p. e28120.
- Goubet, F., Barton, C.J., Mortimer, J.C., Yu, X., Zhang, Z., Miles, G.P., Richens, J., Liepman, A.H., Seffen, K. & Dupree, P. (2009). Cell wall glucomannan in Arabidopsis is synthesised by CSLA glycosyltransferases, and influences the progression of embryogenesis. *The Plant Journal*, 60(3), pp. 527-538.
- Green, P.B. (1962). Mechanism for Plant Cellular Morphogenesis. *Science*, 138(3548), pp. 1404-1405.
- Green, P.B. (1965). Pathways of Cellular Morphogenesis: A Diversity in Nitella. *J Cell Biol*, 27(2), pp. 343-363.
- Groover, A. & Robischon, M. (2006). Developmental mechanisms regulating secondary growth in woody plants. *Current Opinion in Plant Biology*, 9(1), pp. 55-58.
- Gu, Y., Kaplinsky, N., Bringmann, M., Cobb, A., Carroll, A., Sampathkumar, A., Baskin, T.I., Persson, S. & Somerville, C.R. (2010). Identification of a cellulose synthase-associated protein required for cellulose biosynthesis. *Proceedings of the National Academy of Sciences*, 107(29), pp. 12866-12871.
- Guerriero, G., Fugelstad, J. & Bulone, V. (2010). What Do We Really Know about Cellulose Biosynthesis in Higher Plants? *Journal of Integrative Plant Biology*, 52(2), pp. 161-175.
- Gutierrez, R., Lindeboom, J.J., Paredez, A.R., Emons, A.M.C. & Ehrhardt, D.W. (2009). Arabidopsis cortical microtubules position cellulose synthase delivery to the plasma membrane and interact with cellulose synthase trafficking compartments. *Nat Cell Biol*, advanced online publication.
- Ha, M.-A., Apperley, D.C., Evans, B.W., Huxham, I.M., Jardine, W.G., Viëtor, R.J., Reis, D., Vian, B. & Jarvis, Michael C. (1998). Fine structure in cellulose microfibrils: NMR evidence from onion and quince. *The Plant Journal*, 16(2), pp. 183-190.
- Hamada, T. (2007). Microtubule-associated proteins in higher plants. *Journal of Plant Research*, 120(1), pp. 79-98.
- Hamada, T., Nagasaki-Takeuchi, N., Kato, T., Fujiwara, M., Sonobe, S., Fukao, Y. & Hashimoto, T. (2013). Purification and Characterization of Novel Microtubule-Associated Proteins from Arabidopsis Cell Suspension Cultures. *Plant Physiology*, 163(4), pp. 1804-1816.
- Harholt, J., Suttangkakul, A. & Vibe Scheller, H. (2010). Biosynthesis of Pectin. *Plant Physiol.*, 153(2), pp. 384-395.

- Hashimoto, T. (2013). Dissecting the cellular functions of plant microtubules using mutant tubulins. *Cytoskeleton*, 70(4), pp. 191-200.
- Hatton, D., Sablowski, R., Yung, M.-H., Smith, C., Schuch, W. & Bevan, M. (1995). Two classes of cis sequences contribute to tissue-specific expression of a PAL2 promoter in transgenic tobacco. *The Plant Journal*, 7(6), pp. 859-876.
- Heath, I.B. (1974). A unified hypothesis for the role of membrane bound enzyme complexes and microtubules in plant cell wall synthesis. *J Theor Biol*, 48(2), pp. 445-449.
- Hedenström, M., Wiklund-Lindström, S., Öman, T., Lu, F., Gerber, L., Schatz, P., Sundberg, B. & Ralph, J. (2009). Identification of Lignin and Polysaccharide Modifications in Populus Wood by Chemometric Analysis of 2D NMR Spectra from Dissolved Cell Walls. *Molecular Plant*, 2(5), pp. 933-942.
- Hertzberg, M., Aspeborg, H., Schrader, J., Andersson, A., Erlandsson, R., Blomqvist, K., Bhalerao, R., Uhlen, M., Teeri, T.T., Lundeberg, J., Sundberg, B., Nilsson, P. & Sandberg, G. (2001). A transcriptional roadmap to wood formation. *Proceedings of the National Academy of Sciences of the United States of America*, 98(25), pp. 14732-14737.
- Himmelspach, R., Williamson, R.E. & Wasteneys, G.O. (2003). Cellulose microfibril alignment recovers from DCB-induced disruption despite microtubule disorganization. *The Plant Journal*, 36(4), pp. 565-575.
- Hinchee, M., Rottmann, W., Mullinax, L., Zhang, C., Chang, S., Cunningham, M., Pearson, L. & Nehra, N. (2009). Short-rotation woody crops for bioenergy and biofuels applications. *In Vitro Cellular & Developmental Biology - Plant*, 45(6), pp. 619-629.
- Huntley, S.K., Ellis, D., Gilbert, M., Chapple, C. & Mansfield, S.D. (2003). Significant Increases in Pulping Efficiency in C4H-F5H-Transformed Poplars: Improved Chemical Savings and Reduced Environmental Toxins. *Journal of Agricultural and Food Chemistry*, 51(21), pp. 6178-6183.
- Hussey, S.G., Mizrachi, E., Creux, N.M. & Myburg, A.A. (2013). Navigating the transcriptional roadmap regulating plant secondary cell wall deposition. *Frontiers in Plant Science*, 4.
- Ishida, T., Kaneko, Y., Iwano, M. & Hashimoto, T. (2007). Helical microtubule arrays in a collection of twisting tubulin mutants of Arabidopsis thaliana. *Proceedings of the National Academy of Sciences*, 104(20), pp. 8544-8549.
- Ivakov, A. & Persson, S. (2013). Plant cell shapes: Modulators and Measurements. *Frontiers in Plant Science*, 4.
- Jansson, S. & Douglas, C.J. (2007). Populus: A Model System for Plant Biology. *Annual Review of Plant Biology*, 58(1), pp. 435-458.
- Kaloriti, D., Galva, C., Parupalli, C., Khalifa, N., Galvin, M. & Sedbrook, J.C. (2007). Microtubule associated proteins in plants and the processes they manage. *Journal of Integrative Plant Biology*, 49, pp. 1164-1173.
- Kaneda, M., Rensing, K.H., Wong, J.C.T., Banno, B., Mansfield, S.D. & Samuels, A.L. (2008). Tracking Monolignols during Wood Development in Lodgepole Pine. *Plant Physiol.*, 147(4), pp. 1750-1760.
- Karimi, M., Inze, D. & Depicker, A. (2002). GATEWAY(TM) vectors for Agrobacterium-mediated plant transformation. *Trends in Plant Science*, 7(5), pp. 193-195.

- Kawamura, E. & Wasteneys, G.O. (2008). MOR1, the Arabidopsis thaliana homologue of Xenopus MAP215, promotes rapid growth and shrinkage, and suppresses the pausing of microtubules in vivo. *J Cell Sci*, 121(24), pp. 4114-4123.
- Kennedy, C., Cameron, G., Šturcová, A., Apperley, D., Altaner, C., Wess, T. & Jarvis, M. (2007). Microfibril diameter in celery collenchyma cellulose: X-ray scattering and NMR evidence. *Cellulose*, 14(3), pp. 235-246.
- Kim, W.-C., Kim, J.-Y., Ko, J.-H., Kim, J. & Han, K.-H. (2013). Transcription factor MYB46 is an obligate component of the transcriptional regulatory complex for functional expression of secondary wall-associated cellulose synthases in Arabidopsis thaliana. *Journal of Plant Physiology*, 170(15), pp. 1374-1378.
- Kim, W.-C., Ko, J.-H. & Han, K.-H. (2012a). Identification of a cis-acting regulatory motif recognized by MYB46, a master transcriptional regulator of secondary wall biosynthesis. *Plant Molecular Biology*, 78(4-5), pp. 489-501.
- Kim, W.-C., Ko, J.-H., Kim, J.-Y., Kim, J., Bae, H.-J. & Han, K.-H. (2012b). MYB46 directly regulates the gene expression of secondary wall-associated cellulose synthases in Arabidopsis. *The Plant Journal*, pp. n/a-n/a.
- Kimura, S., Laosinchai, W., Itoh, T., Cui, X.J., Linder, C.R. & Brown, R.M. (1999). Immunogold labeling of rosette terminal cellulose-synthesizing complexes in the vascular plant *Vigna angularis*. *Plant Cell*, 11(11), pp. 2075-2085.
- Ko, J.-H., Kim, W.-C. & Han, K.-H. (2009). Ectopic expression of MYB46 identifies transcriptional regulatory genes involved in secondary wall biosynthesis in Arabidopsis. *The Plant Journal*, 60(4), pp. 649-665.
- Ko, J.-H., Kim, W.-C., Kim, J.-Y., Ahn, S.-J. & Han, K.-H. (2012). MYB46-Mediated Transcriptional Regulation of Secondary Wall Biosynthesis. *Molecular Plant*, 5(5), pp. 961-963.
- Ko, J.H., Han, K.H., Park, S. & Yang, J.M. (2004). Plant body weight-induced secondary growth in Arabidopsis and its transcription phenotype revealed by whole-transcriptome profiling. *Plant Physiology*, 135(2), pp. 1069-1083.
- Korolev, A.V., Buschmann, H., Doonan, J.H. & Lloyd, C.W. (2007). AtMAP70-5, a divergent member of the MAP70 family of microtubule-associated proteins, is required for anisotropic cell growth in Arabidopsis. *J Cell Sci*, 120(13), pp. 2241-2247.
- Korolev, A.V., Chan, J., Naldrett, M.J., Doonan, J.H. & Lloyd, C.W. (2005). Identification of a novel family of 70 kDa microtubule-associated proteins in Arabidopsis cells. *Plant Journal*, 42(4), pp. 547-555.
- Kubo, M., Udagawa, M., Nishikubo, N., Horiguchi, G., Yamaguchi, M., Ito, J., Mimura, T., Fukuda, H. & Demura, T. (2005). Transcription switches for protoxylem and metaxylem vessel formation. *Genes & Development*, 19(16), pp. 1855-1860.
- Kumar, M., Thammannagowda, S., Bulone, V., Chiang, V., Han, K.-H., Joshi, C.P., Mansfield, S.D., Mellerowicz, E., Sundberg, B., Teeri, T. & Ellis, B.E. (2009). An update on the nomenclature for the cellulose synthase genes in Populus. *Trends in Plant Science*, 14(5), pp. 248-254.
- Larson, P.R. (1994). *The vascular cambium : development and structure*. Berlin ; New York: Springer-Verlag. Available from: <http://forward.library.wisconsin.edu/catalog/ocm30033721>.

- Li, E., Bhargava, A., Qiang, W., Friedmann, M.C., Forneris, N., Savidge, R.A., Johnson, L.A., Mansfield, S.D., Ellis, B.E. & Douglas, C.J. (2012a). The Class II KNOX gene KNAT7 negatively regulates secondary wall formation in Arabidopsis and is functionally conserved in Populus. *New Phytologist*, 194(1), pp. 102-115.
- Li, E., Wang, S., Liu, Y., Chen, J.-G. & Douglas, C.J. (2011a). OVATE FAMILY PROTEIN4 (OFP4) interaction with KNAT7 regulates secondary cell wall formation in Arabidopsis thaliana. *The Plant Journal*, 67(2), pp. 328-341.
- Li, J., Wang, X., Qin, T., Zhang, Y., Liu, X., Sun, J., Zhou, Y., Zhu, L., Zhang, Z., Yuan, M. & Mao, T. (2011b). MDP25, A Novel Calcium Regulatory Protein, Mediates Hypocotyl Cell Elongation by Destabilizing Cortical Microtubules in Arabidopsis. *The Plant Cell Online*, 23(12), pp. 4411-4427.
- Li, S., Lei, L., Somerville, C.R. & Gu, Y. (2012b). Cellulose synthase interactive protein 1 (CS11) links microtubules and cellulose synthase complexes. *Proceedings of the National Academy of Sciences*, 109(1), pp. 185-190.
- Li, X., Bergelson, J. & Chapple, C. (2010). The ARABIDOPSIS Accession Pna-10 Is a Naturally Occurring sng1 Deletion Mutant. *Molecular Plant*, 3(1), pp. 91-100.
- Li, X., Weng, J.-K. & Chapple, C. (2008). Improvement of biomass through lignin modification. *The Plant Journal*, 54(4), pp. 569-581.
- Li, Y., Qian, Q., Zhou, Y., Yan, M., Sun, L., Zhang, M., Fu, Z., Wang, Y., Han, B., Pang, X., Chen, M. & Li, J. (2003). BRITTLE CULM1, Which Encodes a COBRA-Like Protein, Affects the Mechanical Properties of Rice Plants. *Plant Cell*, 15(9), pp. 2020-2031.
- Liang, Y.-K., Dubos, C., Dodd, I.C., Holroyd, G.H., Hetherington, A.M. & Campbell, M.M. (2005). AtMYB61, an R2R3-MYB Transcription Factor Controlling Stomatal Aperture in Arabidopsis thaliana. *Current Biology*, 15(13), pp. 1201-1206.
- Liepmann, A.H., Wightman, R., Geshi, N., Turner, S.R. & Scheller, H.V. (2010). Arabidopsis – a powerful model system for plant cell wall research. *The Plant Journal*, 61(6), pp. 1107-1121.
- Liu, C.-J., Miao, Y.-C. & Zhang, K.-W. (2011). Sequestration and Transport of Lignin Monomeric Precursors. *Molecules*, 16(1), pp. 710-727.
- Liu, X., Qin, T., Ma, Q., Sun, J., Liu, Z., Yuan, M. & Mao, T. (2013). Light-Regulated Hypocotyl Elongation Involves Proteasome-Dependent Degradation of the Microtubule Regulatory Protein WDL3 in Arabidopsis. *The Plant Cell Online*, 25(5), pp. 1740-1755.
- Lloyd, C. (2006). PLANT SCIENCE: Enhanced: Microtubules Make Tracks for Cellulose. *Science*, 312(5779), pp. 1482-1483.
- Lloyd, C. & Chan, J. (2008). The parallel lives of microtubules and cellulose microfibrils. *Current Opinion in Plant Biology*, 11(6), pp. 641-646.
- Lloyd, C. & Hussey, P. (2001). Microtubule-associated proteins in plants - Why we need a map. *Nature Reviews Molecular Cell Biology*, 2(1), pp. 40-47.
- Mansfield, S., Kang, K.-Y. & Chapple, C. (2012). Designed for deconstruction - poplar trees altered in cell wall lignification improve the efficacy of bioethanol production. *New Phytol*, 194, pp. 91 - 101.
- Mao, G., Buschmann, H., Doonan, J.H. & Lloyd, C.W. (2006). The role of MAP65-1 in microtubule bundling during Zinnia tracheary element formation. *J Cell Sci*, 119(4), pp. 753-758.

- Mao, T., Jin, L., Li, H., Liu, B. & Yuan, M. (2005). Two Microtubule-Associated Proteins of the Arabidopsis MAP65 Family Function Differently on Microtubules. *Plant Physiol.*, 138(2), pp. 654-662.
- Marita, J.M., Ralph, J., Hatfield, R.D. & Chapple, C. (1999). NMR characterization of lignins in Arabidopsis altered in the activity of ferulate 5-hydroxylase. *Proceedings of the National Academy of Sciences*, 96(22), pp. 12328-12332.
- McCarthy, R.L., Zhong, R., Fowler, S., Lyskowski, D., Piyasena, H., Carleton, K., Spicer, C. & Ye, Z.-H. (2010). The Poplar MYB Transcription Factors, PtrMYB3 and PtrMYB20, are Involved in the Regulation of Secondary Wall Biosynthesis. *Plant and Cell Physiology*, 51(6), pp. 1084-1090.
- McCarthy, R.L., Zhong, R. & Ye, Z.-H. (2009). MYB83 Is a Direct Target of SND1 and Acts Redundantly with MYB46 in the Regulation of Secondary Cell Wall Biosynthesis in Arabidopsis. *Plant Cell Physiol.*, 50(11), pp. 1950-1964.
- McCarthy, R.L., Zhong, R. & Ye, Z.-H. (2011). Secondary wall NAC binding element (SNBE), a key cis-acting element required for target gene activation by secondary wall NAC master switches. *Plant Signaling & Behavior*, 6(9), pp. 1282-1285.
- Meier, D., Fortmann, I., Odermatt, J. & Faix, O. (2005). Discrimination of genetically modified poplar clones by analytical pyrolysis–gas chromatography and principal component analysis. *Journal of Analytical and Applied Pyrolysis*, 74(1-2), pp. 129-137.
- Mellerowicz, E.J., Baucher, M., Sundberg, B. & Boerjan, W. (2001). Unravelling cell wall formation in the woody dicot stem. *Plant Molecular Biology*, 47(1-2), pp. 239-274.
- Mellerowicz, E.J. & Sundberg, B. (2008). Wood cell walls: biosynthesis, developmental dynamics and their implications for wood properties. *Current Opinion in Plant Biology*, 11(3), pp. 293-300.
- Meyer, K., Cusumano, J.C., Somerville, C. & Chapple, C.C. (1996). Ferulate-5-hydroxylase from Arabidopsis thaliana defines a new family of cytochrome P450-dependent monooxygenases. *Proceedings of the National Academy of Sciences*, 93(14), pp. 6869-6874.
- Meyer, K., Shirley, A.M., Cusumano, J.C., Bell-Lelong, D.A. & Chapple, C. (1998). Lignin monomer composition is determined by the expression of a cytochrome P450-dependent monooxygenase in Arabidopsis. *Proceedings of the National Academy of Sciences*, 95(12), pp. 6619-6623.
- Miao, Y.-C. & Liu, C.-J. (2010). ATP-binding cassette-like transporters are involved in the transport of lignin precursors across plasma and vacuolar membranes. *Proceedings of the National Academy of Sciences*.
- Mitsuda, N., Iwase, A., Yamamoto, H., Yoshida, M., Seki, M., Shinozaki, K. & Ohme-Takagi, M. (2007). NAC Transcription Factors, NST1 and NST3, Are Key Regulators of the Formation of Secondary Walls in Woody Tissues of Arabidopsis. *Plant Cell*, 19(1), pp. 270-280.
- Mitsuda, N., Seki, M., Shinozaki, K. & Ohme-Takagi, M. (2005). The NAC Transcription Factors NST1 and NST2 of Arabidopsis Regulate Secondary Wall Thickenings and Are Required for Anther Dehiscence. *The Plant Cell Online*, 17(11), pp. 2993-3006.
- Morreel, K., Ralph, J., Kim, H., Lu, F., Goeminne, G., Ralph, S., Messens, E. & Boerjan, W. (2004). Profiling of Oligolignols Reveals Monolignol Coupling Conditions in Lignifying Poplar Xylem. *Plant Physiology*, 136(3), pp. 3537-3549.

- Mutwil, M., Øbro, J., Willats, W.G.T. & Persson, S. (2008). GeneCAT—novel webtools that combine BLAST and co-expression analyses. *Nucleic Acids Research*, 36(suppl 2), pp. W320-W326.
- Nakajima, K., Furutani, I., Tachimoto, H., Matsubara, H. & Hashimoto, T. (2004). SPIRAL1 Encodes a Plant-Specific Microtubule-Localized Protein Required for Directional Control of Rapidly Expanding Arabidopsis Cells. *Plant Cell*, 16(5), pp. 1178-1190.
- Nakamura, M., Naoi, K., Shoji, T. & Hashimoto, T. (2004). Low Concentrations of Propyzamide and Oryzalin Alter Microtubule Dynamics in Arabidopsis Epidermal Cells. *Plant and Cell Physiology*, 45(9), pp. 1330-1334.
- Nakano, Y., Nishikubo, N., Gou, eacute, Nadia, Ohtani, M., Yamaguchi, M., Katayama, Y. & Demura, T. (2010). MYB transcription factors orchestrating the developmental program of xylem vessels in Arabidopsis roots. *Plant Biotechnology*, 27(3), pp. 267-272.
- Neff, R.A., Parker, C.L., Kirschenmann, F.L., Tinch, J. & Lawrence, R.S. (2011). Peak Oil, Food Systems, and Public Health. *American Journal of Public Health*, 101(9), pp. 1587-1597.
- Newman, L.J., Perazza, D.E., Juda, L. & Campbell, M.M. (2004). Involvement of the R2R3-MYB, AtMYB61, in the ectopic lignification and dark-photomorphogenic components of the det3 mutant phenotype. *The Plant Journal*, 37(2), pp. 239-250.
- Nick, P. (2008). *Plant Microtubules: Development and Flexibility*. Second. ed: Springer. Available from: <http://books.google.se/books?id=uoyMYtF3RgkC>.
- Nick, P. (2012). Microtubules and the tax payer. *Protoplasma*, 249(2), pp. 81-94.
- Nieminen, K.M., Kauppinen, L. & Helariutta, Y. (2004). A Weed for Wood? Arabidopsis as a Genetic Model for Xylem Development. *Plant Physiol.*, 135(2), pp. 653-659.
- Nishikubo, N., Takahashi, J., Roos, A.A., Derba-Maceluch, M., Piens, K., Brumer, H., Teeri, T.T., Stålbrand, H. & Mellerowicz, E.J. (2011). Xyloglucan endo-Transglycosylase-Mediated Xyloglucan Rearrangements in Developing Wood of Hybrid Aspen. *Plant Physiology*, 155(1), pp. 399-413.
- Novaes, E., Kirst, M., Chiang, V., Winter-Sederoff, H. & Sederoff, R. (2010). Lignin and Biomass: A Negative Correlation for Wood Formation and Lignin Content in Trees. *Plant Physiology*, 154(2), pp. 555-561.
- Oakley, R.V., Wang, Y.-S., Ramakrishna, W., Harding, S.A. & Tsai, C.-J. (2007). Differential Expansion and Expression of α - and β -Tubulin Gene Families in Populus. *Plant Physiology*, 145(3), pp. 961-973.
- Oda, Y. & Fukuda, H. (2012a). Initiation of Cell Wall Pattern by a Rho- and Microtubule-Driven Symmetry Breaking. *Science*, 337(6100), pp. 1333-1336.
- Oda, Y. & Fukuda, H. (2012b). Secondary cell wall patterning during xylem differentiation. *Current Opinion in Plant Biology*, 15(1), pp. 38-44.
- Oda, Y. & Fukuda, H. (2013a). The dynamic interplay of plasma membrane domains and cortical microtubules in secondary cell wall patterning. *Frontiers in Plant Science*, 4.
- Oda, Y. & Fukuda, H. (2013b). Rho of Plant GTPase Signaling Regulates the Behavior of Arabidopsis Kinesin-13A to Establish Secondary Cell Wall Patterns. *The Plant Cell Online*, 25(11), pp. 4439-4450.
- Oda, Y. & Fukuda, H. (2013c). Spatial organization of xylem cell walls by ROP GTPases and microtubule-associated proteins. *Current Opinion in Plant Biology*, 16(6), pp. 743-748.

- Oda, Y., Iida, Y., Kondo, Y. & Fukuda, H. (2010). Wood Cell-Wall Structure Requires Local 2D-Microtubule Disassembly by a Novel Plasma Membrane-Anchored Protein. *Current Biology*, 20(13), pp. 1197-1202.
- Oda, Y., Mimura, T. & Hasezawa, S. (2005). Regulation of Secondary Cell Wall Development by Cortical Microtubules during Tracheary Element Differentiation in Arabidopsis Cell Suspensions. *Plant Physiol.*, 137(3), pp. 1027-1036.
- Oh, S., Park, S. & Han, K.H. (2003). Transcriptional regulation of secondary growth in Arabidopsis thaliana. *Journal of Experimental Botany*, 54(393), pp. 2709-2722.
- Ohashi-Ito, K. & Fukuda, H. (2010). Transcriptional regulation of vascular cell fates. *Current Opinion in Plant Biology*, 13(6), pp. 670-676.
- Ohashi-Ito, K., Oda, Y. & Fukuda, H. (2010). Arabidopsis VASCULAR-RELATED NAC-DOMAIN6 Directly Regulates the Genes That Govern Programmed Cell Death and Secondary Wall Formation during Xylem Differentiation. *Plant Cell*, p. tpc.110.075036.
- Paredez, A.R., Somerville, C.R. & Ehrhardt, D.W. (2006). Visualization of Cellulose Synthase Demonstrates Functional Association with Microtubules. *Science*, 312(5779), pp. 1491-1495.
- Patten, A.M., Jourdes, M., Cardenas, C.L., Laskar, D.D., Nakazawa, Y., Chung, B.-Y., Franceschi, V.R., Davin, L.B. & Lewis, N.G. (2010). Probing native lignin macromolecular configuration in Arabidopsis thaliana in specific cell wall types: Further insights into limited substrate degeneracy and assembly of the lignins of ref8, fah 1-2 and C4H::F5H lines. *Molecular BioSystems*, 6(3), pp. 499-515.
- Penfield, S., Meissner, R.C., Shoue, D.A., Carpita, N.C. & Bevan, M.W. (2001). MYB61 Is Required for Mucilage Deposition and Extrusion in the Arabidopsis Seed Coat. *The Plant Cell Online*, 13(12), pp. 2777-2791.
- Perrin, R.M., Wang, Y., Yuen, C.Y.L., Will, J. & Masson, P.H. (2007). WVD2 is a novel microtubule-associated protein in Arabidopsis thaliana. *The Plant Journal*, 49(6), pp. 961-971.
- Persson, S., Paredez, A., Carroll, A., Palsdottir, H., Doblin, M., Poindexter, P., Khitrov, N., Auer, M. & Somerville, C.R. (2007). Genetic evidence for three unique components in primary cell-wall cellulose synthase complexes in Arabidopsis. *Proceedings of the National Academy of Sciences*, 104(39), pp. 15566-15571.
- Persson, S., Wei, H.R., Milne, J., Page, G.P. & Somerville, C.R. (2005). Identification of genes required for cellulose synthesis by regression analysis of public microarray data sets. *Proceedings of the National Academy of Sciences of the United States of America*, 102(24), pp. 8633-8638.
- Pesquet, E., Korolev, A.V., Calder, G. & Lloyd, C.W. (2010). The Microtubule-Associated Protein AtMAP70-5 Regulates Secondary Wall Patterning in Arabidopsis Wood Cells. *Current Biology*, 20(8), pp. 744-749.
- Pesquet, E. & Lloyd, C. (2011). Microtubules, MAPs and Xylem Formation The Plant Cytoskeleton. In: Liu, B. (ed. (Advances in Plant Biology, 2) Springer New York, pp. 277-306. Available from: http://dx.doi.org/10.1007/978-1-4419-0987-9_13.
- Pesquet, E., Ranocha, P., Legay, S., Digonnet, C., Barbier, O., Pichon, M. & Goffner, D. (2005). Novel Markers of Xylogenesis in Zinnia Are Differentially Regulated by Auxin and Cytokinin. *Plant Physiology*, 139(4), pp. 1821-1839.

- Pesquet, E., Zhang, B., Gorzsás, A., Puhakainen, T., Serk, H., Escamez, S., Barbier, O., Gerber, L., Courtois-Moreau, C., Alatalo, E., Paulin, L., Kangasjärvi, J., Sundberg, B., Goffner, D. & Tuominen, H. (2013). Non-Cell-Autonomous Postmortem Lignification of Tracheary Elements in *Zinnia elegans*. *The Plant Cell Online*, 25(4), pp. 1314-1328.
- Petersen, P.D., Lau, J., Ebert, B., Yang, F., Verherbruggen, Y., Kim, J.S., Varanasi, P., Suttangkakul, A., Auer, M., Loque, D. & Scheller, H.V. (2012). Engineering of plants with improved properties as biofuels feedstocks by vessel-specific complementation of xylan biosynthesis mutants. *Biotechnology for Biofuels*, 5(1), p. 84.
- Plomion, C., Leprovost, G. & Stokes, A. (2001). Wood formation in trees. *Plant Physiology*, 127(4), pp. 1513-1523.
- Porth, I., Klapšte, J., Skyba, O., Hannemann, J., McKown, A.D., Guy, R.D., DiFazio, S.P., Muchero, W., Ranjan, P., Tuskan, G.A., Friedmann, M.C., Ehling, J., Cronk, Q.C.B., El-Kassaby, Y.A., Douglas, C.J. & Mansfield, S.D. (2013). Genome-wide association mapping for wood characteristics in *Populus* identifies an array of candidate single nucleotide polymorphisms. *New Phytologist*, 200(3), pp. 710-726.
- Preston, R.D. (1982). The case for multinet growth in growing walls of plant cells. *Planta*, 155(4), pp. 356-363.
- Pyo, H., Demura, T. & Fukuda, H. (2007). TERE; a novel cis-element responsible for a coordinated expression of genes related to programmed cell death and secondary wall formation during differentiation of tracheary elements. *The Plant Journal*, 51(6), pp. 955-965.
- Qiu, D., Wilson, I.W., Gan, S., Washusen, R., Moran, G.F. & Southerton, S.G. (2008). Gene expression in Eucalyptus branch wood with marked variation in cellulose microfibril orientation and lacking G-layers. *New Phytologist*, 179(1), pp. 94-103.
- Raes, J., Rohde, A., Christensen, J.H., Van de Peer, Y. & Boerjan, W. (2003). Genome-wide characterization of the lignification toolbox in *Arabidopsis*. *Plant Physiology*, 133(3), pp. 1051-1071.
- Rajangam, A.S., Kumar, M., Aspeborg, H., Guerriero, G., Arvestad, L., Pansri, P., Brown, C.J.L., Hober, S., Blomqvist, K., Divne, C., Ezcurra, I., Mellerowicz, E., Sundberg, B., Bulone, V. & Teeri, T.T. (2008a). MAP20, a Microtubule-Associated Protein in the Secondary Cell Walls of Hybrid Aspen, Is a Target of the Cellulose Synthesis Inhibitor 2,6-Dichlorobenzonitrile. *Plant Physiol.*, 148(3), pp. 1283-1294.
- Rajangam, A.S., Yang, H., Teeri, T.T. & Arvestad, L. (2008b). Evolution of a domain conserved in microtubule-associated proteins of eukaryotes. *Advances and Applications in Bioinformatics and Chemistry*, 2008(1), pp. 51-69.
- Ralph, J., Lundquist, K., Brunow, G., Lu, F., Kim, H., Schatz, P., Marita, J., Hatfield, R., Ralph, S., Christensen, J. & Boerjan, W. (2004). Lignins: Natural polymers from oxidative coupling of 4-hydroxyphenyl- propanoids. *Phytochemistry Reviews*, 3(1-2), pp. 29-60.
- Ranocha, P., Denancé, N., Vanholme, R., Freydier, A., Martinez, Y., Hoffmann, L., Köhler, L., Pouzet, C., Renou, J.-P., Sundberg, B., Boerjan, W. & Goffner, D. (2010). Walls are thin 1 (WAT1), an *Arabidopsis* homolog of *Medicago truncatula* NODULIN21, is a tonoplast-localized protein required for secondary wall formation in fibers. *The Plant Journal*, 63(3), pp. 469-483.

- Ranocha, P., Dima, O., Nagy, R., Felten, J., Corratgé-Faillie, C., Novák, O., Morreel, K., Lacombe, B., Martinez, Y., Pfrunder, S., Jin, X., Renou, J.-P., Thibaud, J.-B., Ljung, K., Fischer, U., Martinoia, E., Boerjan, W. & Goffner, D. (2013). Arabidopsis WAT1 is a vacuolar auxin transport facilitator required for auxin homeostasis. *Nat Commun*, 4.
- Raven, P.H., Evert, R.F. & Eichhorn, S.E. (1999). *Biology of Plants*. Sixth. ed: W.H. Freeman and Company/Worth Publishers. Available from: <http://books.google.com/books?id=8tz2aB1-jb4C>.
- Rose, J.K.C., Braam, J., Fry, S.C. & Nishitani, K. (2002). The XTH family of enzymes involved in xyloglucan endotransglucosylation and endohydrolysis: Current perspectives and a new unifying nomenclature. *Plant and Cell Physiology*, 43(12), pp. 1421-1435.
- Roudier, F., Schindelman, G., DeSalle, R. & Benfey, P.N. (2002). The COBRA family of putative GPI-anchored proteins in Arabidopsis. A new fellowship in expansion. *Plant Physiology*, 130(2), pp. 538-548.
- Roussel, M.R. & Lim, C. (1995). Dynamic Model of Lignin Growing in Restricted Spaces. *Macromolecules*, 28(1), pp. 370-376.
- Rowell, R.M. (2012). *Handbook of Wood Chemistry and Wood Composites*. Second. ed: CRC Press, Taylor & Francis Group, LLC. Available from: <http://www.crcpress.com/product/isbn/9781439853801>.
- Ruegger, M., Meyer, K., Cusumano, J.C. & Chapple, C. (1999). Regulation of Ferulate-5-Hydroxylase Expression in Arabidopsis in the Context of Sinapate Ester Biosynthesis. *Plant Physiology*, 119(1), pp. 101-110.
- Sablowski, R.W., Baulcombe, D.C. & Bevan, M. (1995). Expression of a flower-specific Myb protein in leaf cells using a viral vector causes ectopic activation of a target promoter. *Proceedings of the National Academy of Sciences*, 92(15), pp. 6901-6905.
- Sablowski, R.W., Moyano, E., Cullianez-Macia, F.A., Schuch, W., Martin, C. & Bevan, M. (1994). A flower-specific Myb protein activates transcription of phenylpropanoid biosynthetic genes. *The EMBO journal*, 13(1), pp. 128-137.
- Sampathkumar, A., Gutierrez, R., McFarlane, H.E., Bringmann, M., Lindeboom, J., Emons, A.-M., Samuels, L., Ketelaar, T., Ehrhardt, D.W. & Persson, S. (2013). Patterning and Lifetime of Plasma Membrane-Localized Cellulose Synthase Is Dependent on Actin Organization in Arabidopsis Interphase Cells. *Plant Physiology*, 162(2), pp. 675-688.
- Sampathkumar, A., Lindeboom, J.J., Debolt, S., Gutierrez, R., Ehrhardt, D.W., Ketelaar, T. & Persson, S. (2011). Live Cell Imaging Reveals Structural Associations between the Actin and Microtubule Cytoskeleton in Arabidopsis. *The Plant Cell Online*, 23(6), pp. 2302-2313.
- Sasabe, M. & Machida, Y. (2006). MAP65: a bridge linking a MAP kinase to microtubule turnover. *Current Opinion in Plant Biology*, 9(6), pp. 563-570.
- Scheller, H.V. & Ulvskov, P. (2010). Hemicelluloses. *Annual Review of Plant Biology*, 61(1), pp. 263-289.
- Schindelman, G., Morikami, A., Jung, J., Baskin, T.I., Carpita, N.C., Derbyshire, P., McCann, M.C. & Benfey, P.N. (2001). COBRA encodes a putative GPI-anchored protein, which is polarly localized and necessary for oriented cell expansion in Arabidopsis. *Genes & Development*, 15(9), pp. 1115-1127.

- Sedbrook, J.C. (2004). MAPs in plant cells: delineating microtubule growth dynamics and organization. *Current Opinion in Plant Biology*, 7(6), pp. 632-640.
- Sedbrook, J.C. & Kaloriti, D. (2008). Microtubules, MAPs and plant directional cell expansion. *Trends in Plant Science*, 13(6), pp. 303-310.
- Sederoff, R.R., MacKay, J.J., Ralph, J. & Hatfield, R.D. (1999). Unexpected variation in lignin. *Current Opinion in Plant Biology*, 2(2), pp. 145-152.
- Shoji, T., Narita, N.N., Hayashi, K., Asada, J., Hamada, T., Sonobe, S., Nakajima, K. & Hashimoto, T. (2004). Plant-specific microtubule-associated protein SPIRAL2 is required for anisotropic growth in arabidopsis. *Plant Physiology*, 136(4), pp. 3933-3944.
- Sibout, R. & Höfte, H. (2012). Plant Cell Biology: The ABC of Monolignol Transport. *Current Biology*, 22(13), pp. R533-R535.
- Siedlecka, A., Wiklund, S., Péronne, M.-A., Micheli, F., Leśniewska, J., Sethson, I., Edlund, U., Richard, L., Sundberg, B. & Mellerowicz, E.J. (2008). Pectin Methyl Esterase Inhibits Intrusive and Symplastic Cell Growth in Developing Wood Cells of Populus. *Plant Physiology*, 146(2), pp. 554-565.
- Sims, R.E.H., Mabee, W., Saddler, J.N. & Taylor, M. (2010). An overview of second generation biofuel technologies. *Bioresource Technology*, 101(6), pp. 1570-1580.
- Sindhu, A., Langewisch, T., Olek, A., Multani, D.S., McCann, M.C., Vermerris, W., Carpita, N.C. & Johal, G. (2007). Maize Brittle stalk2 Encodes a COBRA-Like Protein Expressed in Early Organ Development But Required for Tissue Flexibility at Maturity. *Plant Physiol.*, 145(4), pp. 1444-1459.
- Sjödin, A., Street, N.R., Sandberg, G., Gustafsson, P. & Jansson, S. (2009). The Populus Genome Integrative Explorer (PopGenIE): a new resource for exploring the Populus genome. *New Phytologist*, 182(4), pp. 1013-1025.
- Smertenko, A.P., Kaloriti, D., Chang, H.-Y., Fiserova, J., Opatrny, Z. & Hussey, P.J. (2008). The C-Terminal Variable Region Specifies the Dynamic Properties of Arabidopsis Microtubule-Associated Protein MAP65 Isoforms. *Plant Cell*, 20(12), pp. 3346-3358.
- Somerville, C. (2006). Cellulose synthesis in higher plants. *Annual Review of Cell and Developmental Biology*, 22, pp. 53-78.
- Soyano, T., Thitamadee, S., Machida, Y. & Chua, N.-H. (2008). ASYMMETRIC LEAVES2-LIKE19/LATERAL ORGAN BOUNDARIES DOMAIN30 and ASL20/LBD18 Regulate Tracheary Element Differentiation in Arabidopsis. *The Plant Cell Online*, 20(12), pp. 3359-3373.
- Spokevicius, A.V., Southerton, S.G., MacMillan, C.P., Qiu, D., Gan, S., Tibbits, J.F.G., Moran, G.F. & Bossinger, G. (2007). beta-tubulin affects cellulose microfibril orientation in plant secondary fibre cell walls. *Plant Journal*, 51(4), pp. 717-726.
- Stelte, W., Sanadi, A.R., Shang, L., Holm, J.K., Ahrenfeldt, J. & Henriksen, U.B. (2012). RECENT DEVELOPMENTS IN BIOMASS PELLETIZATION – A REVIEW. *BioResources*, 7(3), pp. 4451-4490.
- Sterky, F., Bhalerao, R.R., Unneberg, P., Segerman, B., Nilsson, P., Brunner, A.M., Charbonnel-Campaa, L., Lindvall, J.J., Tandré, K., Strauss, S.H., Sundberg, B., Gustafsson, P., Uhlen, M., Bhalerao, R.P., Nilsson, O., Sandberg, G., Karlsson, J., Lundeberg, J. & Jansson, S. (2004). A

- Populus EST resource for plant functional genomics. *Proceedings of the National Academy of Sciences of the United States of America*, 101(38), pp. 13951-13956.
- Stoppin-Mellet, V., Gaillard, J. & Vantard, M. (2003). Plant katanin, a microtubule severing protein. *Cell Biology International*, 27(3), pp. 279-279.
- Stoppin-Mellet, V., Gaillard, J. & Vantard, M. (2006). Katanin's severing activity favors bundling of cortical microtubules in plants. *The Plant Journal*, 46(6), pp. 1009-1017.
- Strabala, T.J. & MacMillan, C.P. (2013). The Arabidopsis wood model—the case for the inflorescence stem. *Plant Science*, 210(0), pp. 193-205.
- Stracke, R., Werber, M. & Weisshaar, B. (2001). The R2R3-MYB gene family in Arabidopsis thaliana. *Current Opinion in Plant Biology*, 4(5), pp. 447-456.
- Studer, M.H., DeMartini, J.D., Davis, M.F., Sykes, R.W., Davison, B., Keller, M., Tuskan, G.A. & Wyman, C.E. (2011). Lignin content in natural Populus variants affects sugar release. *Proceedings of the National Academy of Sciences*, 108(15), pp. 6300-6305.
- Sugimoto, K., Himmelspach, R., Williamson, R.E. & Wasteneys, G.O. (2003). Mutation or Drug-Dependent Microtubule Disruption Causes Radial Swelling without Altering Parallel Cellulose Microfibril Deposition in Arabidopsis Root Cells. *Plant Cell*, 15(6), pp. 1414-1429.
- Sugimoto, K., Williamson, R.E. & Wasteneys, G.O. (2000). New Techniques Enable Comparative Analysis of Microtubule Orientation, Wall Texture, and Growth Rate in Intact Roots of Arabidopsis. *Plant Physiology*, 124(4), pp. 1493-1506.
- Szymanski, D.B. & Cosgrove, D.J. (2009). Dynamic Coordination of Cytoskeletal and Cell Wall Systems during Plant Cell Morphogenesis. *Current Biology*, 19(17), pp. R800-R811.
- Tamuri, A.U. & Laskowski, R.A. (2010). ArchSchema: a tool for interactive graphing of related Pfam domain architectures. *Bioinformatics*, 26(9), pp. 1260-1261.
- Taylor, G. (2002). Populus: Arabidopsis for forestry. Do we need a model tree? *Annals of Botany*, 90(6), pp. 681-689.
- Taylor, N.G., Howells, R.M., Huttly, A.K., Vickers, K. & Turner, S.R. (2003). Interactions among three distinct CesA proteins essential for cellulose synthesis. *Proceedings of the National Academy of Sciences of the United States of America*, 100(3), pp. 1450-1455.
- The Arabidopsis Genome Initiative (2000). Analysis of the genome sequence of the flowering plant Arabidopsis thaliana. *Nature*, 408(6814), pp. 796-815.
- Thitamadee, S., Tsuchihara, K. & Hashimoto, T. (2002). Microtubule basis for left-handed helical growth in Arabidopsis. *Nature*, 417(6885), pp. 193-196.
- Timmers, J., Vernhettes, S., Desprez, T., Vincken, J.-P., Visser, R.G.F. & Trindade, L.M. (2009). Interactions between membrane-bound cellulose synthases involved in the synthesis of the secondary cell wall. *Febs Letters*, 583(6), pp. 978-982.
- Turner, S.R. & Somerville, C.R. (1997). Collapsed xylem phenotype of Arabidopsis identifies mutants deficient in cellulose deposition in the secondary cell wall. *Plant Cell*, 9(5), pp. 689-701.
- Tuskan, G.A., DiFazio, S., Jansson, S., Bohlmann, J., Grigoriev, I., Hellsten, U., Putnam, N., Ralph, S., Rombauts, S., Salamov, A., Schein, J., Sterck, L., Aerts, A., Bhalerao, R.R., Bhalerao, R.P., Blaudez, D., Boerjan, W., Brun, A., Brunner, A., Busov, V., Campbell, M., Carlson, J., Chalot, M., Chapman, J., Chen, G.L., Cooper, D., Coutinho, P.M., Couturier, J., Covert, S., Cronk, Q., Cunningham, R., Davis, J., Degroove, S., Dejardin, A., Depamphilis,

- C., Detter, J., Dirks, B., Dubchak, I., Duplessis, S., Ehlting, J., Ellis, B., Gendler, K., Goodstein, D., Gribskov, M., Grimwood, J., Groover, A., Gunter, L., Hamberger, B., Heinze, B., Helariutta, Y., Henrissat, B., Holligan, D., Holt, R., Huang, W., Islam-Faridi, N., Jones, S., Jones-Rhoades, M., Jorgensen, R., Joshi, C., Kangasjarvi, J., Karlsson, J., Kelleher, C., Kirkpatrick, R., Kirst, M., Kohler, A., Kalluri, U., Larimer, F., Leebens-Mack, J., Leple, J.C., Locascio, P., Lou, Y., Lucas, S., Martin, F., Montanini, B., Napoli, C., Nelson, D.R., Nelson, C., Nieminen, K., Nilsson, O., Pereda, V., Peter, G., Philippe, R., Pilate, G., Poliakov, A., Razumovskaya, J., Richardson, P., Rinaldi, C., Ritland, K., Rouze, P., Ryaboy, D., Schmutz, J., Schrader, J., Segerman, B., Shin, H., Siddiqui, A., Sterky, F., Terry, A., Tsai, C.J., Uberbacher, E., Unneberg, P., Vahala, J., Wall, K., Wessler, S., Yang, G., Yin, T., Douglas, C., Marra, M., Sandberg, G., de Peer, Y.V. & Rokhsar, D. (2006). The genome of black cottonwood, *Populus trichocarpa* (Torr. & Gray). *Science*, 313(5793), pp. 1596-1604.
- Wade, R.H. & Hyman, A.A. (1997). Microtubule structure and dynamics. *Current Opinion in Cell Biology*, 9(1), pp. 12-17.
- Van Acker, R., Vanholme, R., Storme, V., Mortimer, J., Dupree, P. & Boerjan, W. (2013). Lignin biosynthesis perturbations affect secondary cell wall composition and saccharification yield in *Arabidopsis thaliana*. *Biotechnology for Biofuels*, 6(1), p. 46.
- Van Damme, D., Van Poucke, K., Boutant, E., Ritzenthaler, C., Inze, D. & Geelen, D. (2004). In Vivo Dynamics and Differential Microtubule-Binding Activities of MAP65 Proteins. *Plant Physiol.*, 136(4), pp. 3956-3967.
- Wang, H.-Z. & Dixon, R.A. (2011). On–Off Switches for Secondary Cell Wall Biosynthesis. *Molecular Plant*.
- Wang, X., Zhang, J., Yuan, M., Ehrhardt, D.W., Wang, Z. & Mao, T. (2012). Arabidopsis MICROTUBULE DESTABILIZING PROTEIN40 Is Involved in Brassinosteroid Regulation of Hypocotyl Elongation. *The Plant Cell Online*, 24(10), pp. 4012-4025.
- Wang, X., Zhu, L., Liu, B., Wang, C., Jin, L., Zhao, Q. & Yuan, M. (2007). Arabidopsis MICROTUBULE-ASSOCIATED PROTEIN18 Functions in Directional Cell Growth by Destabilizing Cortical Microtubules. *Plant Cell*, 19(3), pp. 877-889.
- Wang, Z., Gerstein, M. & Snyder, M. (2009). RNA-Seq: a revolutionary tool for transcriptomics. *Nat Rev Genet*, 10(1), pp. 57-63.
- Vanholme, R., Demedts, B., Morreel, K., Ralph, J. & Boerjan, W. (2010). Lignin Biosynthesis and Structure. *Plant Physiol.*, 153(3), pp. 895-905.
- Vanholme, R., Morreel, K., Darrah, C., Oyarce, P., Grabber, J.H., Ralph, J. & Boerjan, W. (2012). Metabolic engineering of novel lignin in biomass crops. *New Phytologist*, 196(4), pp. 978-1000.
- Vanholme, R., Morreel, K., Ralph, J. & Boerjan, W. (2008). Lignin engineering. *Current Opinion in Plant Biology*, 11(3), pp. 278-285.
- Wasteneys, G.O. (2002). Microtubule organization in the green kingdom: chaos or self-order? *Journal of Cell Science*, 115(7), pp. 1345-1354.
- Wasteneys, G.O. (2004). Progress in understanding the role of microtubules in plant cells. *Current Opinion in Plant Biology*, 7(6), pp. 651-660.
- Waterman-Storer, C.M. & Salmon, E.D. (1997). Microtubule dynamics: Treadmilling comes around again. *Current Biology*, 7(6), pp. R369-R372.

- Weng, J.-K., Li, X., Bonawitz, N.D. & Chapple, C. (2008). Emerging strategies of lignin engineering and degradation for cellulosic biofuel production. *Current Opinion in Biotechnology*, 19(2), pp. 166-172.
- Wertz, J.-L., Bédoué, O. & Mercier, J.P. (2010). *Cellulose Science and Technology*. First. ed: EPFL Press. Available from: <http://books.google.se/books?id=XI4nfkRyfGQC>.
- Whittington, A.T., Vugrek, O., Wei, K.J., Hasenbein, N.G., Sugimoto, K., Rashbrooke, M.C. & Wasteneys, G.O. (2001). MOR1 is essential for organizing cortical microtubules in plants. *Nature*, 411(6837), pp. 610-613.
- Wightman, R., Chomicki, G., Kumar, M., Carr, P. & Turner, Simon R. (2013). SPIRAL2 Determines Plant Microtubule Organization by Modulating Microtubule Severing. *Current Biology*, 23(19), pp. 1902-1907.
- Wightman, R. & Turner, S. (2010). Trafficking of the Plant Cellulose Synthase Complex. *Plant Physiol.*, 153(2), pp. 427-432.
- Wightman, R. & Turner, S.R. (2007). Severing at sites of microtubule crossover contributes to microtubule alignment in cortical arrays. *The Plant Journal*, 52(4), pp. 742-751.
- Wightman, R. & Turner, S.R. (2008). The roles of the cytoskeleton during cellulose deposition at the secondary cell wall. *The Plant Journal*, 54(5), pp. 794-805.
- Wilkins, O., Nahal, H., Foong, J., Provart, N.J. & Campbell, M.M. (2009). Expansion and Diversification of the Populus R2R3-MYB Family of Transcription Factors. *Plant Physiol.*, 149(2), pp. 981-993.
- Willats, W.G.T., McCartney, L., Mackie, W. & Knox, J.P. (2001). Pectin: cell biology and prospects for functional analysis. *Plant Molecular Biology*, 47(1-2), pp. 9-27.
- Williamson, R.E., Burn, J.E. & Hocart, C.H. (2002). Towards the mechanism of cellulose synthesis. *Trends in Plant Science*, 7(10), pp. 461-467.
- Wittmann, T., Wilm, M., Karsenti, E. & Vernos, I. (2000). TPX2, A Novel Xenopus MAP Involved in Spindle Pole Organization. *J. Cell Biol.*, 149(7), pp. 1405-1418.
- Vos, J.W., Pieuchot, L., Evrard, J.-L., Janski, N., Bergdoll, M., de Ronde, D., Perez, L.H., Sardon, T., Vernos, I. & Schmit, A.-C. (2008). The Plant TPX2 Protein Regulates Prospindle Assembly before Nuclear Envelope Breakdown. *Plant Cell*, 20(10), pp. 2783-2797.
- Yamaguchi, M. & Demura, T. (2010). Transcriptional regulation of secondary wall formation controlled by NAC domain proteins. *Plant Biotechnology*, 27(3), pp. 237-242.
- Yamaguchi, M., Goué, N., Igarashi, H., Ohtani, M., Nakano, Y., Mortimer, J.C., Nishikubo, N., Kubo, M., Katayama, Y., Kakegawa, K., Dupree, P. & Demura, T. (2010a). VASCULAR-RELATED NAC-DOMAIN6 and VASCULAR-RELATED NAC-DOMAIN7 Effectively Induce Transdifferentiation into Xylem Vessel Elements under Control of an Induction System. *Plant Physiology*, 153(3), pp. 906-914.
- Yamaguchi, M., Kubo, M., Fukuda, H. & Demura, T. (2008). VASCULAR-RELATED NAC-DOMAIN7 is involved in the differentiation of all types of xylem vessels in Arabidopsis roots and shoots. *The Plant Journal*, 55(4), pp. 652-664.
- Yamaguchi, M., Mitsuda, N., Ohtani, M., Ohme-Takagi, M., Kato, K. & Demura, T. (2011). VASCULAR-RELATED NAC-DOMAIN 7 directly regulates the expression of a broad range of genes for xylem vessel formation. *The Plant Journal*, 66(4), pp. 579-590.

- Yamaguchi, M., Ohtani, M., Mitsuda, N., Kubo, M., Ohme-Takagi, M., Fukuda, H. & Demura, T. (2010b). VND-INTERACTING2, a NAC Domain Transcription Factor, Negatively Regulates Xylem Vessel Formation in Arabidopsis. *The Plant Cell Online*, 22(4), pp. 1249-1263.
- Yang, C., Xu, Z., Song, J., Conner, K., Vizcay Barrena, G. & Wilson, Z.A. (2007). Arabidopsis MYB26/MALE STERILE35 Regulates Secondary Thickening in the Endothecium and Is Essential for Anther Dehiscence. *The Plant Cell Online*, 19(2), pp. 534-548.
- Yazaki, K. (2006). ABC transporters involved in the transport of plant secondary metabolites. *Febs Letters*, 580(4), pp. 1183-1191.
- Yuan, J.S., Tiller, K.H., Al-Ahmad, H., Stewart, N.R. & Stewart Jr, C.N. (2008). Plants to power: bioenergy to fuel the future. *Trends in Plant Science*, 13(8), pp. 421-429.
- Yuen, C.Y.L., Pearlman, R.S., Silo-suh, L., Hilson, P., Carroll, K.L. & Masson, P.H. (2003). WVD2 and WDL1 Modulate Helical Organ Growth and Anisotropic Cell Expansion in Arabidopsis. *Plant Physiol.*, 131(2), pp. 493-506.
- Zakzeski, J., Jongerius, A.L., Bruijninx, P.C.A. & Weckhuysen, B.M. (2012). Catalytic Lignin Valorization Process for the Production of Aromatic Chemicals and Hydrogen. *ChemSusChem*, 5(8), pp. 1602-1609.
- Zhang, J., Elo, A. & Helariutta, Y. (2011). Arabidopsis as a model for wood formation. *Current Opinion in Biotechnology*, 22(2), pp. 293-299.
- Zhao, C., Avci, U., Grant, E.H., Haigler, C.H. & Beers, E.P. (2008). XND1, a member of the NAC domain family in Arabidopsis thaliana, negatively regulates lignocellulose synthesis and programmed cell death in xylem. *The Plant Journal*, 53(3), pp. 425-436.
- Zhao, C., Craig, J.C., Petzold, H.E., Dickerman, A.W. & Beers, E.P. (2005). The Xylem and Phloem Transcriptomes from Secondary Tissues of the Arabidopsis Root-Hypocotyl. *Plant Physiol.*, 138(2), pp. 803-818.
- Zhao, Q. & Dixon, R.A. (2011). Transcriptional networks for lignin biosynthesis: more complex than we thought? *Trends in Plant Science*, 16(4), pp. 227-233.
- Zhao, Q., Wang, H., Yin, Y., Xu, Y., Chen, F. & Dixon, R.A. (2010). Syringyl lignin biosynthesis is directly regulated by a secondary cell wall master switch. *Proceedings of the National Academy of Sciences*, 107(32), pp. 14496-14501.
- Zhong, R., Burk, D.H., Morrison, W.H., III & Ye, Z.-H. (2002). A Kinesin-Like Protein Is Essential for Oriented Deposition of Cellulose Microfibrils and Cell Wall Strength. *Plant Cell*, 14(12), pp. 3101-3117.
- Zhong, R., Demura, T. & Ye, Z.-H. (2006). SND1, a NAC Domain Transcription Factor, Is a Key Regulator of Secondary Wall Synthesis in Fibers of Arabidopsis. *Plant Cell*, 18(11), pp. 3158-3170.
- Zhong, R., Lee, C., McCarthy, R.L., Reeves, C.K., Jones, E.G. & Ye, Z.-H. (2011a). Transcriptional Activation of Secondary Wall Biosynthesis by Rice and Maize NAC and MYB Transcription Factors. *Plant and Cell Physiology*, 52(10), pp. 1856-1871.
- Zhong, R., Lee, C. & Ye, Z.-H. (2010a). Evolutionary conservation of the transcriptional network regulating secondary cell wall biosynthesis. *Trends in Plant Science*, 15(11), pp. 625-632.
- Zhong, R., Lee, C. & Ye, Z.-H. (2010b). Functional Characterization of Poplar Wood-Associated NAC Domain Transcription Factors. *Plant Physiol.*, 152(2), pp. 1044-1055.

- Zhong, R., Lee, C. & Ye, Z.-H. (2010c). Global Analysis of Direct Targets of Secondary Wall NAC Master Switches in Arabidopsis. *Molecular Plant*.
- Zhong, R., Lee, C., Zhou, J., McCarthy, R.L. & Ye, Z.-H. (2008). A Battery of Transcription Factors Involved in the Regulation of Secondary Cell Wall Biosynthesis in Arabidopsis. *Plant Cell*, 20(10), pp. 2763-2782.
- Zhong, R., McCarthy, R.L., Haghghat, M. & Ye, Z.-H. (2013). The Poplar MYB Master Switches Bind to the SMRE Site and Activate the Secondary Wall Biosynthetic Program during Wood Formation. *PLoS ONE*, 8(7), p. e69219.
- Zhong, R., McCarthy, R.L., Lee, C. & Ye, Z.-H. (2011b). Dissection of the Transcriptional Program Regulating Secondary Wall Biosynthesis during Wood Formation in Poplar. *Plant Physiology*, 157(3), pp. 1452-1468.
- Zhong, R., Richardson, E. & Ye, Z.-H. (2007a). Two NAC domain transcription factors, SND1 and NST1, function redundantly in regulation of secondary wall synthesis in fibers of Arabidopsis. *Planta*, 225(6), pp. 1603-1611.
- Zhong, R., Richardson, E.A. & Ye, Z.-H. (2007b). The MYB46 Transcription Factor Is a Direct Target of SND1 and Regulates Secondary Wall Biosynthesis in Arabidopsis. *Plant Cell*, 19(9), pp. 2776-2792.
- Zhong, R. & Ye, Z.-H. (2007). Regulation of cell wall biosynthesis. *Current Opinion in Plant Biology*, 10(6), pp. 564-572.
- Zhong, R. & Ye, Z.-H. (2009). Transcriptional regulation of lignin biosynthesis. *Plant Signaling & Behavior*, 4(11), pp. 1028-1034.
- Zhong, R. & Ye, Z.-H. (2012). MYB46 and MYB83 Bind to the SMRE Sites and Directly Activate a Suite of Transcription Factors and Secondary Wall Biosynthetic Genes. *Plant and Cell Physiology*, 53(2), pp. 368-380.
- Zhou, J., Lee, C., Zhong, R. & Ye, Z.-H. (2009). MYB58 and MYB63 Are Transcriptional Activators of the Lignin Biosynthetic Pathway during Secondary Cell Wall Formation in Arabidopsis. *Plant Cell*, 21(1), pp. 248-266.
- Zhou, J., Qiu, J. & Ye, Z.-H. (2007). Alteration in Secondary Wall Deposition by Overexpression of the Fragile Fiber1 Kinesin-Like Protein in Arabidopsis. *Journal of Integrative Plant Biology*, 49(8), pp. 1235-1243.
- Zhu, C. & Dixit, R. (2011). Single Molecule Analysis of the Arabidopsis FRA1 Kinesin Shows that It Is a Functional Motor Protein with Unusually High Processivity. *Molecular Plant*, 4(5), pp. 879-885.

Acknowledgements

My PhD studies were preceded by my Master studies, which I started almost 10 years ago. Since then, I got to know many other PhD students and Post Docs that enriched my stay at UPSC. Some are still around, but most have already departed. It is impossible for me to recall all the people who deserve to be acknowledged for contributing to this thesis, but I will give it a try anyway. I apologize if anyone feels left out and should have been credited.

First of all, I sincerely thank my main supervisor, **Björn S**, for supporting me all the way to the finish line and for the financing all these years, both through “good karma” and “bad karma”, project wise. Also, importantly, for critical reading of the manuscripts and the whole thesis; this was crucial.

Second of all, I owe special thanks to my co-supervisor, **Ewa M**, for critical reading of the thesis, other scientific input and also for motivating me to enrol with PhD studies after I completed my Master’s under her supervision.

Thanks to all the members, past and present, of the FuncFiber colloquium and journal club for stimulating discussions and feedback on the work we do. Hope it will continue in the same good spirit with essential input from the PIs.

Past and present members of the big lab on floor 5, including **Ai-Min W**, **Ajaya B**, **Anna P**, **Bernard W**, **Bo Z**, **Christian K**, **Daniel H**, **Delphine G**, **Ellinor E**, **Emma H**, **Gergely M**, **Grit Z**, **Ingela S**, **Jeanette N**, **Junko S**, **Marta M**, **Mathieu C**, **Mélanie M**, **Robert N**, **Sara P**, **Shashank S**, **Siamsa D**, **Stefana G**, **Sully P**, **Sunil S** and **Vaibhav S**. Also, **Mikael J** and **Peter K**, previously working at Fysbot, UmU, who I got to know during my Master’s.

Before I relocated to the cell wall lab, I shared offices with **Alexander M**, **Christine R** and **Ilkka S**. Thank you all for your personal opinions, even down-to-Earth matters, and for exchanging knowledge and experiences.

At my new office in the cell wall lab, we are several groups performing research on wood formation, interacting on a daily basis. Here follows some of the PIs and their group members, past and present, to be considered.

My own group: **András G, Jonathan L, Judith F, Kjell O, Lorenz G, Melissa R, Peter I, Sara G, Simon B** and **Suhita D**.

Totte N group: **Amir M, Gaia C, Hanna H, Louise D, Umut R, Valentina F, Weiya X** and, of course, “**Titti**”.

Urs F group: **Christoffer J, Daniela L, Hardy H** and **Xu J**.

During my last years, I was funded by the BioImprove program, for which I’m grateful to, not only my supervisor, but also **Hannele T**. To the remaining PhD students in the program, including **Henrik S, Melis K, Ogonna O, Prashant P, Sacha E** and **Szymon T**, I wish you all the best in your efforts to obtain a PhD, as well. Keep up the good work and don’t give up!

Technical/administrative staff: **Carin O, Gun-Britt L, Inga-Britt C, Inga-Lis J, Marie N** and **Veronica B; Stefan L** and **Kjell E** for IT-coordination.

Not to forget, some old friends from my undergraduate studies, and friends working at other institutes than SLU: **Erik S, Marcus W** and **Ulf P**.

For most of the projects I was involved in, there was always some sort of collaboration, for which the following people need recognition of their efforts: **Brecht D, Brian E, Ines E, Ingo B, Mattias H** and **Wout B**.

The last part is dedicated to acknowledge the people who, aside from my main supervisor, made such a substantial contribution to my PhD thesis work that it would for sure not have been possible for me to ever finish it otherwise.

Edouard P, I appreciate all the help I’ve received from you. You brought new life into one of the longest-running projects ever and offered alternative point of views. Your expertise, constructive feedback and motivation were crucial for progress and wrapping up the stories into manuscripts. *Thanks*.

Sergey M, I can’t express my gratitude enough for all the feedback I received and the responsibility you took to help me finalize the manuscripts and my thesis. A sign of goodwill from your side, since I think you sometimes had to sacrifice more time than you were supposed to. I truly enjoyed our team work; it was an excellent complementation of our different skills. *Thanks*.

Manoj K, without your never-ending support and ability to carry out a variety of tasks quickly, this thesis would have been difficult to finalize. We’ve attended many conferences and meetings together and became more than just colleagues. I remember all the late Friday movie nights, exercises at IKSU and all the struggles with the projects. Thanks for also inviting me to England twice and for your hospitality. Hope we’ll always keep in touch in the future.

Last, but not least, I would like to thank my family and close friends who I spend most of my spare time with, and who have little to almost no clue about the purpose of my work. Nevertheless, I’ll give you a hard copy anyway. ☺

11 May 2014